

# 博士論文（要約）

(PhD Dissertation (Abridged))

## Study on hydrodynamic river model with reservoirs for improved simulation of floods in a low-lying floodplain

（低平氾濫原の洪水シミュレーション改善に向けた  
貯水池を含む水文動的河川モデルに関する研究）

チェリー メイ ロセッテ マテオ

Cherry May Rosete Mateo

# Dissertation Summary

Floods are complex processes that are affected by human-natural system interactions. The accelerating human interventions to the hydrological cycle necessitates the representation of coupled human-natural systems in analysing and understanding water management options. The operation of artificial reservoirs is among the human interventions with the largest impact to the hydrological cycle. While multiple benefits can be gained from reservoir operation, the multi-functional nature of reservoirs makes their operation difficult – trade-offs may exist between each competing functions. Integrated models are necessary for addressing such issues. While the impacts of the operation of large reservoirs on augmenting limited water supply (e.g. through irrigation, water scarcity, water withdrawal related studies) have already been assessed through integrated models, their impacts on large scale flooding and flood inundation are rarely assessed. The increasing flood risks necessitates the development of better tools which takes into account the impacts of artificial reservoirs to flood inundation.

This dissertation aims to improve the representation of human impacts, particularly of reservoirs and their operation, in a hydrodynamic river model. This goal is attained by representing reservoirs in elevation maps and integrating their operation as a subroutine in a state-of-the-art global hydrodynamic model, CaMa-Flood Model. The reservoir operation subroutine is based from the reservoir operation algorithm and module in one of the pioneering integrated water resources model, H08. By doing so, a new tool which allows more seamless large-scale assessments of human impacts to hydrodynamic flows is developed.

To ensure the local applicability of the model, it is applied and tested in the Chao Phraya River Basin, the largest and most important geographical unit in Thailand. The lowermost region is a delta which empties into the Gulf of Thailand. These geographic features make the region highly prone to flood inundation. In 2011, successive and excessive rainfall resulted to an immense flood catastrophe in the Chao Phraya River Basin. To date, the Thailand flood of 2011 is said to be the most economically damaging flood in history, both in overall losses and insured losses.

Several studies have already been conducted to analyze the Thai floods but most of them have focused on the natural factors that impacted the flood event. This dissertation contains one of the pioneering research which assessed the impacts of large-scale reservoir operation on the Thai flood inundation. H08, an integrated water resources model with a reservoir operation module, was combined with CaMa-Flood, a river routing model for the representation of flood dynamics. The combined H08-CaMa model was applied to simulate and assess the historical and alternative reservoir operation rules in the two largest reservoirs in the basin, Bhumibol and Sirikit Reservoirs. The combined H08-CaMa model effectively simulated the 2011 flood: regulated flows at a major

gauging station have high daily NSE-coefficient of 92% as compared with observed discharge; spatiotemporal extent of simulated flood inundation match well with those of satellite observations. Simulation results show that through the operation of reservoirs in 2011, flood volume was reduced by 8.6 billion m<sup>3</sup> and both flood depth and flood area were reduced by 40% on the average. Nonetheless, simple modifications in reservoir operation proved to further reduce the flood volume by 2.4 million m<sup>3</sup> and the flood depth and flood area by 20% on the average. A more realistic simulation of the 2011 Thai flood was made possible by modeling reservoir operation with a hydrodynamic model; the possibility of reducing flood inundation through improved reservoir management was quantified.

The utility of the combined H08-CaMa model in simulating the impacts of climate change and reservoir operation to the water balance and flood inundation in Chao Phraya River Basin was also demonstrated. The ensemble means of the simulation results using eight bias-corrected CMIP5 general circulation models (GCMs) under two representative concentration path scenarios (RCP), RCP4.5 and RCP8.5, for the near future from 2041 to 2059 and far future from 2081-2099 were compared with the base period simulation from 1981 to 1999. While the percent change in evapotranspiration within the catchment area of the two reservoirs in both RCP scenarios will not significantly increase, precipitation may significantly increase. This results to an increase in runoff of 40-50% in RCP8.5. While the change in dry season ranges from -10mm to 10mm, the wet season runoff could increase by as much as 160mm in RCP8.5. Hence, the frequency of reservoir emptying will decrease while spilling will increase by as much as 5 times of that of the base period in RCP8.5. Consequently, flooding in the basin will be more frequent and more severe. It was found that the mean inundated area downstream of the two reservoirs will increase by about 130% in RCP8.5. These results clearly indicate that under a changing climate, in the future, a shift of reservoir operation towards prioritizing flood mitigation over drought mitigation will be beneficial in the Chao Phraya River Basin. The study is thus relevant for preparing necessary adaptation measures to minimize the damages in the future.

These studies demonstrate the relevance of including anthropogenic effects in advanced global hydrological and river routing models for improving water resources management and flood mitigation in the present as well as in the future. However, several challenges still remain for the model to be useful for operation or practical purposes: (1) relatively coarse resolution, (2) low predictive skill of flooding in delta, and (3) several physical inconsistencies in forcing CaMa-Flood with the reservoir operation flows.

While numerous studies have shown that finer resolutions result to better predictions of catchment-scale floods using catchment-scale hydrodynamic models, the impact of finer spatial

resolution on flood predictions using global-scale river models is rarely examined. Hence, the suitability of CaMa-Flood river model with a new complex flow scheme which represents multi-directional downstream connectivity (MDC), in hyperresolution modelling of large-scale floods was assessed. The impacts of (1) spatial resolution, and (2) representation of sub-grid processes on simulating the inundated area and discharge during the immense flood in 2011 in Chao Phraya River Basin, Thailand was examined. Using several statistical metrics, it was found that when MDC is considered, simulation results slightly improved with finer spatial resolution. However, when MDC is ignored, the predictive capability of the model significantly declined with finer spatial resolution; Nash-Sutcliffe Efficiency coefficient decreased by more than 35% in simulation results at 1km resolution as compared with those at 10km resolution. In coarser spatial resolutions, floodplains flow along the same direction as the main channels. When simulating in finer spatial resolutions, areas that were expressed as floodplains in coarser spatial resolutions are discretized into small river channels. This results to disconnected floodplains which may only flow towards the main channels. Hence, the flow capacity of such floodplains is greatly reduced. In the event of heavy flooding, the reduced flow connectivity and flow capacity result to unrealistic “build-ups” and backflows. MDC pathways reduce such impacts by allowing water to flow in between floodplains, thereby maintaining the similar flow capacity as in coarser resolutions. The representation of MDC thereby results to more realistic flows between floodplains and deltas in hyperresolution modelling. These results indicate that large-scale flood predictions may not necessarily improve with hyperresolution modelling – improved physical process representation will have to be implemented.

Several models have already succeeded in representing artificial reservoir operation in hydrological and river routing models. These representations usually rely on virtual representations of reservoirs and manipulations of volumetric flows from storage relationships. Physically representing reservoirs in models will be beneficial for biogeochemical assessments, calculation of nutrient cycling and flows, and ecological assessments, among others.

Due to the limitation in satellite observations, dams and their corresponding reservoirs are typically physically represented in existing topography maps as shallow, elevated lakes that suddenly fall to its downstream. The volume of water impounded in dams are thereby underrepresented and underestimated. To improve the representation of reservoir operation, Bhumibol and Sirikit Reservoirs were explicitly represented by using interpolation techniques to modify the elevation of the areas identified as “flat” in the original elevation maps. A new algorithm was developed to detect the dams and their corresponding reservoirs using existing DEMs and river flow maps derived from SRTM and HydroSHEDS; the topography underlying the water surface was inferred



and interpolated using the following information: the elevation of the inflow and outflow grids, river lengths, and river sequence map. To integrate the reservoir operation algorithm previously used in H08, a similar computer code was then written as a subroutine in CaMa-Flood. The new code uses empirically-derived dam storage-water level relationships to convert the simulated water level to reservoir storage. The dam outflows were calculated using the reservoir storage and release rules. The outflows, water level, and dam storage in the downstream grid is then updated.

It was found that the natural flows would significantly change when the bathymetry is changed. The flat elevation in the original DEMs significantly reduces the flow gradient within the reservoirs. Such topography causes water to create a pool of water upstream of the reservoir in order to create a sufficient gradient for water to flow downstream. The pooling of water results to delayed and lower peaks in discharge, particularly during the dry season. It also results to lower flow fluctuations, suggesting slower response to rainfall and runoff. Such effects may be significant during droughts and when intense rainfall suddenly occurs after a dry spell.

Such changes in the natural flows were taken into account in the reservoir operation algorithm. By using the new elevation and the new modelling framework, it was found that the reservoir storage and water levels can be more realistically simulated. The flat elevation in the original DEMs cause extensive backflows when the reservoir operation algorithm is used. By representing the bathymetry of the reservoirs, such unrealistic backflows can be avoided, resulting to a significant improvement in the simulated flood inundation within the areas surrounding the reservoir. Hence, the efficiency of the model in simulating flows in the reservoirs and the surrounding areas have significantly improved.

In summary, this research demonstrated that global hydrological and river models can be used to provide locally-relevant information such as those needed for better water management, disaster mitigation, and climate change adaptation. New techniques for representing human impacts, particularly, reservoir operation, were developed and have been implemented in global models, H08, integrated water resources model and CaMa-Flood, hydrodynamic model. The relative impacts of finer spatial scales and subgrid processes representation on flood prediction have also been assessed. It was found that CaMa-Flood can be suitably used for hyperresolution modelling provided that floodplain flow processes are adequately represented.

To conclude, the results of this research are deemed to be important in directing efforts in modelling anthropogenic impacts with hydrodynamics in regional to global scales. The discussions provided are essential for improving our understanding of the underlying issues of scale and the necessary representation of physical processes. Overall, this dissertation contributes to progress in physically-based modelling and their application for better prediction of large-scale floods.

# Publications List

## First-authored:

- Mateo, C. M., D. Yamazaki, H. Kim, A. Champathong, and T. Oki, Will hyperresolution modelling always simulate flood inundation in large-scales better? (in preparation, to be submitted to WRR)
- Mateo, C. M., N. Hanasaki, D. Komori, K. Tanaka, M. Kiguchi, A. Champathong, T. Sukhaphunnaphan, D. Yamazaki, and T. Oki (2014), Assessing the impacts of reservoir operation to floodplain inundation by combining hydrological, reservoir management, and hydrodynamic models, *Water Resour. Res.*, 50, 7245–7266, doi:10.1002/2013WR014845.
- Mateo, C. M., N. Hanasaki, D. Komori, K. Yoshimura, M. Kiguchi, A. Champathong, T. Sukhaphunnaphan, D. Yamazaki, and T. Oki (2013), A simulation study on modifying reservoir operation rules: Tradeoffs between flood mitigation and water supply, in *Considering Hydrological Change in Reservoir Planning and Management*, edited by A. Schumann (IAHS Publ. 362) pp. 33–40, IAHS Press, Wallingford, U. K.

## Co-authored:

- Watanabe, S., Y. Hirabayashi, S. Kotsuki, N. Hanasaki, K. Tanaka, C. M. R. Mateo, M. Kiguchi, E. Ikoma, S. Kanae, and T. Oki (2014), Application of performance metrics to climate models for projecting future river discharge in the Chao Phraya River basin, *Hydrol. Res. Lett.* 8(1) 33-38.

## Conference proceedings:

- Mateo, C. M., et al., “Simulating the spatiotemporal impacts of large-scale reservoir operation on the 2011 Thai flood inundation through a combined modelling framework”, *Proceedings of the 26th International Union of Geodesy and Geophysics (IUGG) General Assembly*, June 22-July 2, 2015, Prague, Czech Republic
- Mateo, C. M., et al., “Simulating the impacts of large-scale reservoir operation on the 2011 Thai flood inundation,” *Proceedings of the Third Symposium of Sultan Qaboos Academic Chairs: Managing Water Resources for Sustainable Development*, October 2014, Ito Hall, Ito International Research Center B2, Hongo Campus, The University of Tokyo.
- Mateo, C. M. R., et al., “Modeling the impacts of climate change to reservoir operation and flood inundation in Chao Phraya River Basin,” *Proceedings of the 7th International Scientific Conference on the Global Water and Energy Cycle (GEWEX 2014)*, 14-17 July 2014, The Hague, Netherlands.
- Mateo C. M., N. Hanasaki, D. Yamazaki, S. Watanabe, M. Kiguchi, D. Komori, and T. Oki, “A combined model for assessing the impacts of reservoir operation on the spatial extent of flooding within a river basin”, *Proceedings of the 15th International Summer Symposium, Japan Society of Civil Engineers*, September 2013, College of Industrial Technology, Nihon Univ. Tsudanuma Campus, Japan, CS2-27.

# Acknowledgements

*"At times, our own light goes out and is rekindled by a spark from another person. Each of us has cause to think with deep gratitude of those who have lighted the flame within us." -Albert Schweitzer*

My own skills, knowledge, and wisdom would have not flourished and would have been insufficient for writing a dissertation without the inspiration, instruction, guidance, support, and acquaintance I have received. With utmost gratitude, I would like to thank everyone who have accompanied me in this worthwhile journey.

To my adviser and supervisor, Prof. Taikan Oki, I will forever be grateful and proud to have been instructed and trained by a brilliant man. I would have never embarked on this journey, particularly conduct research on modelling, without his encouragement, support, and instruction. He constantly inspires and challenges me to pursue a greater and deeper understanding of my work while ascertaining that my work integrates with and contributes to the overall pursuits of the hydrological and general society. He will always be my inspiration for conducting great, purposeful research and for pursuing to be a great academician.

To my co-advisers and panelists, Prof. Hiroaki Furumai, Dr. Naota Hanasaki, Dr. Yukiko Hirabayashi, and Prof. Toshio Koike, I greatly appreciate how they have challenged and encouraged me to deliver a creative work which is scientifically sound and useful to the society. Especially, I am thankful to Dr. Hanasaki who introduced me to modelling and critically checked and helped me in writing my journal articles.

To Dr. Dai Yamazaki, I am thankful for the enormous support I have received in understanding and modifying CaMa-Flood. His work and dedication inspires me to aspire to become an outstanding researcher.

To Dr. Hyugjun Kim, I would have not been able to produce the figures in this dissertation with efficiency and beauty if not for his dedication to teach us Python. Together with Dr. Nobuyuki Utsumi, they have taught me how to navigate through and use the lab servers. They have also ensured that the computing resources of the lab are working well for the students.

To Dr. Masashi Kiguchi, Dr. Daisuke Komori, Dr. Shinichiro Nakamura, Mr. Adisorn Champathong, and all the members of the IMPAC-T project, I greatly appreciate your help throughout the project. They have all been generous and elemental in providing me with the data I need to conduct this research. In the same manner, I am thankful to the Royal Irrigation Department, Thai Meteorological Department, and Electricity Generation Authority of Thailand for allowing me to use their data for research purposes.

To Dr. Kazuo Oki, Dr. Kei Yoshimura, Dr. Goro Mouri, Dr. Keigo Noda, and Dr. Michio Murakami, I am thankful for all their insightful comments, critical judgment, and thoughtful suggestions. They have all helped me fortify my understanding of and widen my perspective about hydrology and other related fields.

To all the former and current student members of Oki Lab, thank you for patiently receiving my comments and multiple questions during the lab meetings. Especially, I am thankful to Dr. Satoh, Mr. Okazaki, Ms. Hatono, Ms. Yoshida, and all the hardworking members who inspire me to always do my best and set a higher standard for myself. It was a joy working and being acquainted with all of you.

To the efficient, hardworking, and gorgeous secretaries of Oki Lab, Ms. Toi, Ms. Tsukada, and especially to Ms. Kurosawa, thank you for your generosity and for helping me with my documents. Handling such matters would have been next to impossible without your help. Similarly, I am thankful to the secretaries of the Civil Engineering Department, especially to Ms. Aoyama.

To the Japanese government and the people of Japan, I will forever be grateful for granting me the opportunity to study in one of the best universities in the world. In the same manner, I am thankful to the Department of Civil Engineering and its Foreign Student Office for all the opportunities and privileges they have granted to me. Todai used to be just a dream. The MEXT scholarship through the International Graduate Program are elemental in making that dream my reality for the last five years.

I would also like to acknowledge and thank all the people who have helped me live a balanced life and have provided support which extends beyond academic pursuits.

To my friends, thank you for providing me with the much needed camaraderie and encouragement. To Amelia, Ana, and Ahmad, thank you for making lab life much more interesting and fun. The lab overnights, weekend work days, last minute preparations, and bad coding days would have been unbearable without your company and silly stories over tea. To Ralph, it was such a relief to have a friend who is in the same boat and totally understands what we are going through. The same could be said about Sandy, my best friend and housemate who willingly listens to and scrutinizes every new idea that I have. Thank you for hearing out my rants over lengthy lunches or dinners.

To the man who has been patiently waiting for me through the years, cheering me up during the worst of my days, sending me little packages of joy, planning short adventures to somewhere we have not yet explored, and helping me understand, endure, and appreciate every struggle that comes my way, thank you for being there for me from the very beginning of my higher academic (and other) pursuits. Our journey is surely not the most comfortable one can have, but I will forever acknowledge and cherish having someone who lets me fly while assuring me that there will always be someone to go “home” to. You are the certainty to my uncertainties, the anchor to my wandering soul. Thank you, my dearest Bryan.

To my mom, my dad, and my family who dreamed of having a “doctor” in the family and who made me believe in the power of education, thank you very much for passing on your dreams to me, and for instilling in me the values which are needed to achieve them. I would not have been an engineer, a scholar, and a “doctor” if you have not let me be me. Thank your for inspiring me to always aspire for the better.

To all my other acquaintances, friends, and mentors whom I have failed to personally mention but who, in some ways showed their care and encouragement throughout this journey, thank you very much.

# Table of Contents

|                      |   |
|----------------------|---|
| Dissertation Summary | ii  |
| Publications List    | vi  |
| Acknowledgement      | vii   |
| Table of Contents    | ix  |
| List of Figures      | xii   |
| List of Tables       | xiv   |
| <br>                 |   |
| <b>Chapter 1</b>     | <b>Introduction</b>   |
| 1.1                  | Increasing flood risks and vulnerability..... 1   |
| 1.2                  | The importance of river models..... 2   |
| 1.3                  | The importance of artificial reservoirs..... 4  |
| 1.4                  | Objectives and significance of the study..... 4   |
| 1.5                  | Organization of this dissertation..... 5  |
| <br>                 |   |
| <b>Chapter 2</b>     | <b>The state-of-the-art in flood inundation and reservoir operation modelling</b>                               |
| 2.1                  | The state-of-the-art in flood inundation modelling using hydrodynamic models..... 7                             |
| 2.2                  | Gaps and limitations: Hydrodynamic modelling in large scales..... 12  |
| 2.3                  | The state-of-the-art in representations of reservoirs and their operation in regional to global scales ..... 14 |
| 2.3.1                | Increasing importance of reservoir modelling ..... 14   |
| 2.3.2                | Integration of reservoir operation schemes in global models ..... 16  |
| 2.4                  | Gaps and limitations: Integrated reservoir modelling in large scales..... 17                                    |
| 2.5                  | Bridging gaps through this dissertation ..... 18  |
| <br>                 |   |
| <b>Chapter 3</b>     | <b>Overview of models and their applicability to the test basin</b>   |
| 3.1                  | H08 integrated water resources model..... 20  |
| 3.1.1                | H08 land surface processes module ..... 22  |
| 3.1.2                | H08 river processes module ..... 24   |

|                  |  |    |
|------------------|--|----|
| 3.1.3            | H08 reservoir operation module .....   | 24 |
| 3.2              | CaMa-Flood hydrodynamic flood inundation model.....  | 25 |
| 3.2.1            | River network map .....  | 27 |
| 3.2.2            | Hydrodynamic flow equation .....   | 28 |
| 3.2.3            | Flow connectivity scheme .....   | 29 |
| 3.3              | Chao Phraya River Basin.....   | 32 |
| 3.4              | Input data and simulation setup.....   | 34 |
| 3.5              | Applicability of the models in the Chao Phraya River Basin.....  | 35 |
| <b>Chapter 4</b> | <b>Improved representation of reservoir operation in the combined H08-CaMa Flood model</b>                                 |    |
| 4.1              | Introduction: the 2011 Thai flood and the importance of reservoir operation  | 41 |
| 4.2              | Representation of reservoir operation in H08-CaMa model.....   | 43 |
| 4.2.1            | Combined H08-CaMa Flood model with reservoir operation.....  | 44 |
| 4.2.2            | Development of algorithms to represent the historical reservoir operation .....  | 45 |
| 4.3              | Simulation of the 2011 Thai flood .....  | 51 |
| 4.4              | Assessment of improvements in reservoir operation schemes.....   | 59 |
| 4.5              | Projection of the combined impacts of climate change and reservoir operation.....  | 70 |
| 4.6              | Contributions, caveats, and future works .....   | 71 |
| 4.6.1            | On improving the operation of Bhumibol and Sirikit Reservoirs.....   | 71 |
| 4.6.2            | On improving water resources management representation in global models .....  | 73 |
| 4.6.3            | On improving the simulation and assessment of flood events .....   | 74 |
| <b>Chapter 5</b> | <b>Impacts of varying spatial resolution and representation of complex Flow processes on large-scale flood predictions</b> | 76 |
| <b>Chapter 6</b> | <b>Physical representation and integration of reservoir operation in CaMa-Flood</b>  | 77 |

|                   |  |           |
|-------------------|--|-----------|
| <b>Chapter 7</b>  | <b>Summary, contributions, future works, and conclusions</b> | <b>78</b> |
| 7.1               | Summary .....  | 78        |
| 7.2               | Contributions .....  | 80        |
| 7.3               | Limitations and future works .....                           | 81        |
| 7.4               | Conclusions .....  | 83        |
| <b>References</b> |  | <b>84</b> |
| <b>Appendix A</b> |  | <b>97</b> |

# List of Figures

|     |   |    |
|-----|---|----|
| 3.1 | Schematic diagram of the modules (and sources) consisting the H08 integrated water resources model.....   | 21 |
| 3.2 | Schematic diagrams of the subgrid topography parameterization in CaMa-Flood .....   | 26 |
| 3.3 | Schematic diagrams of the multi-directional downstream connectivity in CaMa-Flood   | 30 |
| 3.4 | The Chao Phraya River Basin model domain, elevation map (shown in 1km resolution), river network, and validation stations.....  | 32 |
| 3.5 | Monthly basin averaged rainfall (as calculated from the reanalyzed observed rainfall forcing data) and observed reservoir inflows at Bhumibol and Sirikit Reservoirs from 1981-2004 .....             | 34 |
| 3.6 | Modelling framework for simulating natural flows.....   | 36 |
| 3.7 | Comparison between natural flow simulation results using plain H08 model ( <i>Nat-H08 Plain</i> ), combined H08 and CaMa-Flood model ( <i>Nat-H08-CaMa</i> ), and naturalized observed discharge..... | 37 |
| 3.8 | Daily natural hydrographs (in mm/day) at the validation stations.....   | 40 |
| 4.1 | Simulation process diagrams of the combined H08 Integrated Water Resources Model and CaMa-Flood River Routing Model.....  | 44 |
| 4.2 | Illustration of the upper and lower guide curves and the actual reservoir operation of the Sirikit and Bhumibol Reservoir.....  | 46 |
| 4.3 | Representation of algorithms used for reservoir storage constraints and reservoir releases for the locally-adapted and alternative reservoir operation schemes.....                                   | 48 |
| 4.4 | Comparison of the simulated daily regulated discharge using several reservoir operation algorithms with the observed in (a) 1993-1995, and (b) 2011.....  | 52 |



|      |   |    |
|------|---|----|
| 4.5  | Simulated and observed ratio of inundated areas (inundated area/total area).....  | 54 |
| 4.6  | Total volume of water stored in floodplains (flooded volume) downstream of the two<br>reservoirs .....                                  | 56 |
| 4.7  | Comparison of and difference in flood inundation between without and with dam<br>operation.....   | 57 |
| 4.8  | Alternative reservoir operation rules.....  | 60 |
| 4.9  | Comparison of the daily discharge simulated by the five reservoir operation rules<br>with those of the observed in flood year 2011..... | 61 |
| 4.10 | Reduction in flood volume downstream of both reservoirs.....  | 64 |
| 4.11 | Total area inundated by flood at increasing flood depth threshold levels.....   | 66 |
| 4.12 | Reduction in flood depth (FD) in 1-minute x 1-minute spatial resolution.....  | 68 |

## List of Tables

|     |   |    |
|-----|---|----|
| 3.1 | CaMa-Flood sub-grid parameters in Figure 3.2a .....   | 25 |
| 3.2 | Distinguishing features of the CaMa-Flood version used in the chapters of this<br>dissertation .....                      | 27 |
| 3.3 | Meteorological input data used to run H08.....  | 35 |
| 3.4 | Performance statistics related to the natural discharge simulation using plain H08<br>and combined H08-CaMa model.....    | 39 |
| 4.1 | Reservoir operation release algorithms for simulating the historical operation of<br>Bhumibol and Sirikit Reservoirs..... | 50 |
| 4.2 | Nash-Sutcliffe efficiency coefficients for the reservoir operation algorithms .....                                       | 51 |
| 4.3 | Parameters describing the alternative reservoir operation of Bhumibol and Sirikit<br>Reservoirs.....                      | 60 |
| 4.4 | Reliability of the reservoir operation schemes .....  | 63 |
| A1  | Model parameters calibrated in the study .....  | 97 |

# CHAPTER 1

## Introduction

*“Anthropogenic alterations of hydrology can have a major impact on ecosystems, agriculture, and other biogeochemical systems.”*

*–Vörösmarty and Sabagian, 2000*

*“With the current acceleration of human impacts, it is becoming increasingly clear that improved accounting for change, interactions and feedbacks is necessary to reach a better interpretation of coupled human-natural systems.” “...it is necessary to study and represent the connection between water and humans more deeply, as this is one of the main drivers of change and is connected to both sustainable water use and sustainable development.”*

*– Montanari et al., 2015 (Panta Rhei)*

*“The largest impact of human intervention on the hydrological cycle arises from the operation of reservoirs that drastically changes the seasonal pattern of horizontal water transport in the river system and thereby directly and indirectly affects a number of processes such as ability to decompose organic matter or the cycling of nutrients in the river system.”*

*-Wisser et al., 2010*

### 1.1 INCREASING FLOOD RISKS AND VULNERABILITY

Catastrophes due to extensive, large scale flood inundation have become more prevalent, especially in the last two decades [Brakenridge, 2015; EM-DAT, 2015]. On a huge percentage of the world, such flood risks are projected to increase with changing climate and increasing population [Milly et al., 2002; Dankers et al., 2014; Hirabayashi et al., 2013]. Hence, there is an increasing need for

improved capability to predict and forecast flood inundation in regional to global scales. Although flood events typically occur in smaller scales, analyses in large to global scales are essential to identify hotspots, undertake concerted efforts to address future problems in a consistent manner, and provide information for international financing of management and mitigation projects [Döll et al., 2003, Adhikari et al., 2010].

Although a few of these extreme flood events can be attributed to anthropogenic climate change [e.g. Pall et al., 2011], the IPCC special report on extreme events [IPCC, 2012] argues that there is limited to medium evidence of observed changes in magnitude and frequency of floods due to climate change. This is mainly due to limitations in observed flood records and to the difficulty in separating the complex impacts of human impacts such as land use and water resources management to flooding. The latter reason highlights the need for an integrated approach, one that takes into account both natural and anthropogenic influences, in analysing and predicting flood events.

## 1.2 THE IMPORTANCE OF RIVER MODELS

Global river routing and flood inundation models (global river models) are of great importance in understanding and assessing the previously mentioned issues. For the past two decades, global river models have been indispensable for numerous applications such as providing global estimates of the water cycle components, estimating virtual water trade, validating the outputs of general circulation models (GCMs), and for integrated analysis of economical, ecological, and biogeochemical impacts of global changes [Oki and Sud, 1998; Vörösmarty, Green, Salisbury, & Lammers, 2000; Döll et al., 2003; Hanasaki et al., 2008b; Lehner and Grill, 2013].

As compared with more detailed hydrodynamic or flood dynamic inundation models developed for catchment or basin scales, global river models are still preferable for coupling with GCMs and for ensemble predictions. Catchment or basin scale hydrodynamic models usually require discharge estimates as inputs. Hence, when applied in regional or global domains, they are significantly

hindered by the absence or limited availability of discharge estimates [Smith et al., 2015] or by the significant amount of boundary data processing required when using runoff outputs from global hydrological models (GHMs) or GCMs [Yamazaki, Sato, et al., 2014]. Global river models, on the other hand, are typically structured to route or process the gridded outputs of GHMs and GCMs. Earlier versions of these models, however, cannot explicitly simulate flood inundation because of their simpler flow schemes and the lack of representation of sub-grid scale river channels and floodplain topography which control flood dynamics [Yamazaki et al., 2011; Neal et al., 2012b]. Efforts to explicitly simulate flood inundation in global river models have just started recently [e.g. through implementing advanced floodplain inundation schemes (Coe et al., 2008; Decharme et al. 2008; Getirana et al., 2012); by using full St. Venant momentum equation (Paiva et al., 2011, 2013); by using local inertial flow equation (in CaMa-Flood by Yamazaki et al., 2013); and recently, by inclusion of multi-directional downstream flow schemes (the latest version of CaMa-Flood by Yamazaki, Sato, et al., 2014)]. Generally, these newer generation of river models implement better representation of hydrodynamics to simulate the flow and evolution of water storages on the land surface.

As their development have just been very recent, unlike earlier generation of global river models which have been elemental in integrating other water-related processes, the new generation of hydrodynamic river models are yet to be coupled or integrated with other processes such as human interventions with and management of water resources. However, as mentioned previously, flood events are increasingly becoming more complex as they are influenced by the confounding factors caused by anthropogenic interventions – these factors must be considered in order to have more reliable predictions [Di Baldassarre et al. 2013; Kundzewicz et al., 2014; Sivapalan et al., 2011, Wagener et al. 2010]. Hence, advancements towards integrating or incorporating human impact components on a hydrodynamic river model for more realistic flood predictions should be pursued.

### 1.3 THE IMPORTANCE OF ARTIFICIAL RESERVOIRS

Among the anthropogenic interventions to the hydrological cycle, artificial reservoirs are said to have the highest impacts due to their interference with the seasonal availability and flow of water [Hanasaki et al., 2006, Wisser et al., 2010]. They have been essential for protecting the downstream of the river basin from immense flooding. They have also been essential for providing water for irrigation and water supply, thereby making them useful for drought mitigation. Artificial reservoirs are also essential for providing energy through hydropower as well as providing some ecological services. While multiple benefits can be gained from reservoir operation, the multi-functional nature of reservoirs makes their operation difficult – trade-offs may exist between each competing functions [Mateo et al., 2013]. For example, operating reservoirs to highly prioritize flood mitigation in one season can lead to insufficient water for hydropower and for water supply in the subsequent dry season. Models which integrate simplified representation of reservoir operation can be helpful in assessing and balancing such trade-offs as well as understanding how such operation affects the water cycle.

### 1.4 OBJECTIVES AND SIGNIFICANCE OF THE STUDY

While regional to global analyses of flood risks using advanced global river models exist [Dankers et al., 2014; Hirabayashi et al., 2013], flood inundation analyses on the large-scale which include human impacts, particularly of reservoir operation, rarely exist. With the increasing interventions of humans in the Anthropocene, the beneficial and detrimental impacts of reservoirs on large river basins are becoming more apparent. Thus, in order to harness the potential benefits and reduce the impending damages that can be incurred from reservoir operation, the need to quantify and understand their impacts is increasing.

Primarily, this dissertation aims to improve the representation of human impacts, particularly of reservoirs and their operation, in a global hydrodynamic river model. This goal is attained by representing reservoirs in elevation maps and integrating their operation as a subroutine in a state-

of-the-art global hydrodynamic model, CaMa-Flood Model [Yamazaki et al., 2011; Yamazaki, Sato, et al., 2014]. The reservoir operation subroutine is based from the reservoir operation algorithm and module in one of the pioneering integrated water resources model, H08 [Hanasaki et al., 2008a]. With such improvement in modelling capabilities, our capability to understand and assess natural-human impacts on large-scale flood inundation will also be enhanced.

Secondarily, this study aims to assess and improve the applicability of the modelling framework in regional to local scales. To attain this, issues of scale and appropriate physical representation of processes are investigated. The modelling frameworks and tools developed herein are tested and applied in a region with a low-lying floodplain, the Chao Phraya River Basin. The said river basin is prone to both floods and droughts which are alleviated by the management of two large reservoirs upstream, the Bhumibol and Sirikit Reservoirs. Floodplains in low-lying regions which are among the most vulnerable areas to flooding and to the impacts of human interventions are deemed to benefit from this study.

To this end, this thesis contributes towards the ongoing hydrologic community efforts of developing models which have “more comprehensive representation of the links and feedbacks between hydrological and human system” [Montanari et al., 2013 (Panta Rhei)] and which can be “applicable everywhere and are locally relevant” [Bierkens et al., 2015 (Hyperresolution Challenge)].

## 1.5 ORGANIZATION OF THIS DISSERTATION

This dissertation is organized so that the reader may easily follow the improvements implemented on the hydrologic (H08) and hydrodynamic (CaMa) models used. Chapter 2 orients the reader with the state-of-the-art in the research in the two main areas of concern of this dissertation: flood inundation modelling using hydrodynamic river models and reservoir operation modelling in regional to global scales. Chapter 3 gives a brief description of the hydrologic and hydrodynamic models used and the river basin in which the applicability of the models are tested. The applicability of the models in simulating natural flows in the basin will also be demonstrated in this chapter.

Chapter 4 describes the improvements implemented in order to model how the operation of the two huge reservoirs in the river basin adjust to manage the interannual and seasonal variation of water in the river basin. A modelling framework which simulates reservoir operation as an integrated module in H08 and uses the runoff and reservoir release as inputs to CaMa-Flood is used. The applicability of the combined H08-CaMa model with improved reservoir operation algorithm for three purposes are demonstrated: 1) simulating the world's most economically damaging event – the immense 2011 Thai flood, 2) proposing and assessing improvements in reservoir operation, and 3) assessing the combined impacts of climate change and reservoir operation in the river basin. Several issues in the model results or modelling framework will be discussed in detail. Two of these issues will be addressed in the next two chapters. Chapter 5 addresses the issue of overestimation of the flooded areas in the low-lying areas of the basin. It explicates the role of finer spatial resolutions and better physical representation of flow physics in providing more reliable flood inundation predictions in floodplains. Two model configurations of CaMa-Flood are implemented in varying spatial resolutions. Chapter 6 addresses the issue of a more physically-based and more seamless integration of reservoirs in the hydrodynamic model. Two major model developments are implemented in this chapter: (1) rather than using virtual storages, the bathymetry of reservoirs are physically represented in the elevation maps used in CaMa-Flood, and (2) rather than simulating as an integrated module within H08, the reservoir operation algorithm used in Chapter 3 is integrated as a subroutine within CaMa-Flood. Chapter 7 summarizes the key points of the dissertation, expounds on its contributions and limitations, and finally, directs the reader towards possible future directions for improving the flood predictions through hydrodynamic modelling with reservoirs.



## MAJOR RESEARCH GAPS

- Integration or joint use of hydrodynamic models with reservoir operation in the large scales are rarely conducted
- The applicability of regional to global scale hydrodynamic models to finer resolution implementations for better local applicability have never been assessed
- Large scale impacts of reservoir operation to floodplain inundation are rarely conducted

## CHAPTER 2

### The state-of-the-art in flood inundation and reservoir operation modelling

*This chapter reviews published literature on two main research fields from which this dissertation is founded: (1) flood inundation modelling using hydrodynamic models, and (2) representing reservoirs and modelling their operation. While small-scale models (those that are especially made for and applied in small catchments or short reaches), this dissertation and this review focuses on large-scale models (those that use general parameters and globally-available datasets and are applied in regional to global domains). In each of the research fields mentioned, the significant studies and key developments will be discussed, and the gaps and limitations will be identified.*

#### 2.1 THE STATE-OF-THE-ART IN FLOOD INUNDATION MODELLING USING HYDRODYNAMIC MODELS

With the increasing computational capability and the advent and acceleration of advancements in remotely sensed data [Bates et al., 2004], the development of hydrodynamic and flood inundation modelling have greatly accelerated in the past decade. Remotely sensed data provided the information necessary for friction parameterization, topographical parameterization, and wide-area model validation, among others [Bates et al., 2012]. Such information allow for the continued progress in flood inundation modelling.

There are two main families of hydrodynamic river models: those that have been developed to simulate flood inundation at small catchment to basin scales, and those that have been developed to route water in regional to global scales. Because of the differences in their intended purposes, the level of complexity of these models also vary.

Catchment to basin scale hydrodynamic models (also called hydraulic models) were constructed based on a sound understanding of the physical laws governing the movement of water in small scales [Kirchner, 2006]. Compared with global-scale river models, these models usually have a more complete, thereby more complex representation of surface water flow physics. Early investigations in this field used mesh discretization and two-dimensional (2D) finite element codes for solving shallow water equations [e.g. Bates et al., 1992; Bates et al., 1998; Hardy et al., 1999]. Such models proved to be useful in modelling floodplain flows [Baird & Anderson, 1992; Bates et al., 1992], validation and modelling flows in ungauged catchments [e.g. Baird, Gee, & Anderson, 1992], and modelling sediment fluxes and pollution transport [e.g. Hardy, Bates, & Anderson, 2000; Papanicolaou, Krallis, & Edinger, 2008] in small river reaches, estuaries, and floodplains. To reduce the computational costs of such complex models, simplifications to the shallow water equations have also been investigated and applied [Hunter et al., 2007; McMillan & Brasington, 2007]. Using rectangular channels and 1D St. Venant's flow equations solved using parabolic approximations, Oliveri and Santoro [2000] estimated the urban flood damages in Palermo, Italy. Simplifications of the shallow water equations using 1D-2D channel-floodplain approach and using 2D St. Venant's estimation have also been evaluated for predicting flood inundation [e.g. in a 60km reach of River Severn in UK by Horritt and Bates, 2002]. This study, along with other more recent studies examining the complexity of catchment scale hydrodynamic models, have found that topography (and other small-scale, man-made features such as dikes, bridges, and diversion canals), rather than model complexity, is the major factor determining flood inundation patterns [Bates, 2012; Cook and Merwade, 2009; Hardy et al., 1999; Horritt and Bates, 2002]. Hence, such models have been usually implemented in fine spatial resolution and in smaller domains.

The predictive capability of hydrodynamic models deteriorate when implemented in coarser resolutions and when applied to more complex, heterogeneous systems in larger domains [Kirchner, 2006]. When applied in coarser resolution simulations, topographical details which control flow connectivity and boundary necessary for flood wave propagation cannot be represented explicitly [Neal, Schumann, & Bates, 2012 and Neal, Villanueva et al, 2012]. The implementation of hydrodynamic models in very fine resolutions on large- to global-scale domains entails high computational costs. Hence, these hydrodynamic models were usually implemented and assessed in short river reaches to small catchments. Although several small-scale hydrodynamic models have recently been implemented on large river basins by representing sub-grid topographical controls in coarser resolutions [e.g. Wilson et al., 2007; Neal, Schumann, & Bates, 2012], they are yet to be coupled with general circulation models (GCMs). Global or multiple large-scale basins application of small-scale or regional hydrodynamic models coupled with GCMs would require a significant amount of boundary data processing [Yamazaki, Sato, et al., 2014].

Compared with detailed river hydrodynamic models developed for catchment or basin scales, regional or global hydrodynamic models have simpler flow physics representation and have fewer, globally-available parameters [Neal, Schumann, & Bates, 2012; Sood and Smakhtin, 2015]. Most global river models (GRMs) have been typically structured to route or process the gridded outputs of GCMs, land surface models (LSMs), and global hydrological models (GHMs). Earlier versions of global river models typically use flow schemes based on water balance or storage cell model, kinematic wave model, and other variants which ignore some components of the dynamic water flow [e.g. TRIP of Oki and Sud, 1998; HYDRA of Coe, 2000; TRIP2 of Ngo-Duc et al., 2007]. These models, however, cannot explicitly simulate flood inundation because of their simpler flow schemes and the lack of representation of sub-grid scale river channels and floodplain topography which control flood dynamics [Yamazaki et al., 2011; Neal, Schumann, & Bates, 2012]. Efforts to explicitly simulate flood inundation in global river models have just started recently.

To explicitly simulate flood inundation and surface waters dynamics in the Amazon River Basin, Coe et al. [2008] used empirically-based equations to define the sub-grid morphological characteristics of a river (i.e. river width, height, and bank full volume), improved river flow velocity equation, and 1km resolution topographic data from SRTM. With these improvements, they have greatly reduced the error in simulated wet-season flooded area in the Amazon mainstem from 1983-1988 as compared with satellite-derived estimates. Similarly, Decharme et al [2008] used simple yet explicit representations of stream reservoirs (rectangular cross-section) and floodplain reservoirs (cubic cross-section) in the ISBA-TRIP coupled LSM-GRM to analyse and understand the interactions of inundated areas and wetlands with the climate and with the hydrological cycle. This was made possible by coupling the stream and floodplain reservoirs with the soil through infiltration and with the overlying atmosphere through precipitation and evapotranspiration. In addition to improvements in accuracy in simulating discharge and gaining reasonable capability to simulate flood inundation, the offline evaluation of the model over South America found a basin-scale increase in surface evaporation due to wetlands and inundated areas. These simplified representation of rivers and floodplains used statistical or conceptual parameters to infer the relationship between surface water movements and river stages.

Yamazaki et al [2011] improved the subgrid representation of river (or stream) and floodplain topographies through the introduction of the CaMa-Flood model. The subgrid topographic parameters and river networks are derived from fine-resolution flow direction maps and DEMs. Within each unit catchment, the floodplain elevation profile is derived from the cumulative distribution function of the SRTM30 elevation. The simplified function for the floodplain elevation profile is then used to diagnose flooded area fraction at a certain water depth or flood stage. The only prognostic variable is water storage and the rest of the variables are diagnosed from the water storage. Water mass is assumed to be instantaneously exchanged between channel and floodplain such that the water surface elevations in the two reservoirs are the same. Flow through the channel is calculated using diffusive wave equation. With these improvements, the simulation of daily river

discharge in major rivers as well as inundation in floodplains were both improved. However, early peaking of discharge was observed which was attributed to the assumption of instantaneous water exchange between river channels and floodplains.

Similarly, Paiva et al [2013] found that river-floodplain water exchange and storage as well as pressure forces and backwater effects play important roles in attenuating flood waves in the Amazon River hydrodynamics. They used a relatively complex and complete approach to river hydraulics modelling by implementing full St. Venant momentum equations [Paiva et al., 2011]. They also used fine resolution DEM and GIS-based algorithms to discretize the river reaches, and geomorphic in the Solimoes River in Amazon River Basin.

To improve the representation of floodplain dynamics, Getirana et al [2012] combined the main features of CaMa-Flood [Yamazaki et al., 2011] and ISBA-TRIP [Decharme et al., 2008] into a global flow routing scheme called HyMAP. The end goal of developing the model is similar to that of ISBA-TRIP which is to create a hydrodynamic model that can potentially be coupled with atmospheric models. It improved the physical representation of floodplain flows by allowing the water in the floodplain reservoir to flow to the downstream unit-catchment, similar with the flow in the river channel, using kinematic wave equation. Water interchange between floodplain and river channel is still instantaneous but the derivation of the floodplain elevation profile was improved by using a corrected SRTM30 DEM [Yamazaki, Baugh et al., 2012] and by considering the bank-full water surface area of river channels (previously neglected by Yamazaki et al., 2011 and Decharme et al., 2008).

Most of these improvements in flow physics have also been incorporated in the later version of CaMa-Flood [Yamazaki, Lee et al., 2012] by improving the representation of water surface elevations of water stored in floodplains and river channels and allowing the water in floodplains to flow to the downstream unit-catchment using diffusive wave equation. To increase its calculation efficiency, the CaMa-Flood was revised to implement a more complete shallow water equation in the form of the local inertial flow [Bates et al., 2010] for calculating river channel and floodplain

discharge and to use vector instead of raster-based components [Yamazaki et al., 2013]. Most recently, a bifurcation scheme had been incorporated in the model which allows the simulation of flows in braided rivers, artificial canals, and in between floodplains that do not have upstream-downstream relationships [Yamazaki, Sato, et al., 2014]. With these improvements, it can be said that CaMa-Flood model is currently at the frontier of large-scale hydrodynamic and flood inundation modelling.

## 2.2 GAPS AND LIMITATIONS: HYDRODYNAMIC MODELLING IN LARGE SCALES

Despite the developments in hydrological, hydrodynamic, and flood inundation modelling [e.g. Neal, Schumann, & Bates, 2012; Pappenberger et al., 2008; Vergnes and Decharme, 2012; Yamazaki, Sato, et al., 2014], greater availability and accessibility of data [e.g. Lehner and Grill, 2013], and improved remote sensing and assimilation techniques [Bates, 2004, 2012; Schumann et al., 2009], large-scale flood predictions remain uncertain and flood management is often sub-optimal [Arduino et al., 2005; Baldassarre and Uhlenbrook, 2012]. One of the prevailing issues is the spatial scale at which most of the existing global flood inundation studies are implemented – their outputs are too coarse for operational or practical purposes [Wood et al., 2011; Lehner and Grill, 2013]. In order to adequately provide flood as well as other water cycle information critical to the society, Wood et al. [2011] challenged the hydrological community to pursue hyper-resolution modelling. The group defined hyper-resolution modelling as the implementation of models at much higher spatial resolutions: about 1km at the global scale and about 100m at the continental scale. With respect to surface water and flood modelling, they have highlighted the need for high spatial resolution to capture topographical controls which are necessary for flood dynamics and inundation modelling.

In terms of modelling, there are two main approaches in addressing this challenge: expand the implementation of fine resolution, small basin-scale models from short river reaches to continental or global domains, or improve the physical representation of water movement in global-scale

hydrodynamic models and implement them at hyper-resolution. Unlike small-scale hydrodynamic models, the sensitivity to varying spatial scales and suitability for finer to hyper-resolution modelling of global-scale hydrodynamic models are yet to be assessed.

While large- to global-scale models may benefit from finer representation of topographical controls, Beven and Cloke [2012] argued that predictability issues cannot be simply solved by hyper-resolution modelling – heterogeneities will continue to exist even in hyper-resolution simulations. Hence, it is argued that more focus should be given to addressing fundamental issues related to the realistic sub-grid scale parameterization and processes representation [Beven and Cloke, 2012], and the epistemic uncertainties associated with the current prediction methods [Baldassarre and Uhlenbrook, 2012]. Wood et al. [2012] agreed that more research and modelling improvements still need to be done to address scale-appropriate parameterizations but the hydrologic community must work together “to define what is needed to develop robust hyper-resolution Earth System Models that include appropriate hyper-resolution land surface parameterizations.” In a recent review of research activities that have been conducted to respond to this challenge, Bierkens et al. [2015] gave emphasis on the end goal of hyper-resolution modelling – to develop models that are applicable “everywhere and are locally relevant.”

Wood et al [2011] further identified six main issues that need to be addressed in order to achieve hyper-resolution modelling: (1) surface and subsurface interactions, (2) land-atmosphere interactions, (3) human impacts on water cycle, (4) water quality, (5) computational considerations, and (6) observations and data. With respect to hydrodynamic modelling efforts, ISBA-TRIP [Decharme et al., 2008] and HyMAP [Getirana et al., 2012] have started to address issues (1) and (2) by allowing flood inundation to interact with infiltration and evaporation. Yamazaki et al. [2013] have started to address issue (5) by implementing more computationally-efficient schemes. Issue (6) have been partly addressed through the corrections to the SRTM30 DEM for hydrological purposes [Yamazaki, Lee, et al., 2012], and by providing a global width database for large rivers [Yamazaki, O’Loughlin, et al., 2014]. With these ongoing efforts, issues (3) human impacts on water

cycle, and (4) water quality, are yet to be addressed. Indeed, heavily regulated rivers are commonly identified as among the major sources of uncertainties and discrepancies in past studies [e.g. Decharme et al., 2008; Merz and Blöschl, 2008; Ngo-Duc et al., 2005; Ngo-Duc et al., 2007; Van Der Knijff et al., 2010].

## 2.3 THE STATE-OF-THE-ART IN REPRESENTATIONS OF RESERVOIRS AND THEIR OPERATION IN REGIONAL TO GLOBAL SCALES

### 2.3.1 Increasing importance of reservoir modelling

Damming of rivers have been essential for the human civilization to flourish. For more than thousands of years, they have been built to manage the seasonal variability of water; they were used for impounding water to augment low water supply during dry seasons, reduce the excessive and hazardous flows during rainy seasons, controlling water level for navigation, and providing electricity, among others. Due to the increasing need to manage the finite supply of water for an increasing population and developmental demands, the number of dams built and in operation worldwide have also greatly increased. To date, there are more than 58,000 large reservoirs (>15m) with the capacity to impound more than 15,000km<sup>3</sup> of fresh water in the World Registry of Dams [ICOLD, 2015]. This storage in large reservoirs accounts for about one-sixth of the total annual river flow to oceans [Hanasaki, Kanae, & Oki, 2006]. Large reservoirs are thus considered as important components of the terrestrial water cycle and should be considered in global change studies [Vörösmarty et al., 1997].

Recently, there have been increasing awareness of the detrimental impacts of large-scale reservoir operation. River damming results to fragmented rivers, thereby causing fragmentation in fluxes of nutrients, sediments, and movement of species. Lima et al. [2008] found that globally, large reservoirs might release about 104 Tg of CH<sub>4</sub> to the atmosphere annually, thereby contributing to the human-induced warming. Reservoirs have also been found to play important roles in the removal of nitrogen from surface water [Harrison et al., 2009]. Vörösmarty et al. [2003] estimates



that greater than 50% of basin-scale sediment flux are impounded in artificial reservoirs. While soil erosion due to other human interventions contribute to increased sedimentation in river mouths, the massive impoundment of sediments in large reservoirs still result to a net reduction in sediment flux which eventually lead to coastal erosion [Syvitski et al., 2005].

Despite these potential detrimental impacts, reservoir operation remains to be one of the key techniques that is used to manage water resources during floods and droughts as well as to adapt to the uncertainties in the temporal variability of rainfall. Hatcher and Jones [2013], for example, have found that in the Columbia River Basin, the artificial reservoirs have the capacity to overprint the climate change signal, thereby showing the contribution of the reservoirs in ensuring what they termed as “engineering resilience.” Artificial reservoirs remain to be one of the cheaper options for adapting to environmental and climatological changes. Hence, there is a growing concern to understand how the increasing variability and uncertainties in climatologic and socio-economic factors would impact the operation of reservoirs [e.g. Christensen et al., 2004; Eum and Simonovic, 2010]. Consequently, there is an increasing need to understand how reservoirs should be operated in order to adapt to projected changes [e.g. Eum et al., 2012; Payne et al., 2004].

In the Anthropocene, an epoch the natural system is increasingly being governed by human interventions, there is an increasing need to understand how the detrimental impacts of artificial reservoirs can be minimized and how their benefits can be maximized. Models which could explicitly show how reservoir operation impacts the temporal and spatial aspects of inundation and variability of water availability are essential tools for such purposes. As reservoir operation impacts multiple systems, an integrated approach to modelling is preferred. In human-modified hydrological systems, traditional monomeric (single-component) approach to modelling was also found to be inefficient; integrated or holistic hydrological modelling that takes components of human modification into account proved to improve modelling efficiency [Nalbantis et al., 2011].

### 2.3.2 Integration of reservoir operation schemes in global models

Several advancements in integrated modelling of natural hydrological processes and reservoir operation have been achieved in the past decade. Haddeland et al. [2006] implemented a simple reservoir operation algorithm in the VIC model to analyze the combined impacts of reservoir operation and irrigation to surface water fluxes. Hanasaki et al. [2006] developed an algorithm for estimating the reservoir operating rules and integrated it with a global river routing model to quantify the impact of reservoirs on the terrestrial water cycle. Later on, this reservoir module was integrated with several other modules into the H08 model [Hanasaki et al., 2008a] and was used to assess the global water scarcity [Hanasaki et al., 2008b]. Döll et al. [2009] modified the algorithm used by Hanasaki et al. [2006] and integrated it into the WaterGAP model to analyze the combined impacts of reservoirs and withdrawals to river flow alterations globally.

In a recent review of GHMs, Sood and Smakhtin [2015] listed three other existing GHMs have integrated reservoir operation with the natural water cycle: Water Balance Model plus (modified from HDTM 1.0 model by Wisser et al., 2010), PCR-GLOBWB [Wada et al., 2011; van Beek et al., 2011], and LPJmL [Rost et al., 2008]. The reservoir operation module in these models have been used to study the human alteration of the terrestrial water cycle, estimate the global-scale water withdrawal and irrigation demand, and assess the present and future water scarcity and water stress. Analyses of the impacts of reservoir operation on large-scale flooding (i.e. regional to global domains) are rarely conducted. This is most probably due to the limitations in the capability of GRMs integrated with the GHMs to simulate flood inundation. To the author's knowledge, there are only four published studies that used hydrodynamic models to simulate the effects of large-scale reservoirs to regional or large-scale flooding. The first two studies were motivated by the need to understand whether reservoirs can be used to mitigate flooding not only within their vicinity but throughout a huge basin or an entire region. The other two studies were conducted by the author and are included in the body of this thesis.

De Paes and Brandao [2013] used the one-dimensional CLiv hydrodynamic model to assess the capability of the Manso multipurpose reservoir to attenuate and mitigate flooding in Cuiabá, Brazil, a metropolitan area located 285km downstream of the reservoir. They found that while not all flooding can be entirely avoided through reservoir routing, Manso reservoir can be used to mitigate and reduce the frequency of extreme floods. However, a great source of uncertainty in difficulty have been found in processing the vast extent of incremental basin in between Manso reservoir and the city. Thereby, they proposed the integration of the hydrodynamic model with a hydrologic rainfall-runoff model.

Seibert, Skublics, & Ehret [2014] recognized the need to use a joint hydrologic-hydrodynamic modelling system to translate the effect of reservoir operation to its downstream and capture the complex flow in floodplains. They tested the potential for mitigating flood in the Bavarian Danube basin through the coordinated operation of its nine reservoirs. They used hydrologic and hydrodynamic models which were specifically designed and used in the Bavarian Danube. They have found that at least one of the nine reservoirs can be used for coordinated, regional flood mitigation in the basin. Surprisingly, they have also found that the use of a hydrodynamic model in their study did not significantly improve their simulations. They have found, however, that the when observed rather than simulated lateral inflow are used, hydrodynamic simulation setup clearly outperformed the hydrologic routing scheme. With this, they concluded that the advantages of the fine resolution 2D hydrodynamic model cannot be fully exploited when used with the less accurate and “afflicted with systematic errors in volume and timing” inputs from hydrologic models. They proposed a joint calibration of the hydrodynamic and hydrologic model chain.

## 2.4 GAPS AND LIMITATIONS: INTEGRATED RESERVOIR MODELLING IN LARGE SCALES

Primarily developed for analysing river flows to the ocean and calculating the water balance, none of the integrated models previously mentioned have been implemented to analyse the impacts of reservoir operation to inundation and thus, did not necessarily employ a river routing model that

considers flood dynamics. However, implementing reservoir operation models considering flood dynamics may be necessary for a more accurate simulation of human-influenced river channel flows, floodplain flows, and flood inundation. Such information are relevant for planning purposes and damage assessment.

While the past studies and existing databases are able to geo-reference dams and their reservoirs, reservoirs in models remain to be represented by virtual storages. Such representation may be sufficient for the purpose of estimating water availability. However, the other characteristics of the impounded water throughout a reservoir such as its fluctuating surface area, water level, and water velocity which may have significantly affect physical processes are ignored in current models. Such representation limits the capability of models to simulate and analyse the impacts of reservoirs to evaporation (through the exposed water surface), its interaction with infiltration, and the flow dynamics within the reservoir. The analyses of transport processes which may be beneficial for geological (e.g. sediments), ecological (e.g. species), or biogeochemical (e.g. nutrient cycling) fields may also be constrained.

## 2.5 BRIDGING GAPS THROUGH THIS DISSERTATION

Both regional to global-scale hydrodynamic modelling and integrated large-scale reservoir modelling are relatively new fields of study. Both proved to be essential tools for understanding the water cycle, especially for the purpose of managing the limited availability of water as well as the impending risks from hydrometeorological extremes. However, the advantages that could be gained from integrating the two models, i.e. hydrodynamic model with a reservoir operation module, are yet to be fully reaped. This is mainly due to the lack of physically-based models which integrate the two models for application in large domains.

This dissertation bridges this gap by exploring the potential of physically representing reservoirs and integrating their operation with a global hydrodynamic model. Hence, this dissertation will focus on model improvement and development, and their impacts on simulated surface water flows

and flood inundation. It will provide quantification of impact of reservoir operation to low water flows (drought mitigation) but the focus of discussions will be on the impacts on high water flows (flood mitigation). It will assess and analyse the strengths and weaknesses of the developed system in modelling the impacts of reservoir operation on an extreme floodplain inundation in a flood prone region. The modelling framework will also be used for assessing the combined impacts of reservoir operation and climate change. It will also tackle the important issue of local applicability by applying the modelling framework in finer to hyper-resolution. It will, in summary, lay down the foundations and set examples on how artificial reservoirs and their operation can be represented in a hydrodynamic model.

## CHAPTER HIGHLIGHTS

- The two global models used and their unique characteristics were presented
- The unique characteristics of the test river basin were discussed
- The models were shown to be applicable in the Chao Phraya River basin

### Related papers:

- Mateo, C. M. et al. (2013), A simulation study on modifying reservoir operation rules: Tradeoffs between flood mitigation and water supply, in *Considering Hydrological Change in Reservoir Planning and Management*, edited by A. Schumann (IAHS Publ. 362) pp. 33–40, IAHS Press, Wallingford, U. K.
- Mateo, C. M. et al. (2014), Assessing the impacts of reservoir operation to floodplain inundation by combining hydrological, reservoir management, and hydrodynamic models, *Water Resour. Res.*, 50, 7245–7266.

## CHAPTER 3

### Overview of models and their applicability to the test basin

*This chapter aims to build a basic understanding of the modelling tools, data set, and the river basin used in this research. The information and discussions written thereafter are essential for understanding the modelling improvements implemented in the succeeding chapters of this thesis. Two global models, H08, an integrated water resources model, and CaMa-Flood, a hydrodynamic river model are introduced. The characteristics and sources of the input data needed to drive each model are briefly discussed. The characteristics and importance of the Chao Phraya River Basin, the river basin where the results of this thesis are applied to, are presented. Lastly, the applicability of the models in the chosen river basin is discussed by presenting the simulation results obtained by the author during her master's research.*

#### 3.1 H08 INTEGRATED WATER RESOURCES MODEL

H08, a distributed global water resources model [Hanasaki et al., 2008a], is a pioneering model among several models which integrate anthropogenic interventions, such as reservoir operation, with the natural hydrologic processes. It was originally developed to assess global water availability and use in the subannual time scale. The development of the model was based on the fundamental concept of closing the water and balance energy in the land surface area.

H08 integrates six modules into a system (See Figure 3.1) – two

modules which are necessary to simulate natural hydrologic processes, the land processes and river modules, and four modules which are necessary to simulate human interventions, the reservoir operation, anthropogenic water withdrawal, crop growth, and environmental flow modules. Each module can be run separately while a coupled module exists to run all the processes in an integrated manner.

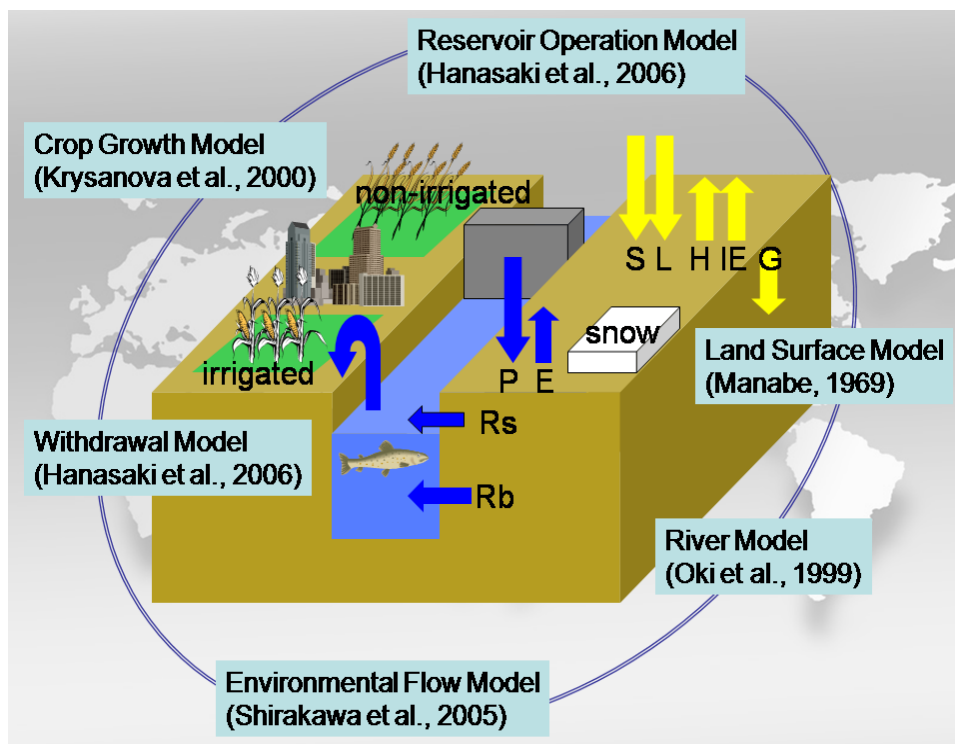


**Figure 3.1. Schematic diagram of the modules (and sources) consisting the H08 integrated water resources model.** *Figure courtesy of Dr. Naota Hanasaki.*

Three modules were used in this study – the land surface processes, river processes, and reservoir operation modules. Thus, the next sections will briefly describe each of these modules. The development, validation, and varied applications of H08 are well-documented. The model is open-source and can be freely obtained for research purposes. For more details about the model, please refer to Hanasaki et al. [2006, 2008a, 2008b] and existing H08 manuals.

### 3.1.1 H08 land surface processes module

The land surface module is based on a “leaky bucket” model which represents a single, 15 cm deep soil moisture layer for all soil and vegetation type. Unlike in the original bucket model [Manabe, 1969; Robock et al., 1995] where runoff is generated only when the bucket is filled to its capacity, the “leaky bucket” continuously drains soil moisture in the bucket. A simple subsurface runoff ( $Q_{sb}$ ) parameterization (equation 3.1) similar to the LPJ model [Gerten et al., 2004] was added to the original bucket model:

$$Q_{sb} = \frac{W_f}{\tau} \left( \frac{W}{W_f} \right)^\gamma \quad (3.1)$$

where  $W_f$  is the soil water content at field capacity (fixed at  $150 \text{ kg m}^{-2}$ ),  $\tau$  is a time constant, and  $\gamma$  is a shape parameter that sets the relationship between soil moisture and subsurface flow. The soil moisture is at field capacity when the bucket is full; it is at wilting point when the bucket is empty. Surface runoff ( $Q_s$ , equation 3.2) is generated when the soil water content ( $W$ ) exceeds the field capacity:

$$Q_s = \begin{cases} W - W_f & W_f < W \\ 0 & W \leq W_f \end{cases} \quad (3.2)$$

The soil water balance is calculated using equation 3.3:

$$\frac{dW}{dt} = \text{Rainfall} + Q_{sm} - E - Q_s - Q_{sb} \quad (3.3)$$

where  $E$  is the evaporation from surface and  $Q_{sm}$  is the snow melt rate. The snow melt is calculated using the snow water balance but because of its tropical climate, snow fall in Thailand is negligible. The calculation of evaporation (equation 3.4) was set similarly with the original bucket model. It is expressed as a function of soil moisture and potential evapotranspiration as follows:

$$E = \beta E_p(T_s) \quad (3.4)$$



where:

$$\beta = \begin{cases} 1 & 0.75W_f \leq W \\ W/0.75W_f & W < 0.75W_f \end{cases} \quad (3.5)$$

and  $E_p(T_s)$  (equation 3.6) is the potential evaporation ( $E_p$ ) at surface temperature ( $T_s$ ):

$$E_p(T_s) = \rho C_D U (q_{SAT}(T_s) - q_a) \quad (3.6)$$

In the equation above,  $\rho$  is the density of air,  $C_D$  is the bulk transfer coefficient,  $U$  is the wind speed,  $q_{SAT}(T_s)$  is the saturated specific humidity, and  $q_a$  is the specific humidity. Energy balance is calculated using equation 3.7:

$$(1 - \alpha)SW^\downarrow + LW^\downarrow = \sigma T_s^4 + lE + H + G \quad (3.7)$$

where  $\alpha$  is the surface albedo,  $SW^\downarrow$  is the downward shortwave radiation,  $LW^\downarrow$  is the downward longwave radiation,  $\sigma$  is the Stefan-Boltzmann constant,  $l$  is the latent heat,  $H$  is the sensible heat flux, and  $G$  is the soil heat flux. The sensible heat flux,  $H$ , is calculated as follows:

$$H = C_p^* \rho C_D U (T_s - T_a) \quad (3.8)$$

where  $C_p^*$  is the specific heat of air, and  $T_a$  is the air temperature. The calculation of surface albedo was set identical to that of Robock et al. [1995]. To reasonably simulate the diurnal cycle of surface temperature, the bucket model was modified. The force restore method [Bhumralkar, 1975; Deardoff, 1978] is used to calculate the soil temperature using three-hourly meteorological forcing inputs.

For a more detailed discussion about the equations used in the land surface hydrology module, please refer to Appendix B of Hanasaki et al. [2008a]. Most of the parameters as described in Hanasaki et al. [2008a] have been used except for the following parameters: soil depth,  $\tau$ ,  $\gamma$ , and  $C_D$ . The said

parameters have been calibrated for the Chao Phraya River Basin as discussed in Appendix A of this dissertation.

### 3.1.2 H08 river processes module

The Total Runoff Integrated Pathways model [TRIP; Oki and Sud, 1998], an idealized global river channel network which give directions for lateral water movement, was used to accumulate the runoff calculated by the land surface processes module and uses hydrologic routing to calculate streamflow. Virtual river elements are depicted as straight lines without any cross-sectional component that flows at a constant velocity to the downstream cell. Flow directions are inferred from digital elevation models which have been manually corrected using atlases. Water from each grid cell is assumed to flow to only one downstream grid and backflow is not considered.

The river water balance is calculated using equation 3.9:

$$\frac{dRivSto}{dt} = RivInf + Q_{tot}A - Rivout \quad (3.9)$$

where  $RivSto$  is the river storage,  $RivInf$  is the river inflow from the upstream grid,  $Q_{tot}$  is the total runoff in the grid, and  $A$  is the area of the grid, and  $RivOut$  is the river flow to the downstream grid. To calculate the river flow,  $RivOut$ , a constant speed of 0.5m/s and a constant meandering ratio of 1.4 over the distance from the calculation grid to the downstream grid are used.

### 3.1.3 H08 reservoir operation module

Using globally available reservoir information, the reservoir module applies simplistic rules on geo-referenced large ( $>10^9 \text{ m}^3$ ) reservoirs. Reservoirs are classified into two main categories based on their stated primary purpose: irrigation or other purposes. Irrigation reservoirs are operated to release water that is proportional to the water demand in the downstream reaches while other reservoirs are operated to minimize the interannual and subannual variations [Hanasaki et al., 2006]. The water demand on irrigated areas is calculated using the crop growth module. In this study, however, the default reservoir

operation rules used for global simulations were overwritten with rules that mimic that of the historical operation of the two reservoirs, Bhumibol and Sirikit.

### 3.2 CAMA-FLOOD HYDRODYNAMIC FLOOD INUNDATION MODEL

Catchment-based Macro-scale Floodplain (CaMa-Flood) model [Yamazaki et al., 2011, 2013, 2014b] is a state-of-the-art river hydrodynamic model that was developed to realistically describe river routing and floodplain inundation dynamics in the global scale. River basins are discretized at the desired spatial scale into unit-catchments which delineated from fine-resolution HydroSHEDS flow direction maps [Lehner et al., 2008] and SRTM3 digital elevation models (DEM) [Farr et al., 2007]. Each unit-catchment is assumed to have a river and floodplain storage (Figure 3.2, Table 3.1), the dimensions and characteristics of which are calculated using explicit sub-grid topography parameters derived from the fine-resolution flow direction maps and DEMs.

**Table 3.1. CaMa-Flood sub-grid parameters in Figure 3.2a [based from Yamazaki et al., 2011].**

| Symbol            | Parameter or Variable Meaning    | Unit  |
|-------------------|----------------------------------|-------|
| <i>Parameters</i> |                                  |       |
| $A_c$             | unit catchment area              | $m^2$ |
| $B$               | bank height                      | m     |
| $L$               | channel length                   | m     |
| $W$               | channel width                    | m     |
| $Z$               | surface altitude                 | m     |
| <i>Variables</i>  |                                  |       |
| $A_f$             | flooded area                     | $m^2$ |
| $D_r$             | river water depth                | m     |
| $D_f$             | floodplain water depth           | m     |
| $S$               | total water storage, $S_r + S_f$ | $m^3$ |
| $S_r$             | river channel water storage      | $m^3$ |
| $S_f$             | Floodplain water storage         | $m^3$ |

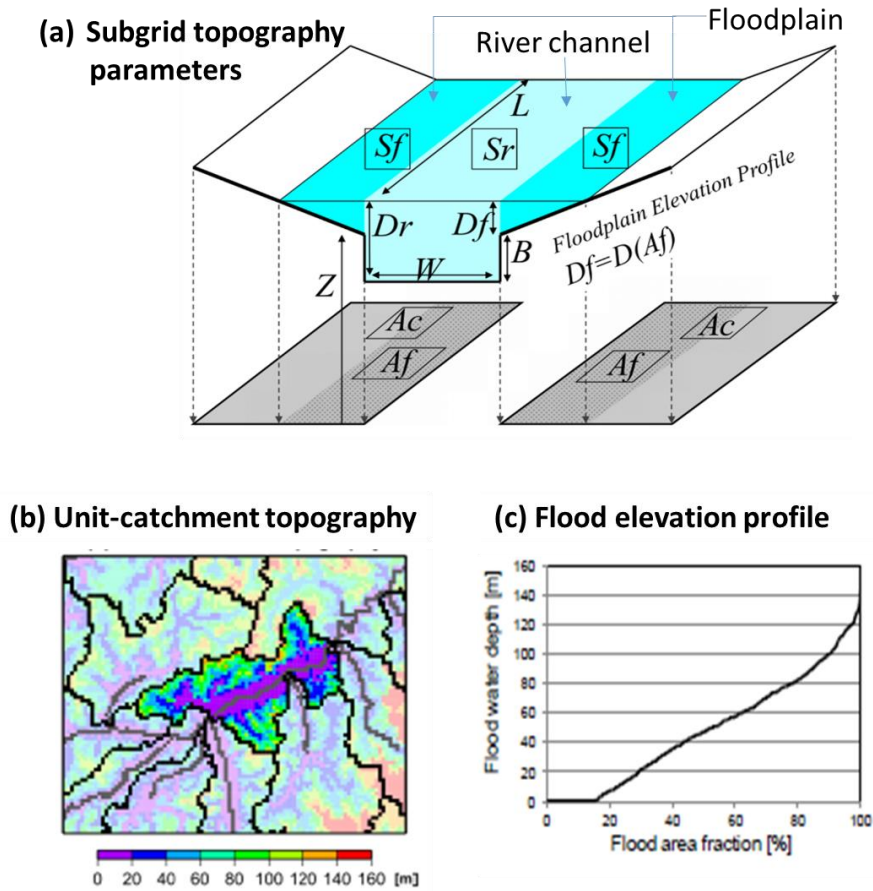


**Figure 3.2. Schematic diagrams of the subgrid topography parameterization in CaMa-Flood;** (a) River channel and floodplain sub-grid parameters. Please refer to Table 1 for definition of variables. (b) An example of unit-catchment topography where the height above the nearest river channel is shown by the background color and the river channels are shown in gray lines. (c) An example of the flood elevation profile, the cumulative distribution function (CDF) of the height above the nearest river channel. It is used to diagnose the flooded area from the flood depth [Figures modified from Yamazaki et al., 2011]

Runoff from a land surface model is used as forcing input to calculate river hydrodynamics in each unit-catchment within the river basin. Through the sub-grid river and floodplain topography representation, two prognostic variables are calculated at each unit-catchment: the volume of water impounded in river and floodplain catchments, and the river discharge. Water flux between each unit-catchment is routed along a river network map. After calculating the river discharges between unit-catchments, the water storage is updated so that water mass is conserved at each unit-catchment. From

the water storage at each time step, other variables, such as water level, inundated area, and velocity, can be diagnosed.

Throughout the development of this dissertation, CaMa-Flood has undergone several model improvements. Correspondingly, this dissertation used the latest available version of the model at the time when each numerical experiment is conducted. The distinguishing features of the model used in each chapter are shown in Table 3.2.

**Table 3.2. Distinguishing features of the CaMa-Flood version used in the chapters of this dissertation.**

| CaMa-Flood Feature         | Chapters 3 and 4                     | Chapter 5   | Chapter 6                                 |
|----------------------------|--------------------------------------|---|---|
| River network map          | Hybrid                               | Vector  | Vector                                    |
| Hydrodynamic flow equation | Diffusive wave                       | Local inertial equation                           | Local inertial equation                   |
| Flow connectivity scheme   | Single downstream connectivity (SDC) | SDC and Multi-directional downstream connectivity | Multi-directional downstream connectivity |

The earlier versions of CaMa-Flood which use the single downstream connectivity (SDC) flow scheme, and the diffusive wave equation to simulate flood flows and inundation were used in this chapter and in Chapter 4. The latest and most efficient version of CaMa-Flood which uses the multi-directional downstream connectivity (MDC) and local inertial flow equation was applied in Chapters 5 and 6 of this study.

### 3.2.1 River network map

Vector-based maps, unlike raster-based maps, discretize a land surface into unit-catchments that are not restricted to a Cartesian coordinate system [Becker and Braun, 1999]. Vector-based maps are more preferable for representing subbasin topography, and have been demonstrated to be more efficient than grid-based maps and hybrid maps [Paiva et al., 2011; Lehner & Grill, 2013; Yamazaki et al., 2013].

### 3.2.2 Hydrodynamic flow equation

The diffusive wave equation (equation 3.10), the flow equation used in the earlier versions of CaMa-Flood, is a simplification of the 1-D St. Venant shallow water flow equation. By ignoring only the acceleration and advection term, the diffusive wave equation can simulate most of the important characteristics that define shallow water flow in regional to global-scales. It is calculated by the following equation:

$$\frac{\partial D_r}{\partial x} + i_0 - i_f = 0 \quad (3.10)$$

where  $D_r$  is the river water depth,  $x$  is the distance along the river channel,  $i_0$  is the riverbed slope, and  $i_f$  is the friction slope. Flow velocity,  $v$ , can be derived and simplified as:

$$v = \frac{i_{sf c}}{|i_{sf c}|} n^{-1} i_{sf c}^{1/2} H^{2/3} \quad (3.11)$$

where  $i_{sf c}$  is the water surface slope,  $n$  is the Manning's roughness coefficient (assumed to be constant in this thesis), and  $H$  is the hydraulic radius. By taking into account the water surface slope, the diffusive wave equation can take into account the backwater flow.

Although the diffusive wave equation was found to be sufficient for most of large to global scale simulation of hydrodynamics [e.g. Yamazaki et al., 2011], it requires smaller time steps when calculating at areas with large water depth and small water surface slope. A more computationally efficient equation, the local inertial equation, was recently proposed by Bates et al. [2010] which allows stable calculation of flow at similar conditions using higher time steps.

The local inertial equation, was then recently implemented in CaMa-Flood to calculate river discharge from each upstream to its downstream unit-catchment [Yamazaki et al., 2013]. It was found that the local inertial equation implemented in CaMa-Flood can result to a 300% increase in computational efficiency [Yamazaki et al., 2013]. By neglecting only the advection term of the 1-D St. Venant

equation, the local inertial equation can explicitly represent backwater effect and allows a more complete representation of shallow water physics. According to Bates et al [2010], the local inertial equation can be discretized and modified to equation 3.12:

$$Q^{t+\Delta t} = \frac{Q^t - \Delta t g A S}{\left(1 + \frac{\Delta t g n^2 |Q^t|}{A h^{4/3}}\right)} \quad (3.12)$$

where  $Q^{t+\Delta t}$  is the discharge between times  $t$  and  $t + \Delta t$ ,  $Q^t$  is the discharge at the previous time step,  $g$  is the gravitational acceleration ( $\text{ms}^{-2}$ ),  $A$  is the flow cross-sectional area ( $\text{m}^2$ ),  $S$  is the water surface slope between the upstream and downstream unit catchments,  $n$  is the Manning's friction coefficient ( $\text{m}^{-1/3} \text{s}$ ), and  $h$  is the flow depth (m).

### 3.2.3 Flow connectivity scheme

Regional to global river models typically route river flows following a “one downstream grid” or single downstream connectivity (SDC) assumption. While the assumption is sufficient in simulating flows in main river channels, it cannot simulate the more complex, diverging flows common in deltas and low-lying floodplains.

The latest version of CaMa-Flood [Yamazaki, Sato et al., 2014] developed a new multi-directional downstream flow scheme to overrule the simplified SDC assumption. Originally intended to simulate the bifurcation processes in deltas, the new scheme is referred to as “bifurcation scheme” and the pathways which allow multi-directional downstream flow as “bifurcation channels” in Yamazaki, Sato et al. [2014]. An algorithm which identifies and represents bifurcation channels in a new river network map had been developed. Bifurcation channels, defined as channels connecting two unit-catchments which do not have upstream-downstream relationships in a river network map, are classified as either “overland pathways” (green lines in Figure 3.3a) or “river pathways” (red lines in Figure 3.3a). Flow routes in floodplains during flooding are represented by overland pathways, while bifurcated river channels with persistent bifurcation flow are represented by river pathways.



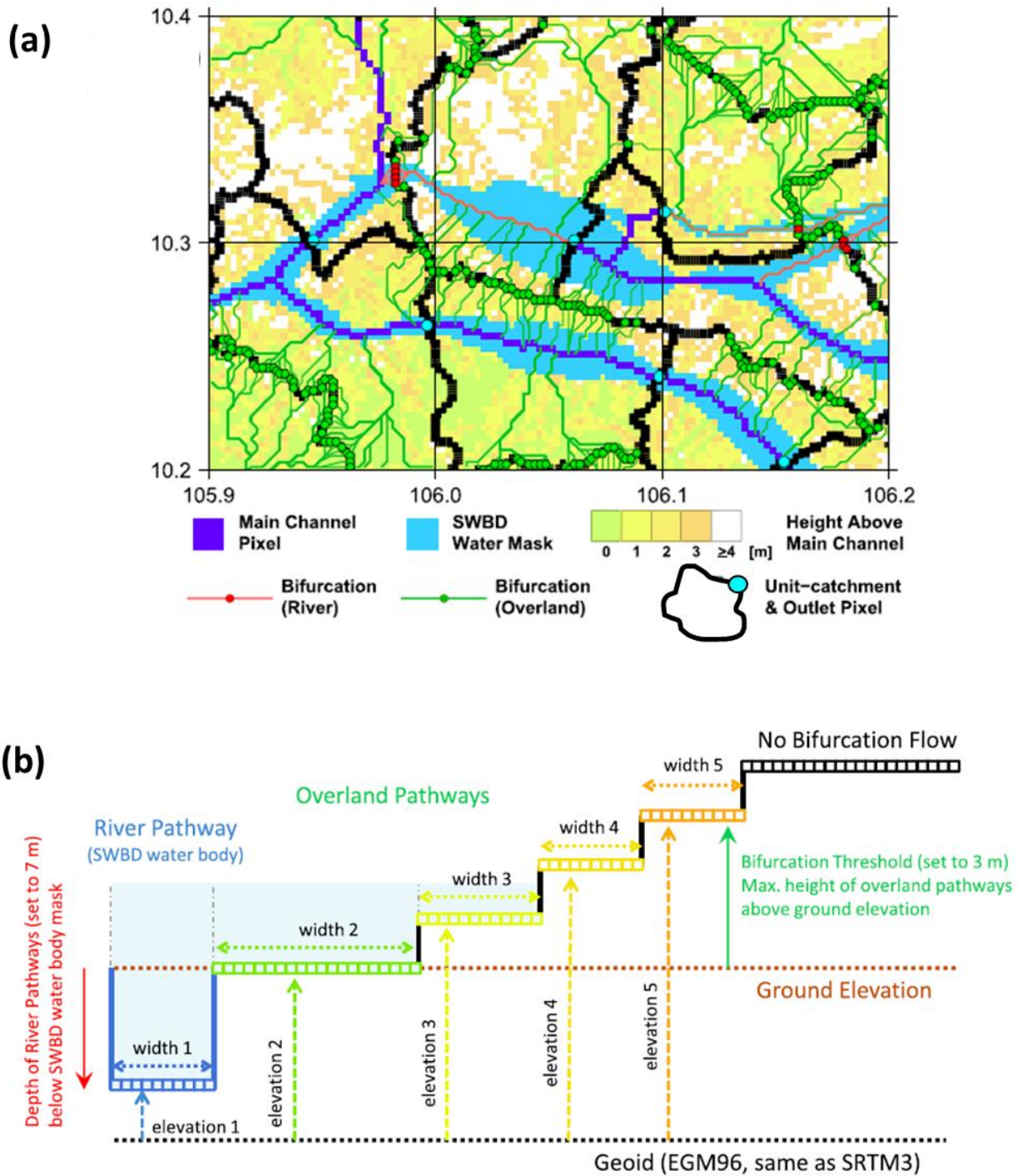


**Figure 3.3. Schematic diagrams of the multi-directional downstream connectivity in CaMa-Flood;** (a) A sample of sub-grid topography and multi-directional downstream connectivity (MDC) pathways. Overland pathways are represented by the green channels while river pathways are represented by the red channels. (b) Representation of MDC channel cross section after aggregating MDC pathways with the same elevations. MDC channel's elevations and effective widths are indicated by the vectors “elevation 1–5” and “width 1–5” [Figures 3.3a (sampled from Mekong River) and 3.3b modified from Yamazaki, Sato et al., 2014].



By defining bifurcation channels as mentioned, flows in braided streams, artificial open canals, diversion channels, and other water pathways that can be detected or inferred from water surface in satellite images can be represented in flood simulations. Hence, the bifurcation scheme is not restricted to representing flow processes in bifurcating deltas and bifurcation channels are not restricted to representing the flow pathways in streams that bifurcate. Generally, the new scheme enables the simulation of an important process in flood propagation and inundation – the Multi-directional Downstream Connectivity (MDC) between grid cells. Therefore, to avoid misconceptions about the function of the scheme, this dissertation will refer to the new scheme as “MDC scheme.” For simplicity, bifurcation channels and pathways will hereby be referred to as “MDC channels” or “MDC pathways.”

Six parameters are used to represent each MDC channel: MDC channel elevation, channel width, channel length, roughness coefficient, upstream unit-catchment ID, and downstream unit-catchment ID. Flow in an MDC channel occurs when the elevation of the channel is lower than the water surface elevation in either upstream or downstream unit-catchment (see schematic diagram in Figure 3.3b). MDC channel flows are also calculated using the local inertial equation. Calculation is implemented after the calculation of river discharge in main channels [Yamazaki, Sato et al., 2014].

The development of CaMa-Flood model is well-documented and its performance, well-validated. For more details about the model, please refer to Yamazaki et al., [2011, 2013], Yamazaki, Lee et al. [2012], Yamazaki, O’Loughlin et al. [2014], Yamazaki, Sato et al. [2014], and the existing CaMa-Flood manuals.

### 3.3 CHAO PHRAYA RIVER BASIN

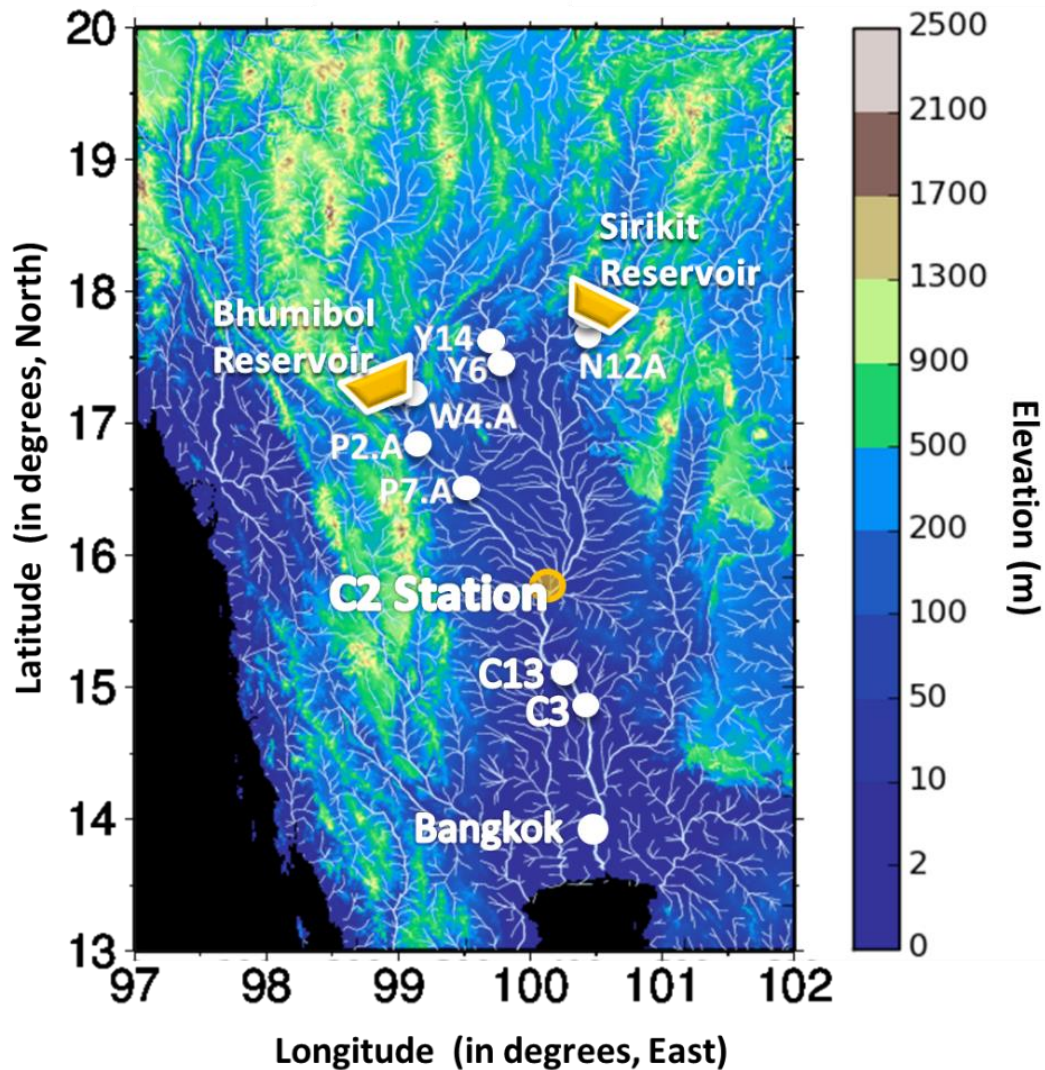


**Figure 3.4.** The Chao Phraya River Basin model domain, elevation map (shown in 1km resolution), river network, and validation stations. The location of the station used for calibration is marked with an orange dot. Validation points are marked with white dots. Dam locations are marked with orange trapezoids.

The Chao Phraya River Basin (Figure 3.4), the largest river basin in Thailand, has eight sub basins with a total catchment area of approximately 158,000 km<sup>2</sup>, a huge area that amounts to more than a third of the total area of Thailand. It is home to about 23 million people (about 40% of the population), 8

million of whom live at the capital city of Bangkok [1996 estimates, ONWRC, 2003]. Thus, it is deemed to be the largest and most important geographical unit in Thailand [Sripong et al., 2000].

The four main sub catchments in the upstream watershed of the basin originate from the northern mountain system which flow down at a point of confluence in the middle of the basin in Nakhon Sawan. The middle region of the basin is a floodplain with a relatively flat slope of approximately 1/15,000 and the lowermost region is a delta which empties into the Gulf of Thailand. These geographic characteristics make the region highly prone and vulnerable to flood inundation. The region is equally susceptible to droughts – in the past, records of water shortages led to over pumping of the groundwater which led to subsequent land subsidence [ONWRC, 2003].

In order to manage water supply and reduce flooding in the basin, two huge reservoirs, Bhumibol (drainage area: 26,400 km<sup>2</sup>) and Sirikit (drainage area: 13,130 km<sup>2</sup>), which have a storage capacity of 23 billion m<sup>3</sup> in total were built in the Ping and Nan Rivers, respectively. A high seasonal variation can be observed in the mean monthly rainfall and inflows (Figure 3.5) in the catchment of the two reservoirs. Reservoir operation during the rainy season critically affects both flood mitigation and the availability of water for the subsequent dry season. Although the general trend in seasonal variations in precipitation within the basin is known, the total volume of precipitation and inflows to the reservoirs during the rainy season are very difficult to predict several months in advance. Thus, long-term reservoir operation policy that is adaptive to annual and seasonal variations in precipitation is preferred in Bhumibol and Sirikit Reservoirs.

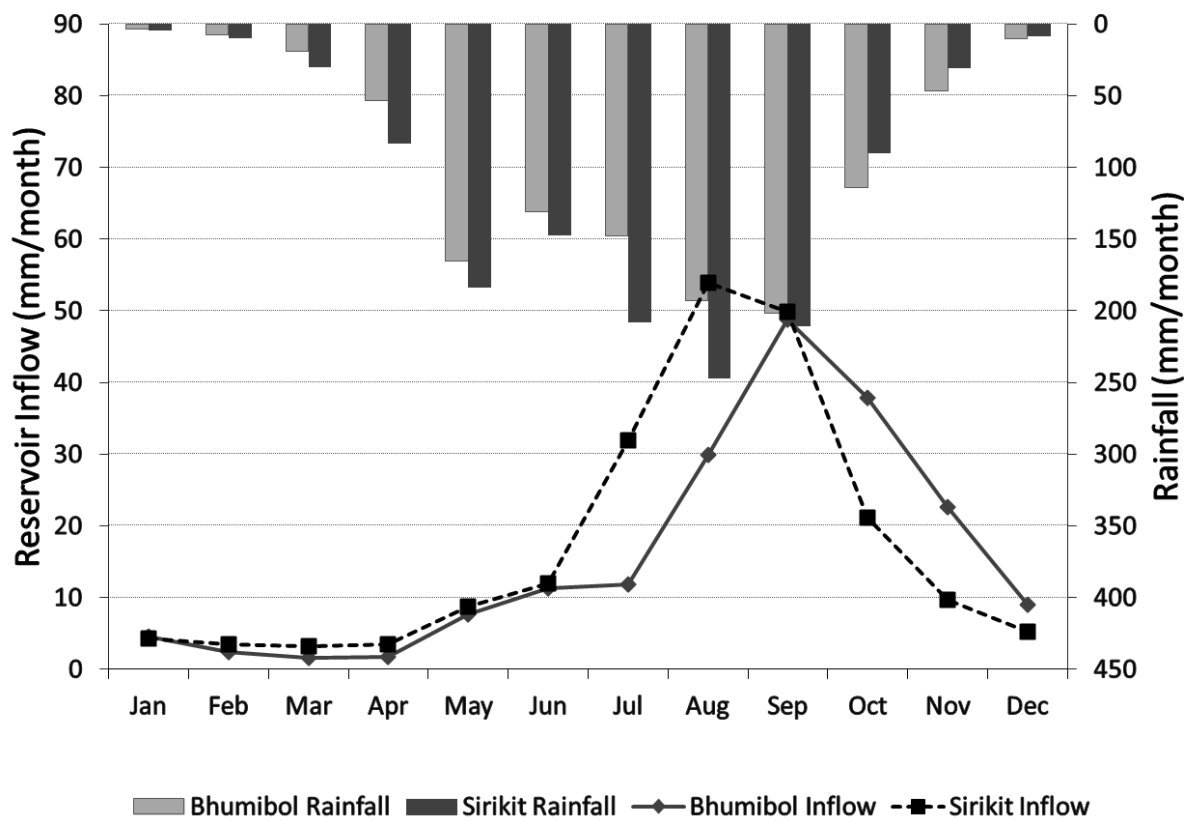


Figure 3.5. Monthly basin averaged rainfall (as calculated from the reanalyzed observed rainfall forcing data) and observed reservoir inflows at Bhumibol and Sirikit Reservoirs from 1981-2004.

### 3.4 INPUT DATA AND SIMULATION SETUP

In this chapter, simulation was conducted on a daily time scale (shorter than 1-day in CaMa-Flood, with the time step automatically adjusted by the CFL condition) at a spatial resolution of  $5' \times 5'$  longitudinal and latitudinal grids, in domains from  $97^\circ\text{E}$  to  $102^\circ\text{E}$  longitude and  $13^\circ\text{N}$  to  $20^\circ\text{N}$  latitude in H08 and  $97.5^\circ\text{E}$  to  $102^\circ\text{E}$  longitude and  $13^\circ\text{N}$  to  $20^\circ\text{N}$  latitude in CaMa-Flood. The meteorological inputs for the simulation periods 1981-2004 and 2010-2011 are shown in Table 3.3.

**Table 3.3. Meteorological input data used to run H08.**

| Meteorological input | 1981-2004 source  | 2010-2011 source                    |
|----------------------|---|-------------------------------------|
| Surface Air Pressure | GAME-T2, 2011   | Yoshimura et al., 2008 (forecasted) |
| Wind Speed           | GAME-T2, 2011   | Yoshimura et al., 2008 (forecasted) |
| Specific Humidity    | Hirabayashi et al., 2008  | Yoshimura et al., 2008 (forecasted) |
| Shortwave Radiation  | Hirabayashi et al., 2008  | Yoshimura et al., 2008 (forecasted) |
| Longwave Radiation   | Hirabayashi et al., 2008  | Yoshimura et al., 2008 (forecasted) |
| Temperature          | Hirabayashi et al., 2008  | Yoshimura et al., 2008 (forecasted) |
| Surface Albedo       | Interpolated from GSWP2   | Yoshimura et al., 2008 (forecasted) |
| Precipitation        | Reanalyzed data by Prof. Kenji Tanaka et al. from observed precipitation data from the Royal Irrigation Department (RID) and Thai Meteorological Department (TMD) |                                     |

### 3.5 APPLICABILITY OF THE MODELS IN THE CHAO PHRAYA RIVER BASIN

Due to its geographical characteristics, a large portion of the Chao Phraya River Basin is prone to inundation. In order to consider the effect of floodplain inundation processes to streamflow, CaMa-Flood was used to substitute the TRIP river routing model originally used within the H08 model. The combination of the two models, hereafter called H08-CaMa model, satisfies the model characteristics necessary for assessing the impacts of reservoir operation on flood inundation: 1) can reasonably simulate the natural hydrologic processes; 2) can model reservoir operation; and 3) can explicitly simulate inundation.

In this section, the capability of the combined H08-CaMa model in simulating the flows without reservoir operation, hereby called *natural flows*, in the Chao Phraya River Basin will be discussed. The natural flows throughout the basin can be simulated either by using the land processes and river processes module in H08 model or by using the H08-CaMa model (see Figure 3.6). Here, the capability of the combined H08-CaMa model to simulate the natural flow is compared with the plain H08 model (simulation results are hereby called referred to as *Nat – H08-CaMa* and *Nat – H08 Plain*, respectively).

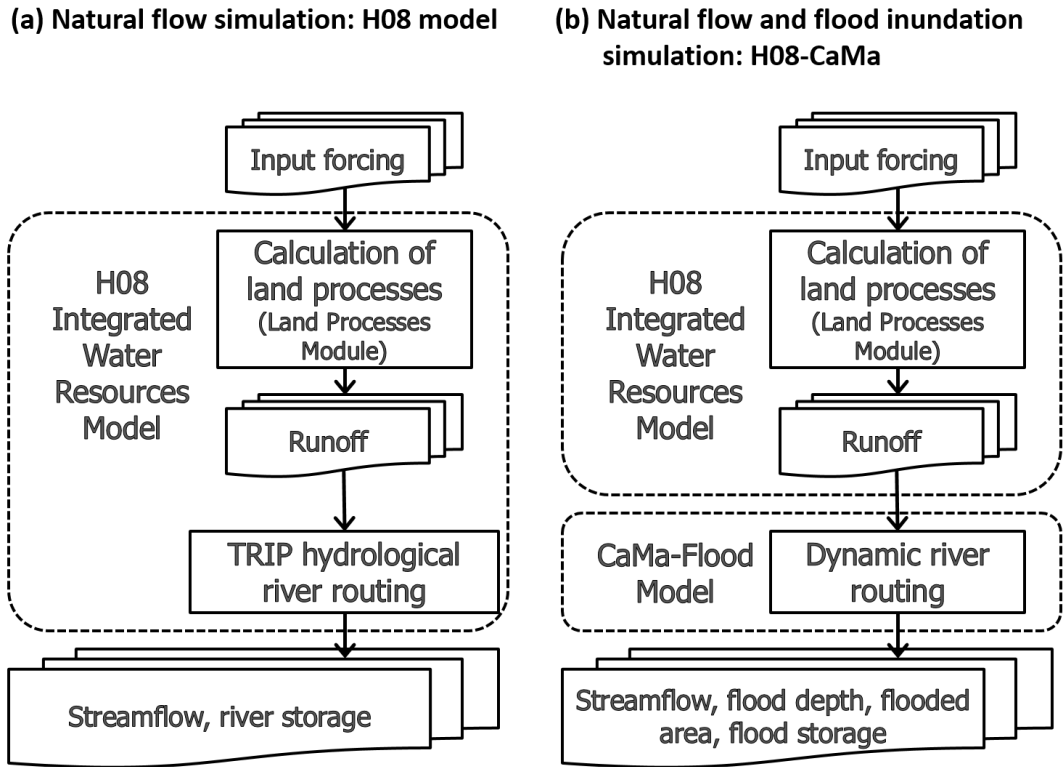


**Figure 3.6** Modelling framework for simulating natural flows (a) using H08 model (Nat – H08 Plain), and (b) using H08-CaMa model (Nat – H08-CaMa)

The daily and monthly discharge hydrographs simulated by the two model setups are compared with those of the naturalized observed at Nakhon Sawan or C2 Station (station used for calibration) in Figure 3.6. The methodology used for calibration is briefly discussed in Appendix A. The naturalized observed discharge at C2 Station was computed by deducting the effects of reservoir operation upstream of the station using equation 3.13:

$$ND_{C2} = OD_{C2} + [I + P - R - S]_{Bhumibol} + [I + P - R - S]_{Sirikit} \quad (3.13)$$

where  $ND$  is naturalized discharge,  $OD$  is observed discharge,  $I$  is reservoir inflow,  $P$  is water pumped into the reservoir,  $R$  is reservoir release, and  $S$  is water released through the spillway. The observed discharge data were obtained from the Royal Irrigation Department (RID) of Thailand. The reservoir



operation data of the Bhumibol Reservoir and Sirikit Reservoir stations were obtained from the Electricity Generating Authority of Thailand (EGAT).

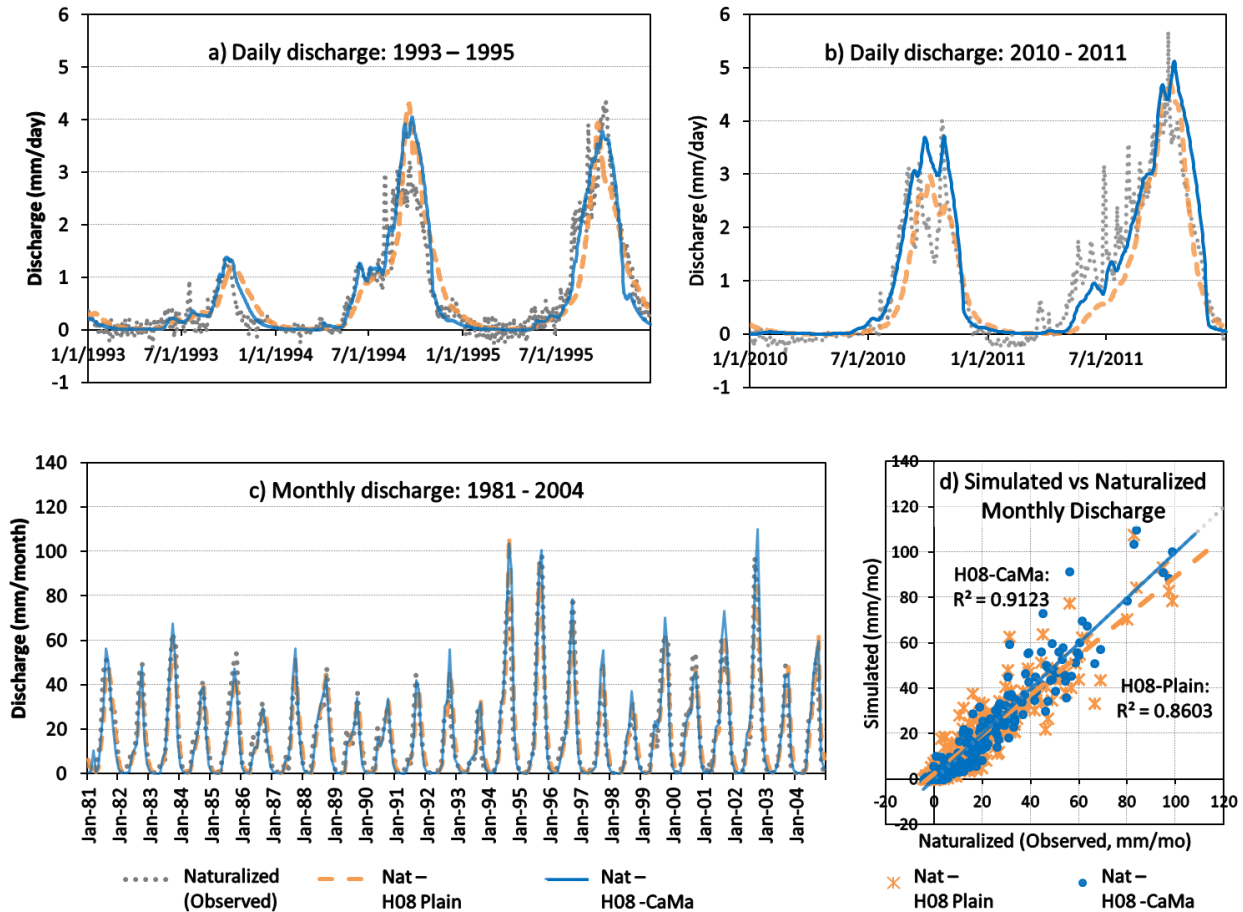


**Figure 3.7.** Comparison between natural flow simulation results using plain H08 model (*Nat – H08 Plain*), combined H08 and CaMa-Flood model (*Nat – H08-CaMa*), and naturalized observed discharge. (a) daily discharge hydrograph from 1993-1995; (b) daily discharge hydrograph from 2010-2011; (c) monthly discharge hydrograph from 1981-2004; and (d) scatter plot comparing the simulated monthly discharges with that of the naturalized observed, orange dashed and blue lines indicate the trend lines for Nat-H08 Plain and Nat-H08-CaMa, respectively. Please refer to Table 3.4 for performance statistics related to this figure.

Within the study period 1981-2004, the worst drought event occurred in 1993 while the worst flood event occurred in 1995 [based on cumulative discharge at C2 Station in Komori et al., 2012]. The flooding in 2011 was the worst in the history of Thailand. The simulated natural flows from 1993-1995

and 2010-2011, respectively shown in Figures 3.7a and 3.7b, demonstrate the reliability of the models in simulating the natural processes within the river basin during extreme events.

Although both *Nat – H08 Plain* and *Nat – H08-CaMa* seem to simulate the natural daily discharge very well, a significant improvement in the magnitude and timing of peak discharge were obtained using the combined H08-CaMa model (Table 3.3). As compared with *Nat – H08 Plain* simulations, the range of percent error in peak magnitude was reduced from [-26%, 31%] to [-14%, 19%] and the maximum absolute value of the error in peak timing (expressed in number of days) was reduced from 18 days to just 9 days using *Nat – H08-CaMa*.

Very good correspondence between the two simulated monthly discharge hydrographs and the observed can be seen in Figures 3.7c and 3.7d. The simulated discharge hydrographs using *Nat – H08-CaMa* also outperform *Nat – H08 Plain* in terms of correlation of determination,  $R^2$ , and Nash-Sutcliffe Efficiency coefficient (NSE-coefficient, Table 3.4). These statistical results indicate that although the plain H08 can be calibrated to simulate the naturalized observed discharge very well, combining the model with CaMa-Flood could further improve the simulation results by improving the simulation of the shape and fluctuations of the hydrograph, peak magnitude, and peak timing.

The applicability of the model to the basin is further validated by comparing the simulated streamflow with the naturalized observed flows at nine other gauge stations throughout the basin. These gauge stations are marked by white circular (hydrologic stations) and orange trapezoidal (dam) markers (Figure 3.4). Gauging stations within the basin with a catchment area greater than 10,000 km<sup>2</sup> and observation years greater than 10 have been chosen for the validation. The gauge stations which are heavily affected by anthropogenic interventions other than reservoirs, i.e. big water canals, have been excluded from the analysis because of the lack of accessible data which are needed to consider the effect of water diversion in the streamflow.



**Table 3.4. Performance statistics related to the natural discharge simulation using plain H08 and combined H08-CaMa model\*.**

| Setting                          | Daily discharge             |                             |                              |                             |                              | Daily discharge               |                               |                               |                               |                               | Monthly<br>NSE-<br>coefficient<br>(1981-2004) |
|----------------------------------|-----------------------------|-----------------------------|------------------------------|-----------------------------|------------------------------|-------------------------------|-------------------------------|-------------------------------|-------------------------------|-------------------------------|---|
|                                  | Peak Magnitude (mm)         |                             |                              |                             |                              | Peak Timing (date: month/day) |                               |                               |                               |                               |   |
|                                  | 1993                        | 1994                        | 1995                         | 2010                        | 2011                         | 1993                          | 1994                          | 1995                          | 2010                          | 2011                          |   |
| Naturalized<br>Observed          | 1.41                        | 3.27                        | 4.40                         | 4.02                        | 5.69                         | 10/03                         | 09/22                         | 10/06                         | 10/22                         | 10/04                         | <i>n.a.</i>                                   |
| <i>Nat –</i><br><i>H08 Plain</i> | 1.19<br>(-16%)              | 4.30<br>(31%)               | <b>3.93</b><br><b>(-11%)</b> | 2.96<br>(-26%)              | 4.59<br>(-19%)               | 10/10<br>(+7 d)               | 09/17<br>(-5 d)               | 09/20<br>(-16 d)              | 10/04<br>(-18 d)              | <b>09/29</b><br><b>(-5 d)</b> | 80.72%  |
| <i>Nat –</i><br><i>H08-CaMa</i>  | <b>1.38</b><br><b>(-2%)</b> | <b>4.06</b><br><b>(19%)</b> | 3.78<br>(-14%)               | <b>3.72</b><br><b>(-7%)</b> | <b>5.12</b><br><b>(-10%)</b> | <b>09/29</b><br><b>(-4 d)</b> | <b>09/23</b><br><b>(+1 d)</b> | <b>09/29</b><br><b>(+7 d)</b> | <b>10/25</b><br><b>(+3 d)</b> | 10/13<br>(+9 d)               | <b>90.43%</b>                                 |

\* The relative errors with respect to the observed are indicated inside parentheses (percent error and number of days for peak magnitude and peak timing (in days), respectively). Values closer to the naturalized observed are shown in bold fonts. *Please refer to Figure 3.7 for the corresponding hydrographs.*

Daily natural flows are shown (see Figure 3.8) from 1993 to 1995 at the seven validation stations, and from 2002-2004 at station N67 because data collection at this station only began in the middle of 1997. Hydrographs in station Y14 are not shown in the figure because they are just very similar to that of Y6 as a result of the geographical proximity of the two stations. It was found that the hydrographs at eight out of nine stations corresponded well with their respective naturalized observed discharge, with their monthly discharge NSE-coefficients ranging from 69.5% to 87.0%. However, a negative NSE-coefficient was obtained at station W4.A which was reported to be a floodplain area by RID officials. The difficulty to measure discharge in a floodplain accurately could have led to several uncertainties. At this point, it can be said that the H08-CaMa model can effectively simulate the natural flows in the Chao Phraya River Basin.

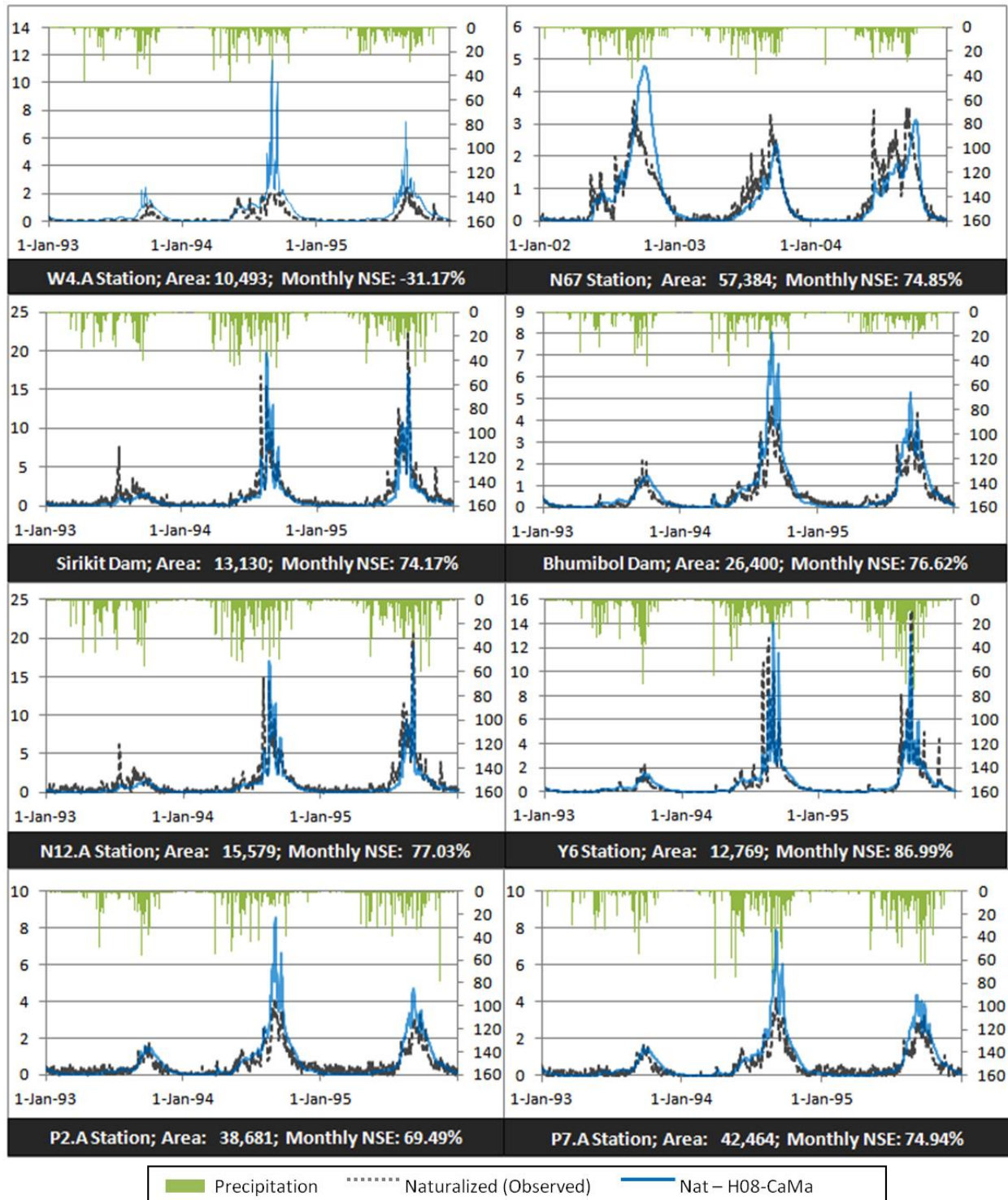


**Figure 3.8. Daily natural hydrographs (in mm/day) at the validation stations.** Simulated natural flows in Bhumibol and Sirikit reservoirs are compared with inflows in the respective reservoirs while those in the rest of the stations are compared with naturalized observed flows; daily natural flow values are shown on the left vertical axis; daily precipitation values are shown on the right vertical axis.

## CHAPTER HIGHLIGHTS

- A new reservoir operation algorithm that can represent interannual and seasonal variations in operation was developed
- Improvements in reservoir operation schemes were proposed and assessed
- The combined impacts of reservoir operation and climate change in the near and far future were assessed

### Related publications:

- Mateo, C. M. et al. (2014a), Modeling the impacts of climate change to reservoir operation and flood inundation in Chao Phraya River Basin, *Proceedings of the 7th International Scientific Conference on the Global Water and Energy Cycle (GEWEX 2014)*, 14-17 July 2014, The Hague, Netherlands.
- Mateo, C. M. et al. (2014b), Assessing the impacts of reservoir operation to floodplain inundation by combining hydrological, reservoir management, and hydrodynamic models, *Water Resour. Res.*, 50, 7245–7266.

# CHAPTER 4

## Improved representation of reservoir operation in the combined H08-CaMa Flood model

*In the previous chapter, the models used in this thesis are introduced and their applicability in simulating the natural flows in the Chao Phraya River Basin was shown. In this chapter, the inclusion of human impacts, particularly reservoir operation, in the modelling framework will be discussed. A new algorithm that can adequately simulate the operation of Bhumibol and Sirikit reservoirs and the corresponding modelling framework used for simulating the impacts of the two reservoirs to flood inundation will be introduced. The utility of the modelling framework in (1) simulating the 2011 Thai flood, (2) proposing and assessing alternative reservoir operation schemes, and (3) assessing the combined impacts of reservoir operation and climate change to future water availability and flood extremes will be demonstrated.*

### 4.1 INTRODUCTION: THE 2011 THAI FLOOD AND THE IMPORTANCE OF RESERVOIR OPERATION

In 2011, massive flooding occurred in Thailand from mid-May to December which is currently ranked as the worst flood event from 1900 to 2012, worldwide, in terms of economic losses [EM-DAT, 2012]. It has caused immense damages which amount to about 1.43 trillion Baht [World Bank, GFDRR, 2012]. To date, the Thailand flood is said to be the most economically damaging flood in history, both in overall

losses and insured losses [Swiss Re, 2012; EM-DAT, 2013; Munich RE, 2013]. The extent of the damages due to this flood event affected not only Thailand but the global supply chain of several industries as well, particularly the computer and automotive industries [Chongvilaivan, 2012; Swiss Re, 2012].

The global extent of the damages have prompted several studies which aim to understand the nature of the 2011 Thai floods, particularly in the Chao Phraya River Basin [e.g. Kotsuki & Tanaka, 2013; Yokoo et al., 2014]. Rakwatin et al. [2013] estimated the flood area and volume during the flood using multi-temporal remote-sensing data and digital elevation model. Komori et al. [2012] reported that the disaster is mainly attributable to the occurrences of several intense rainfalls. The river basin is relatively very flat which makes it prone to long-term flood inundation. They argue that although a significant amount of 10 billion  $\text{m}^3$  (approximately two-thirds of the total flood volume) of water had been stored in the two biggest reservoirs in the basin, if water in the early rainy season (May-July) had been released instead of stored, an additional 1 billion  $\text{m}^3$  may have been stored in each of the two reservoirs during the heavy rainfall season (September). Similarly, Oldenborgh et al. [2012] ascribed the 2011 Thai flood to heavy rainfalls which are not yet attributable to climate change; they stressed the importance of non-meteorological factors such as reservoir management in setting the scale of the disaster. Other studies in the past also suggest that the two largest reservoirs in the basin, Bhumibol and Sirikit, significantly affect the hydrologic regime in the Chao Phraya River Basin [Tebakari et al., 2012; Komori et al., 2013]. The storage capacity of the two reservoirs ( $23 \times 10^9 \text{ m}^3$  in total) can be used to temporarily store flood waters and manage the high seasonal variability and availability of water.

Despite these findings, the impact of operation of the two largest reservoirs to flood inundation in the Chao Phraya River Basin is relatively unexplored. Although several reservoir modeling studies have been previously conducted in Thailand [e.g. Tospornsampan et al., 2005a and 2005b; Suiadee et al., 2007; Pinthong et al., 2009], most have mainly focused on optimizing reservoir operation in relatively

smaller-scale catchments and reservoirs in Thailand. Typically evaluated based on reservoir storages, none of these previous studies have examined and discussed the impacts of reservoir operation neither to an entire river basin nor to flood inundation. Aside from this research, only Wichakul et al. [2013a, 2013b] have incorporated the two large reservoirs in analyzing regulated flows in the 2011 flood in Chao Phraya River Basin. Although they used flood routing models in their analyses, they have not evaluated the impacts of the two reservoirs to flood inundation features such as flooded area and flood volume. A gap in assessing the impacts of large scale reservoirs to the flood inundation in Chao Phraya River Basin still exists.

To bridge this gap, an integrated model which could explicitly simulate the impacts of the operation of the two huge reservoirs to the spatiotemporal aspects of inundation has been developed in this study. The development of an algorithm to represent the operation of the two reservoirs in the H08-CaMa model is presented in the next section. The advantages of using the model in (1) simulating the 2011 Thai flood flows and inundation, (2) proposing and assessing alternative reservoir operation rules to mitigate floods, and (3) assessing the combined impacts of climate change and reservoir operation in the near and far future are demonstrated in sections 4.3, 4.4, and 4.5, respectively.

Several parts of this chapter have already been published and peer-reviewed. Sections 4.1 to 4.4 are based on results and discussions written in Mateo et al. [2013, 2014b]. Preliminary results of section 4.5 have been presented and included in the proceedings of an international conference [see Mateo et al., 2014a] while the latest results presented in this chapter will be submitted for journal publication.

## 4.2 REPRESENTATION OF RESERVOIR OPERATION IN H08-CaMa MODEL

The modelling framework for simulating natural flows using H08-CaMa had already been discussed in the previous chapter. In this section, the development of algorithms to adequately represent reservoir operation and the process of its integration in the H08-CaMa model will be discussed.

#### 4.2.1 Combined H08-CaMa Flood model with reservoir operation

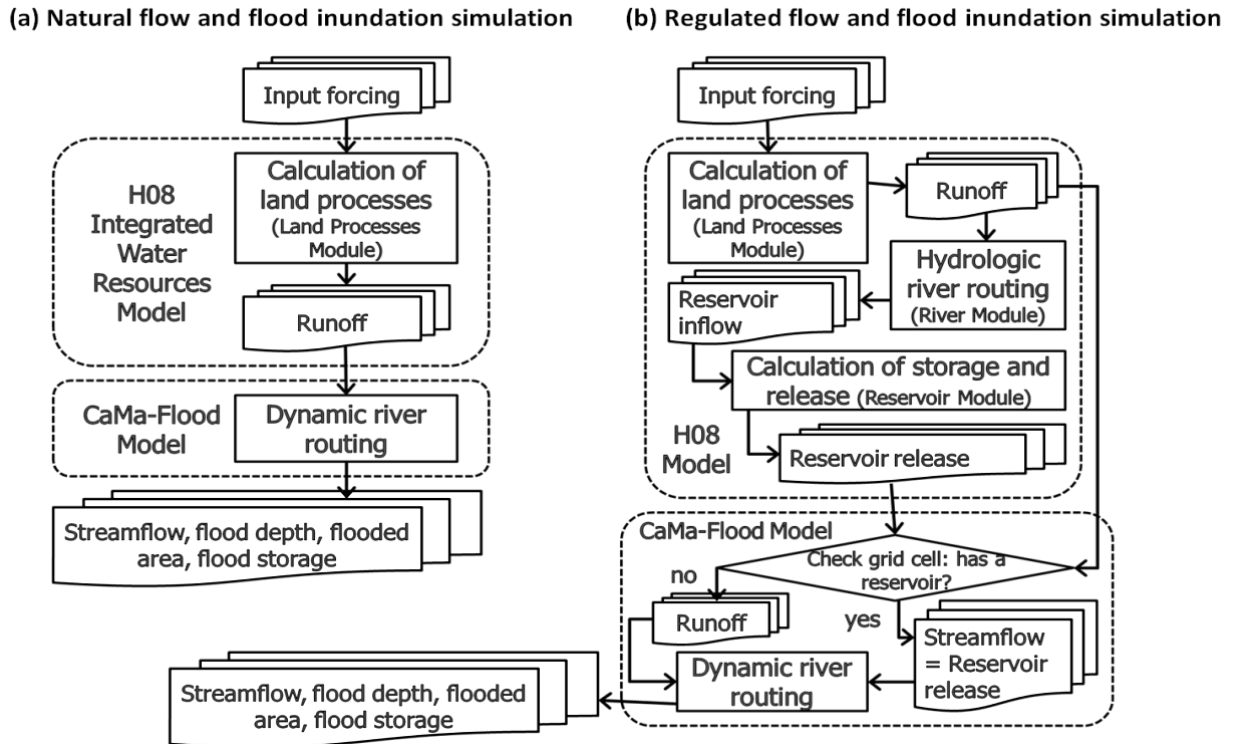


**Figure 4.1. Simulation process diagrams of the combined H08 Integrated Water Resources Model and CaMa-Flood River Routing Model.** (a) Without reservoir operation, i.e. natural flows, and (b) with reservoir operation, i.e. regulated flows [Mateo et al., 2014b]

For reference and clarity of discussion, the process diagram for simulating natural flows (Figure 4.1a, Figure 3.5b in the previous chapter) is contrasted with the process diagram used in simulating discharge considering the impacts of reservoir operation (Figure 4.1b). For brevity, simulated discharge considering the effects of reservoir operation is hereby referred to as *regulated flow*.

In simulating the natural flows, the runoff calculated by the land surface processes module of H08 was used as input to the CaMa-Flood model. In simulating the regulated flows, algorithms representing reservoir operation rules in Bhumibol and Sirikit Reservoirs were encoded into the reservoir module of H08 model. The impacts of operation of other existing reservoirs in the basin were assumed to be negligible because their storage capacities are significantly smaller relative to those of the Bhumibol



and Sirikit Reservoirs. The integrated land surface, river, and reservoir operation modules of H08 model were used to simulate the inflows to and outflows from the two reservoirs. In CaMa-Flood model, boundary conditions have been set at the grid cell locations of Bhumibol and Sirikit reservoirs. The simulated natural flows calculated in these grid cell locations were replaced with the respective reservoir outflows calculated using the integrated modules of H08 model. The streamflow in grid cells other than those of Bhumibol and Sirikit Reservoirs were calculated similar to that of the natural condition. By using this modelling framework, the impacts of modified reservoir operation rules to the availability of water as well as inundation within a river basin can be explicitly analysed.

#### 4.2.2 Development of algorithms to represent the historical reservoir operation

Operation of the Bhumibol and Sirikit reservoirs is governed by upper and lower rule curves as shown in Figure 4.2. These rule curves have been set for each dam based on inflows, storage, and dam operations in the past. The reservoirs are operated such that water storage at any time is within the two guide curves and the irrigation and water supply demands downstream are met. However, as can be seen in Figure 4.2, the water storage sometimes go beyond the two guide curves. Such occurrences can be attributed to natural causes such as the flood year of 2011 and the drought year of 2010, while some were due to decisions made by the reservoir operation managers. Two sets of guide curves, indicated by filled and unfilled markers, can be seen in the figure, indicating a change in the operation rules. The guide curves have been adjusted after the occurrence of the 2011 Thai flood to prevent the occurrence of extreme floods in the future.

Characterizing the historical reservoir operation of the two reservoirs is important in developing a reservoir operation algorithm that mimics their actual operation. As shown in Figure 4.2, there are two distinguishable features of the historical operation of Bhumibol and Sirikit Reservoirs: (1) seasonal variation in reservoir outflows is high, and (2) two storage guide curves are used. Representation of

the seasonal variations in reservoir outflows is necessary to simulate the high flows during heavy rainfall season. Representation of the upper and lower storage guide curves which serve as storage targets or limits can critically affect the simulated volume of water stored in the reservoirs.

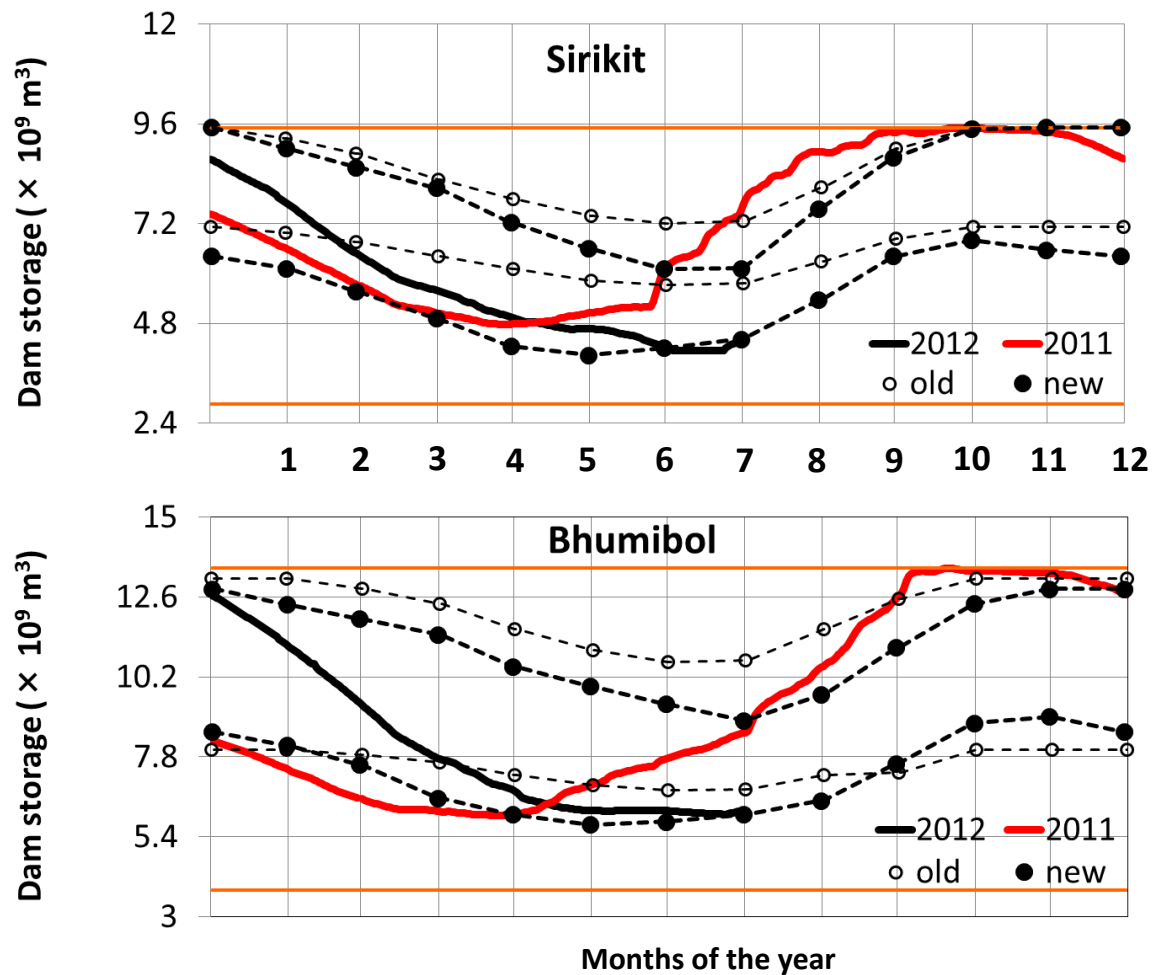


**Figure 4.2** Illustration of the upper and lower guide curves and the actual reservoir operation of the Sirikit and Bhumibol Reservoir. The lines with unfilled, circular markers were used as guides before and during the 2011 flood. The lines with filled markers are the revised rule curves to prioritize flood mitigation after the 2011 flood.

*Illustration courtesy of the Thai Royal Irrigation Department.*



In order to represent these two features in the H08 reservoir operation module, the generic algorithms used for global simulation have to be modified. The following parameters were included in the reservoir operation algorithm (see Figure 4.3): dry season release ( $R_d$  in  $\text{m}^3/\text{s}$ ), wet season release ( $R_w$  in  $\text{m}^3/\text{s}$ ), day when dry season ends ( $M_d$  in day of the year), target storage limit level ( $K_o \cdot C$ , in  $\text{m}^3$ ) which is  $K_o$  ratio of the effective storage capacity  $C$ , and storage limit target date ( $T_o$  in day of the year). For simplicity, target storage limit level will be referred to as “target level” and storage limit target date will be referred to as “target date”.

Initially, these parameters were estimated from the historical operation;  $K_o \cdot C$  and  $T_o$  were inferred from the historical upper storage guide curve (upper curve in dashed line with open circles, Figure 4.3) while  $R_d$ ,  $R_w$ , and  $M_d$  were inferred from the long-term observed release records.  $M_d$  was set as the end of the last month with an observed mean monthly release higher than the observed annual mean release. In this case,  $M_d$  was found to be the last day of May, thereby classifying January to May as dry season release months and the rest as wet season release months. The seasonal release,  $R_d$  and  $R_w$ , were calculated using equation 4.1:

$$R_{d(w)} = \frac{Ia_s}{Ia_o} \cdot R_{do(wo)} \quad (4.1)$$

where  $Ia_s$  and  $Ia_o$  are the simulated and observed mean annual inflows to the reservoirs, respectively, and  $R_{do}$  and  $R_{wo}$  are the observed long-term mean dry and wet season releases, respectively. The use of eq. 4.1 was necessary to take into account the bias between simulated and observed inflows. Releases  $R_d$  and  $R_w$  remain constant throughout the season unless storage exceeds the storage limit or the available volume of stored water is insufficient; in such cases, excess water is spilled or the reservoir is emptied to deliver as much water as possible.

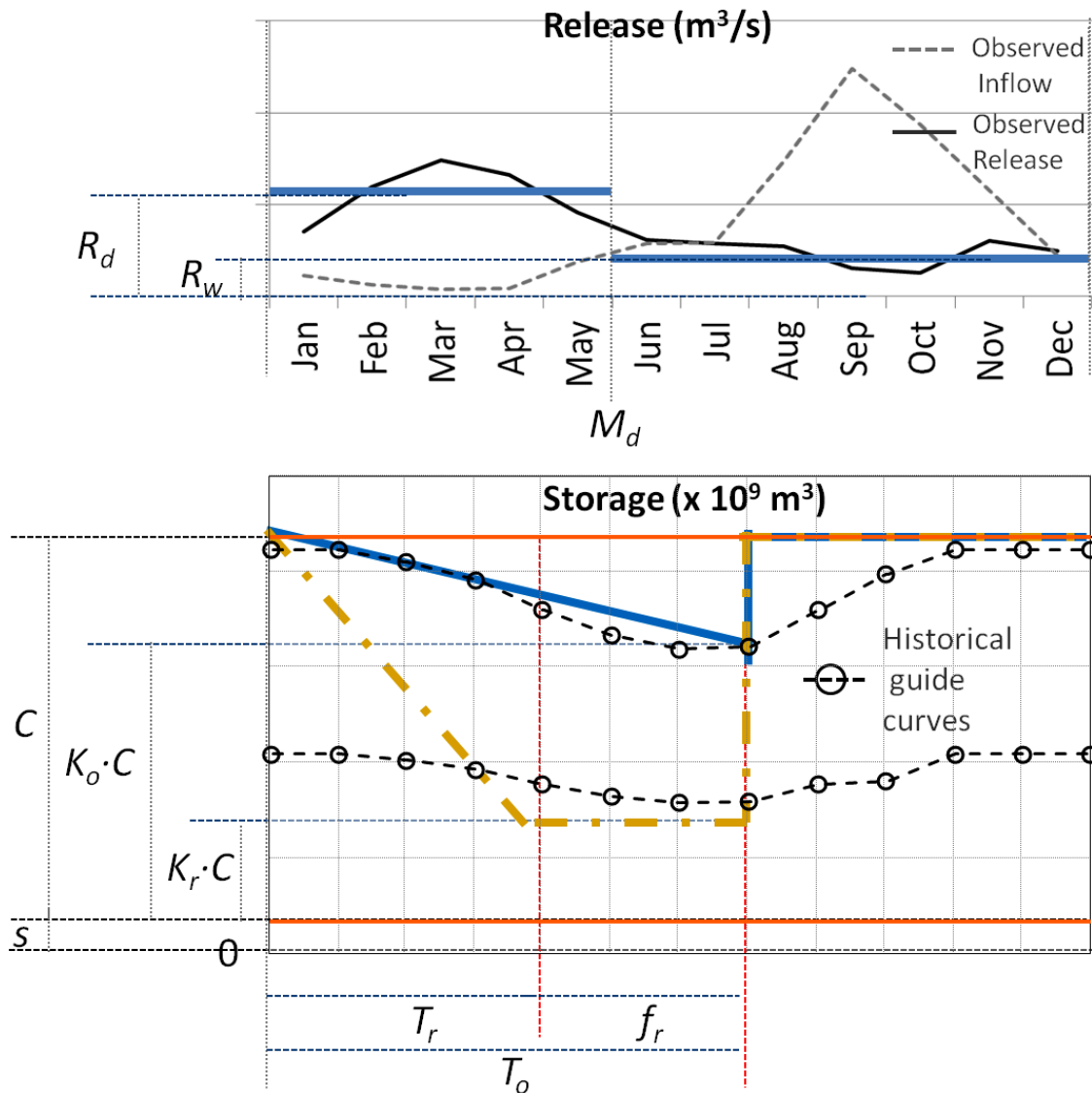


**Figure 4.3. Representation of algorithms used for reservoir storage constraints and reservoir releases for the locally-adapted and alternative reservoir operation schemes** (use with Table 4.1 and Table 4.3). The thin gray lines in the upper panel (reservoir release) indicate the long-term (1981-2004) mean monthly inflow and release in the reservoir. The thick colored lines in the upper panel were then used to represent the simplified reservoir release scheme in all reservoir operation rules. Historically, the operation of the reservoirs were guided by upper and lower storage guide curves as indicated by the thin, gray, dashed lines with circles in the lower panel (dam storage). The thick colored lines in the lower panel indicate the “upper storage constraint” curves in the algorithms used to represent the simplified reservoir operation rules. [modified from Mateo et al., 2013, 2014b]

The upper storage limit in this paper is defined by the simplified and linearized upper guide curve (solid blue line, Figure 4.3); it is represented by a negatively sloped line drawn from the full capacity of the dam at the beginning of the year to the target level  $K_o \cdot C$  on the target date  $T_o$ , and a flat line at reservoir storage capacity,  $C$ , thereafter; the current level of dead storage due to siltation,  $s$ , was set as the constant lower storage limit. This simplified reservoir operation algorithm which uses constant dry season and wet season is hereby referred to as *ThaiOp\_ConRls* (Thai Operation, constant release).

Setting constant seasonal release as  $R_d$  and  $R_w$  in *ThaiOp\_ConRls* takes seasonal variation into account but ignores interannual variability. It was found that although this algorithm can adequately simulate regulated flows and inundation, it tends to cause frequent drying up of reservoirs because the mean seasonal release is quite high for a generally dry year [Mateo et al., 2013]. Rationally, when the stored water level at the beginning of the year is lower than usual or when there is an impending drought, reservoir operators will tend to reduce the water released to prevent reservoirs from drying up during the dry season. Similarly, when stored water level is higher than usual, reservoir operators will tend to release more water to reach a low storage target to prevent reservoirs from overflowing during the rainy season.

In order to represent such water rationing phenomena, a release coefficient,  $k_{rls}$ , similar to that of the H08 generic rules [Hanasaki et al., 2006] was adapted to account for interannual variability. Precipitation in the Chao Phraya River Basin can drastically vary not only interannually but also sub annually or seasonally. A good example is the year 2011 when there was an impending drought due to the low water level in the reservoirs in the earlier months; however, eventually, heavy rainfall started to occur from the middle of the year and several other heavy rainfall occurred towards the end of the year. Hence, in this study, the release coefficient,  $k_{rls}$ , is calculated twice a year – first, at the beginning of the year, and second, at target date  $T_o$ .

The release coefficient  $k_{rls}$  is computed using equation 4.2:

$$k_{rls} = \begin{cases} \frac{S_1}{\alpha \cdot C} & d.o.y. < T_o \\ \frac{S_{T_o}}{\alpha \cdot K_o \cdot C} & T_o \leq d.o.y. \leq 366 \end{cases} \quad (4.2)$$

where  $\alpha$  is an empirically derived release constant,  $S_1$  is the storage at first day of the year (d.o.y.), and  $S_{T_o}$  is the storage on target day  $T_o$ ; in this paper, release constant  $\alpha$  was set at 0.65. Finally, the release coefficient,  $k_{rls}$ , is multiplied accordingly to the seasonal releases,  $R_d$  and  $R_w$ .

Except from the empirically tuned release constant  $\alpha$ , all the other constants used in the equations were calculated based on the mean values of the long-term observed reservoir operation. Hence, hereafter, these local operation-adjusted operation rules is referred to as *ThaiOp\_kRls* (Thai Operation, release varying by coefficient,  $k_{rls}$ ).

For the purpose of comparison, the two reservoir operation algorithms, *ThaiOp\_ConRls* and *ThaiOp\_kRls* are compared with the observed discharge and the simulation results using the observed release from the two reservoirs as input to CaMa-Flood (*Thai\_DamObs*). For clarity, the characteristics of the simulation schemes to be discussed are summarized in Table 4.1.

**Table 4.1. Reservoir operation release algorithms for simulating the historical operation of Bhumibol and Sirikit Reservoirs (to be used with Figure 3).** [Modified from Mateo et al., 2014b]

| Simulation Name      | $K_o^*$   | $T_o(d.o.y.)^*$   |
|----------------------|---|-------------------|
| <i>ThaiOp_ConRls</i> | 1.0   | 212 [end of July] |
| <i>ThaiOp_kRls</i>   | 0.65  | 212 [end of July] |
| <i>Thai_DamObs</i>   | n.a. (observed reservoir release used as forcing) |                   |

\* $K_o$  and  $K_r$  are target storage limit constants;  $T_o$  and  $T_r$  are storage limit target date in days of the year.

### 4.3 SIMULATION OF THE 2011 THAI FLOOD

Simulation of regulated flows using the simplified operation schemes, *ThaiOp\_ConRls* and *ThaiOp\_kRls*, yielded good results which are comparable to that of the simulation which used the actual reservoir releases in the two reservoirs as forcing input, *Thai\_DamObs* (Figure 4.4). For comparison of the efficiency of the reservoirs in reducing the natural peak flow, the natural flows simulated by the *Nat-H08-CaMa* is also shown in the graph. The figures clearly show that the discharge peak had been reduced and its timing delayed because of the impoundment of water in the two huge reservoirs.

The daily Nash-Sutcliffe Efficiency (NSE-coefficients) from the years 1993-1995 and year of 2011 and monthly NSE-coefficients from 1981-2004 using these reservoir operation schemes are summarized in Table 4.2. It can be seen that while both of the algorithms introduced, *ThaiOp\_ConRls* and *ThaiOp\_kRls*, show good performances (“good” performance evaluated as  $65\% < \text{NSE-coefficient} \leq 75\%$ , and  $\pm 10 \leq \text{PBIAS} < \pm 15$  by Moriasi et al. [2007]) in simulation the regulated flows in the basin, the *ThaiOp\_kRls*, the operation which utilized release coefficients, show better performance than the *ThaiOp\_ConRls*, especially in simulating the 2011 Thai flood.

**Table 4.2. Nash-Sutcliffe efficiency coefficients for the reservoir operation algorithms**

| Reservoir<br>operation<br>scheme | Monthly<br>(1981-2004) | Daily<br>(1993-1995) | Daily<br>(2011) |
|----------------------------------|------------------------|----------------------|-----------------|
| <i>Thai_DamObs</i>               | 68.41%                 | 91.70%               | 91.89%          |
| <i>ThaiOp_ConRls</i>             | 65.65%                 | 88.30%               | 66.35%          |
| <i>ThaiOp_kRls</i>               | 68.91%                 | 86.60%               | 91.93%          |

[Modified from Mateo et al., 2014b]

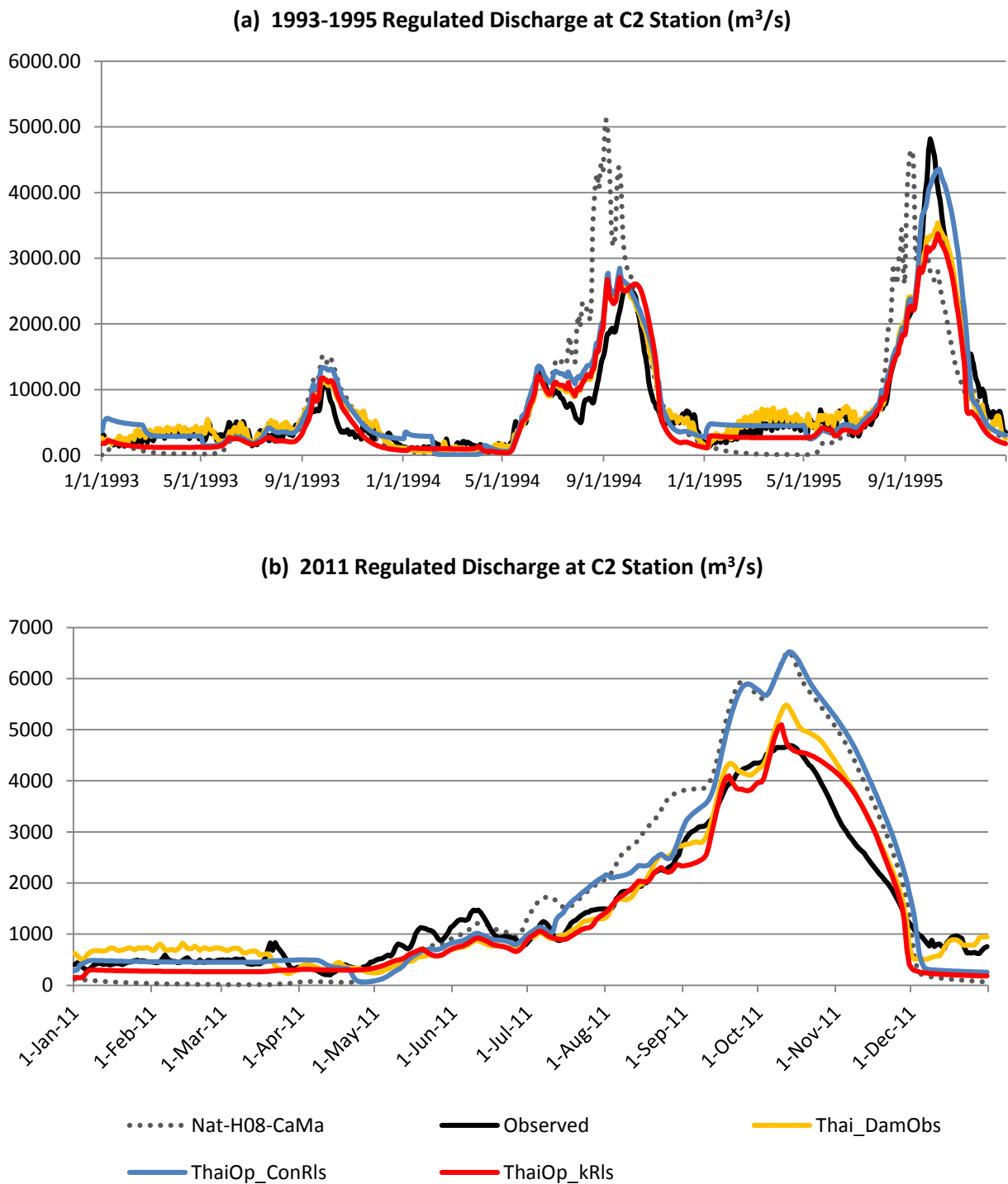


**Figure 4.4.** Comparison of the simulated daily regulated discharge using several reservoir operation algorithms with the observed in (a) 1993-1995, and (b) 2011. The gray dotted line representing Nat-H08-CaMa simulation is shown for reference. [Modified from Mateo et al., 2014b]

In flood year 2011, the simulated regulated daily flows using *ThaiOp\_kRls* showed high agreement with those of the observed discharge (Figure 4.4): NSE-coefficient is 91.93%,  $R^2$  is 0.95, and RMSE is 0.29mm/day (368.80m<sup>3</sup>/s). The observed peak discharge of 3.68 mm/day which occurred in October 13 was replicated well with the simulated peak magnitude (3.99 mm/day) percent error of only 8.74% and simulated peak timing (October 10) error of only 3 days. Thus, it can be said that the simplifications of historical reservoir operation rules applied in *ThaiOp\_kRls* can effectively represent the more complex nature of the actual reservoir operation decisions.

Overall, these statistical results are comparable with the results of Wichakul et al. [2013b] who used a Simplified Xinanjiang (SXAJ) regional hydrological model and a 1-km distributed flow routing model (1K-FRM) for analyzing the 2011 floods in the Chao Phraya River Basin. The applied SXAJ at 15-min spatial resolution and 1-hr temporal resolution while the applied 1K-FRM at 1-km spatial resolution and 10-min temporal resolution. For the flood year 2011, Wichakul et al. reported a NSE-coefficient of 91.0%,  $R^2$  of 0.94, and RMSE of 388m<sup>3</sup>/s at C2 Station. This confirms that albeit the use of global models, the combined H08-CaMa model is sufficient for application on the Chao Phraya River Basin.



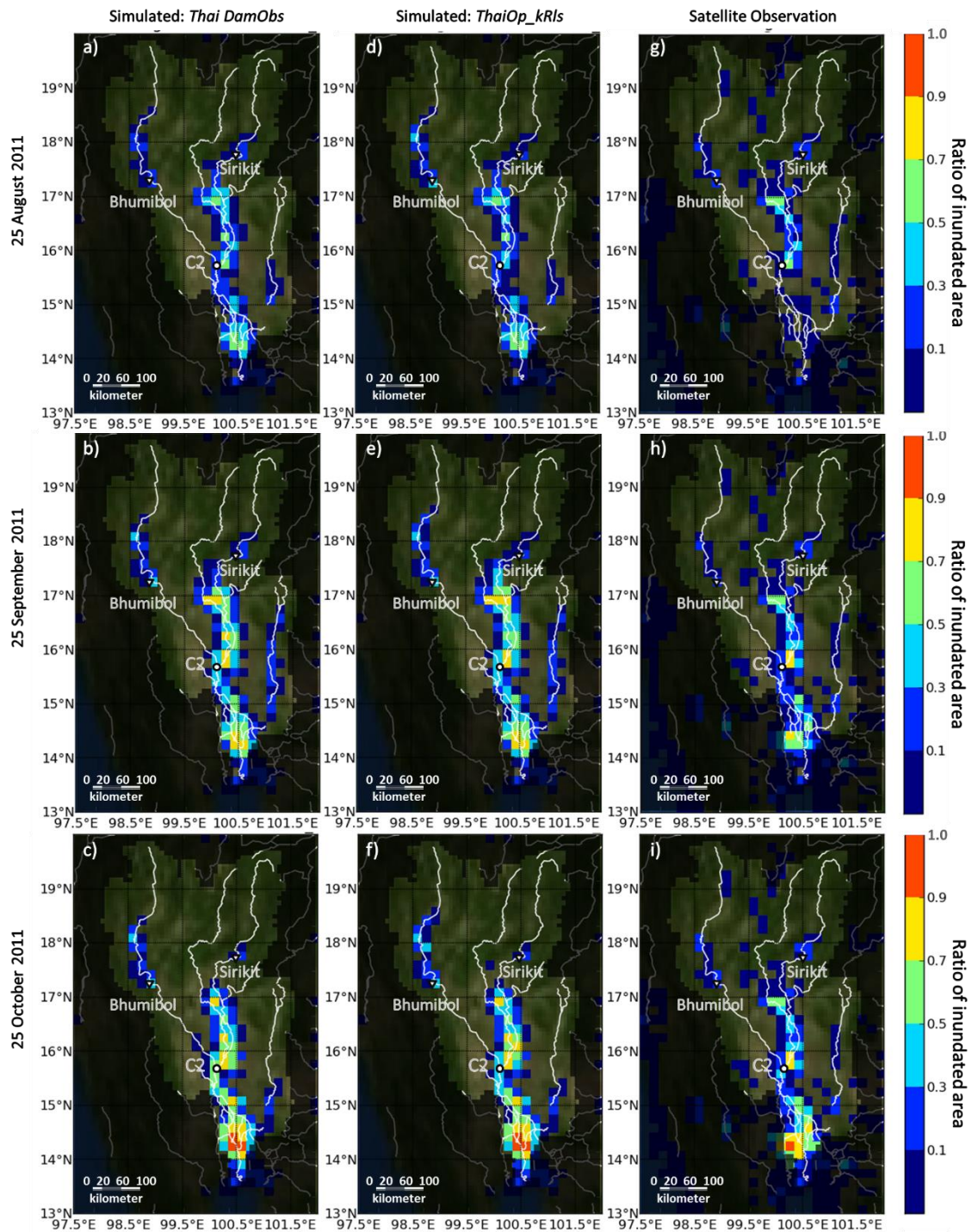


**Figure 4.5.** Simulated and observed ratio of inundated areas (inundated area/total area); figures in the left-most column (a, b, and c) show simulation results using the actual reservoir operation as forcing input (*Thai\_DamObs*); figures in the middle column (d, e, and f) show simulation results using the simplified historical reservoir operation (*ThaiOp\_kRIs*); figures in the right-most column (g, h, and i) show satellite images using combined outputs of MODIS and AMSR-E [Modified from Mateo et al., 2013, 2014b]



A significant advantage of using the H08-CaMa model is that it can explicitly simulate floodplain inundation. Observed satellite images from the combined analysis of the Moderate Resolution Imaging Spectroradiometer (MODIS) and Advanced Microwave Scanning Radiometer for EOS (AMSR-E) [courtesy of Dr. Wataru Takeuchi, Dr. Kazuo Oki, and Dr. Hyungjun Kim, 2012] available from 2010-2011 have been used to validate the inundation simulated by the H08-CaMa model. It is verified that the spatiotemporal change in inundation can be simulated by the H08-CaMa model (Figure 4.5). The extent of flood inundation shown in 1-month intervals from August 25, 2011 to October 25, 2011 simulated using *ThaiOp\_kRls* (Figures 4.5d, 4.5e, and 4.5f) are almost similar to those of *Thai\_DamObs* (Figures 4.5a, 4.5b, and 4.5c). Moreover, albeit the use of simplified reservoir operation rules, the extents of flood inundation in three different months simulated by *ThaiOp\_kRls* correspond quite well with those of the satellite observations (Figures 4.5g, 4.5h, and 4.5i). However, some areas within the basin tend to be overestimated. Most of these areas are within zones that are heavily affected by anthropogenic interventions such as huge canals, diversion channels, or urbanized regions which are not yet considered in the version of the CaMa-Flood model used in this chapter.

The total volume of water stored in floodplains (i.e. out of bank flood volume) calculated for all grid cells downstream of the two reservoirs in natural flow simulation and in each reservoir operation scheme for five worst flood years in the dataset (shown in decreasing order in the figure) is shown in Figure 4.6. Given that all other factors between the simulations other than the reservoir scheme used are the same, the differences between each scheme within each year can be solely attributed to reservoir operation. In the graph, it is evident that the *ThaiOp\_ConRls* scheme tend to overestimate the flood volume as the flood event increase in magnitude. This can be attributed to the constant reservoir release used in *ThaiOp\_ConRls* – the reservoirs tend to easily fill up during extreme events.

On the other hand, *ThaiOp\_kRls* scheme can give reasonable estimates of the flood volume which are comparable with those simulated by *Thai\_DamObs*. The calculated flood volume of 21.6 billion m<sup>3</sup>

using *ThaiOp\_kRls* is slightly overestimated but is comparable to the estimates of Komori et al. [2012] and Rakwatin et al. [2013]. The date when the maximum flood volume occurred (October 16, 2011) also agrees with the results (October 12-18, 2011) of Rakwatin et al [2013]. Further, the reduction in flood volume between *ThaiOp\_kRls* and natural flow simulation, *Nat-H08-CaMa*, of 8.6 billion m<sup>3</sup> is also close to the flood volume stored in the two reservoirs (10 billion m<sup>3</sup>) estimated by Komori et al. [2012].

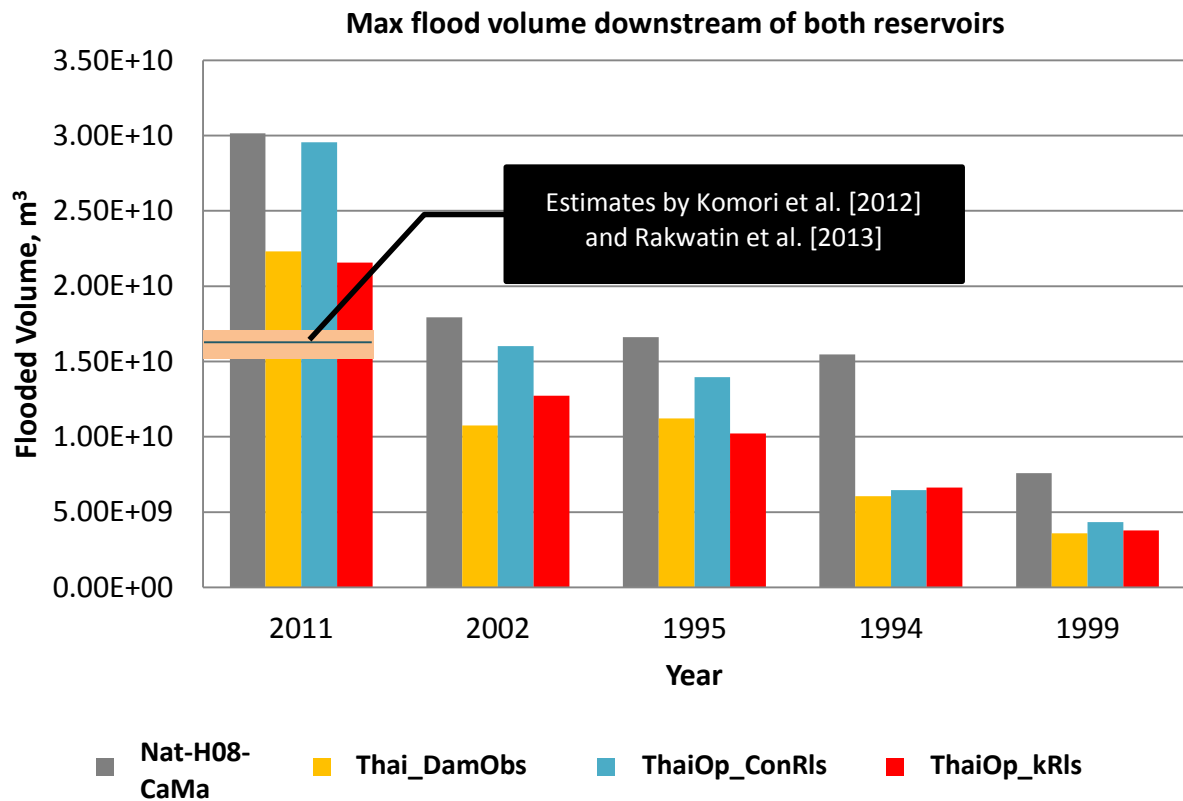


**Figure 4.6. Total volume of water stored in floodplains (flooded volume) downstream of the two reservoirs.** The total volume of water stored in floodplains for each day was calculated for each simulation scheme. After then, the maximum among the daily flooded volume was calculated. Only the grid cells downstream of both reservoirs were included in order to exclude the waters stored in the reservoirs in the analysis and to focus on the impacts of reservoir operation.

[Modified from Mateo et al., 2014b]

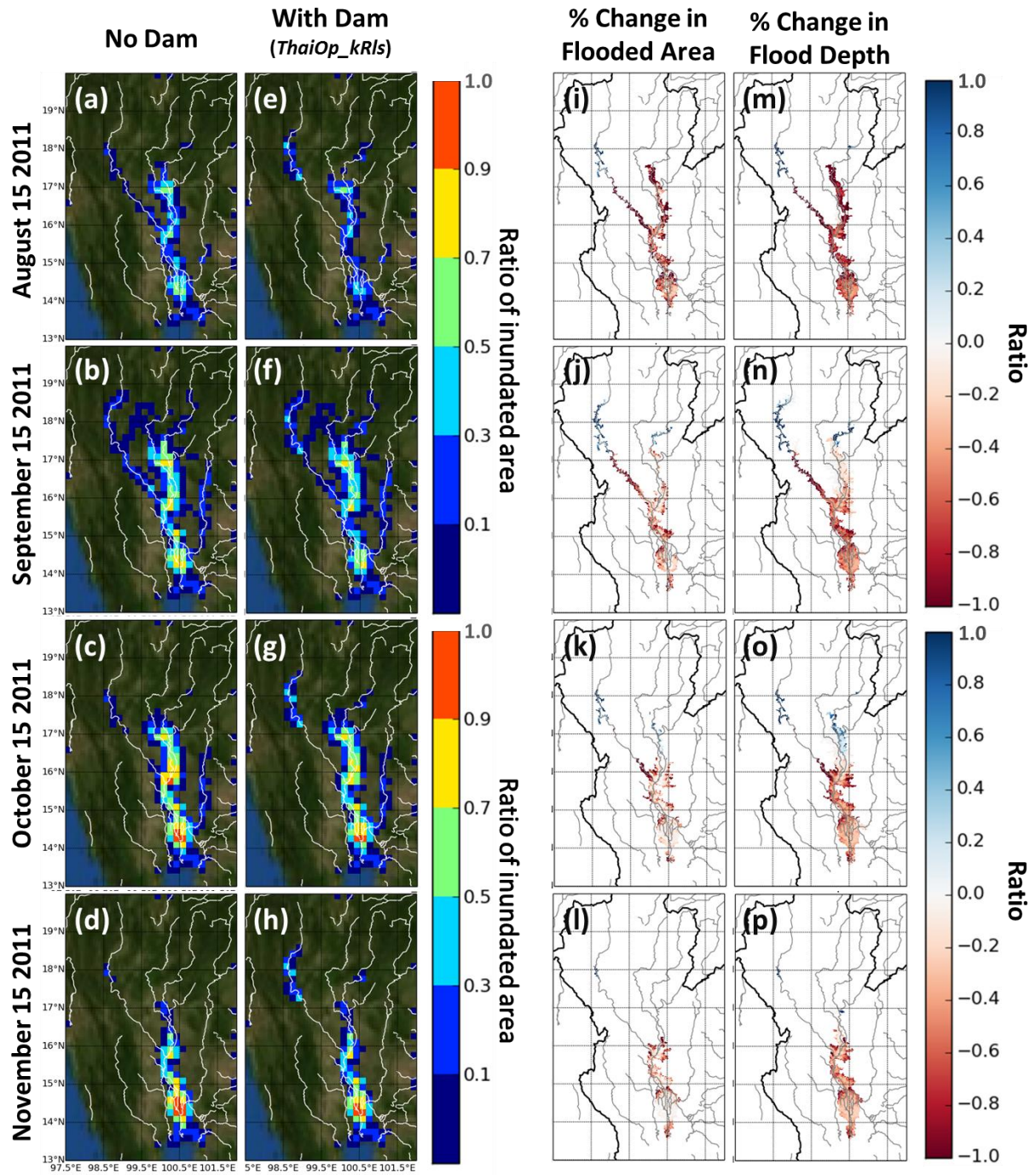


**Figure 4.7 Comparison of and difference in flood inundation between without and with dam operation;** ratio of inundated area in (a-d) without dam operation using *Nat-H08-CaMa* and (e-h) with dam operation using *ThaiOp\_kRLs*; percent difference in (i-l) flooded area and (m-p) flood depth between with and without dam operation simulations. The first two columns from the left (a-h) are shown in 10-min resolution for reference with satellite images (Fig. 4.5) while the last two columns (i-p) are shown in 1-min resolution to show finer details.

The comparison of flood volume estimates clearly show the benefits from flood mitigation through the operation of the two reservoirs. The reduction in flood volume, consequently, resulted to reduction in the inundated areas and flood depth between as shown in Figures 4.7i to 4.7p. While the flood extent and ratio of inundated area do not seem to significantly change between Figures 4.7a to 4.7h, the reduction in flooded areas and flood depth are evident in the dark red pixels in Figures 4.7i to 4.7p. As expected, reduction in flooded area and flood depth are greatest near the border lines (or boundaries) of the flood extents. Percent reduction in flood depths are generally larger and more significant than those in flooded areas. This could be due to the lower absolute values in flood depths as compared with those in flooded areas. As flood damages are usually greatly influenced by flood depths and flooded areas [e.g. Dutta, Herath, & Musiak, 2003; Oliveri and Santoro, 2000], these information are critical for evaluating the efficiency and effectiveness of reservoir operation. Such information are also critical for providing sufficient warnings, planning evacuation procedures, and facilitating disaster response, rescue, and recovery procedures.

The results in Figures 4.6 to 4.7 indicate that flooding throughout the basin cannot be solely mitigated by the two reservoirs. This should be expected given the huge domain of the river basin and the upstream location of the two reservoirs; rainfall that fell outside of their catchment area cannot be intercepted and temporarily stored by the two reservoirs. Hence, the capacity of the reservoirs to mitigate flood disasters will also depend on the spatio-temporal distribution of rainfall. The understanding of such limitations are important in order to not falsely judge the effectiveness (or ineffectiveness) of the operation reservoirs based on bulk damages. Clearly, the results show that the operation of the two reservoirs resulted to significant reduction or mitigation of damages not only to the areas located immediately to their downstream, but to the entire basin as well. This is evident in the reduction in flooded areas and flood depths in the low-lying floodplains within the basin which are located several hundred kilometres downstream of the two reservoirs. Such benefits through

mitigation of damages can be easily overlooked when assessed on relatively coarser spatial resolutions; therefore, the results suggest that flood inundation parameters should be downscaled in order to properly account the benefits (or damages) in local scale. Overall, these results accentuates the importance of assessing the human-natural systems in the river basin in a holistic and integrated manner.

#### 4.4 ASSESSMENT OF IMPROVEMENTS IN RESERVOIR OPERATION SCHEMES

Simple modifications in the historical reservoir operation rules which can possibly mitigate flooding in the basin are presented in this section. Primarily, the concept of pre-release was used wherein low reservoir storage is targeted to prepare for extreme inflows during the rainy season. To simulate the pre-release of water, the target level,  $K_o \cdot C$ , and target date,  $T_o$ , were modified to  $K_r \cdot C$  and  $T_r$ , respectively (dashed yellow line, Figure 4.3). In addition, an option to simulate a low constant storage level  $K_r \cdot C$  for consecutive  $f_r$  days after modified target date  $T_r$  had been added (i.e., a flat storage will be maintained for  $f_r$  days after  $T_r$ ; after then, storage limit is set to be equal to reservoir storage capacity,  $C$ ). For simplicity, the other reservoir release parameters  $R_d$ ,  $R_w$ ,  $k_{rdb}$ , as computed using equations 1 and 2 have been retained.

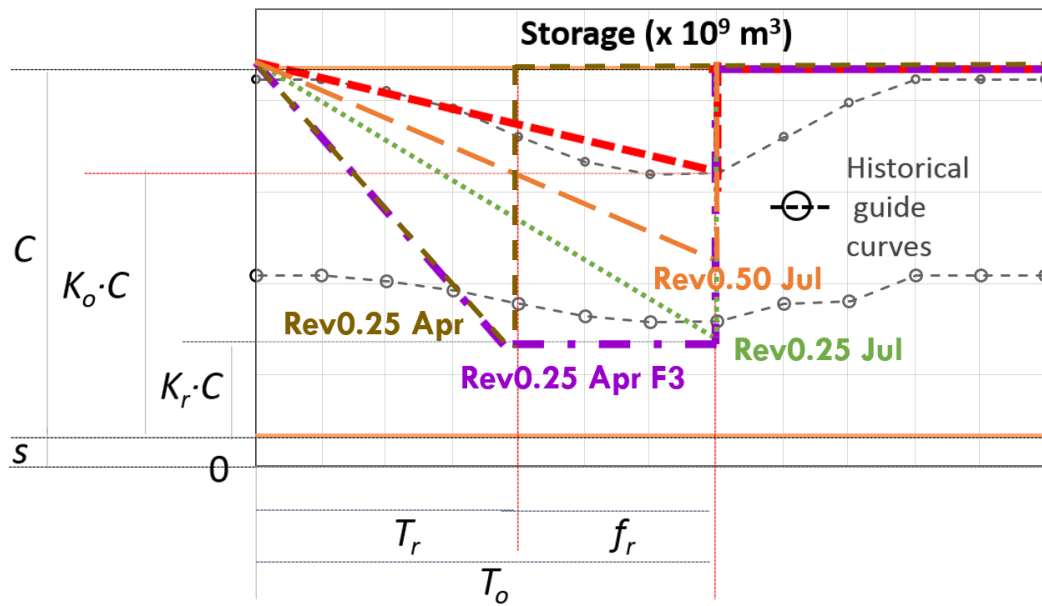


**Figure 4.8. Alternative reservoir operation rules.** Simple modifications to the storage guide curve are proposed by changing the storage targets and target dates. *Please use with Table 4.3.* [Modified from Mateo et al., 2013, 2014b]

**Table 4.3. Parameters describing the alternative reservoir operation of Bhumibol and Sirikit Reservoirs.** The modifications in the upper storage guide curve parameters are compared with the operation scheme that simulates the historical reservoir operation (*ThaiOp\_kRls*). *Please use with Figure 4.8.* [Modified from Mateo et al., 2014b]

| Simulation name       | $K_o^*$ or $K_r^*$ | $T_o^*$ or $T_r^*$ (d.o.y.) | $f_r^*$ (days) |
|-----------------------|--------------------|-----------------------------|----------------|
| <i>ThaiOp_kRls</i>    | 0.65               | 212 [end of Jul]            | 0              |
| <i>Rev0.5 Jul</i>     | 0.50               | 212 [end of Jul]            | 0              |
| <i>Rev0.25 Jul</i>    | 0.25               | 212 [end of Jul]            | 0              |
| <i>Rev0.25 Apr</i>    | 0.25               | 120 [end of Apr]            | 0              |
| <i>Rev0.25 Apr F3</i> | 0.25               | 120 [end of Apr]            | 92 [3 months]  |

$K_o$  and  $K_r$  are target storage limit constants;  $T_o$  and  $T_r$  are storage limit target date in days of the year;  $f_r$  is the number of days after  $T_r$  wherein a flat storage limit equivalent to  $K_r \cdot C$  is maintained.



Several alternative reservoir operation rules have been simulated in this study but only four will be discussed in this chapter (see Figure 4.8 and Table 4.3). These alternative rules were referred to as:  $RevK_r T_r (name\ of\ month) Ff (in\ months)$ , e.g.  $Rev0.25 Apr F3$  means “Revised” operation using a target storage ratio  $K_r$  of 0.25 that has to be reached by date  $T_r$  which is at the end of April. The low storage ratio of 0.25 should be maintained for 3 months after April. These four alternative rules were deemed to be sufficient in showing the impacts of lower target level, earlier target date, and low constant storage level. It should be noted that these four alternative operation rules may not show optimized reservoir operation but may indicate future directions for optimization. Hereon, these four alternative rules will be compared with the  $ThaiOp\_kRls$  operation scheme.

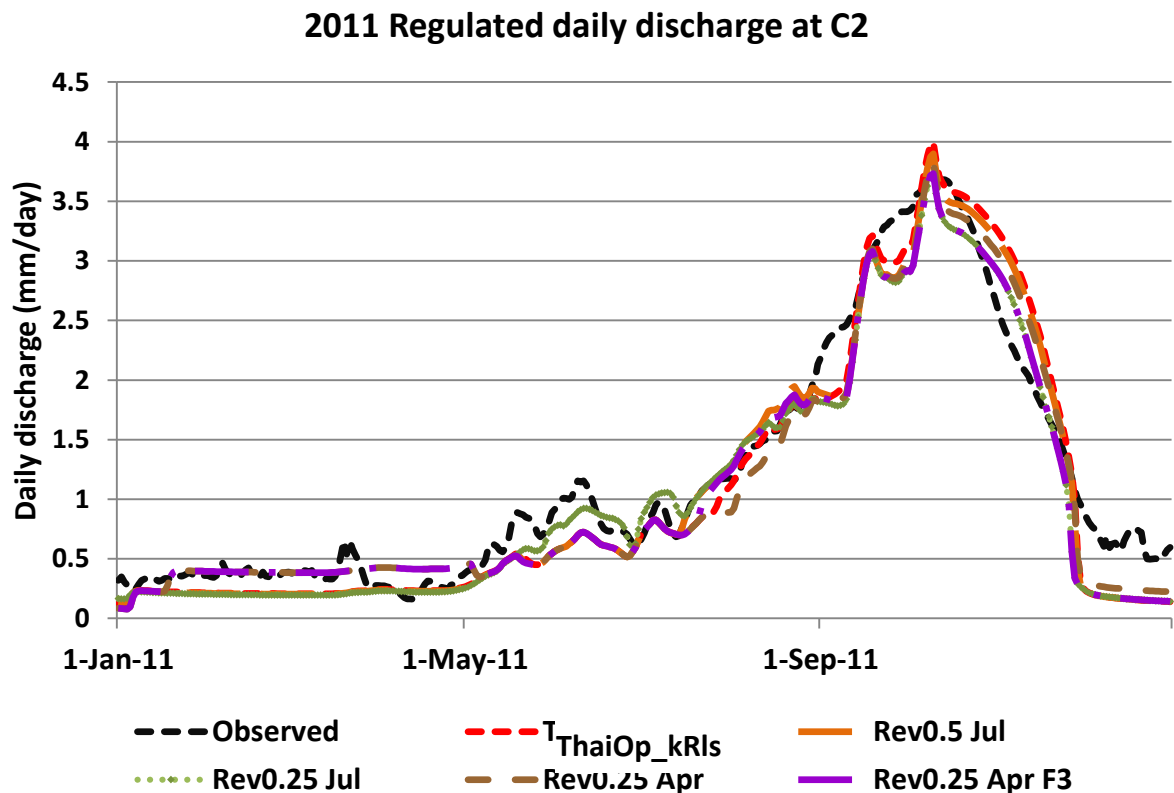


Figure 4.9. Comparison of the daily discharge simulated by the five reservoir operation rules with those of the observed in flood year 2011. [Modified from Mateo et al., 2014b]

The four operations marginally reduce the magnitude of peak discharge at C2 Station (Figure 4.9); maximum reduction is about 7% in both *Rev0.25 Jul* and *Rev0.25 Apr F3* while the minimum reduction is about 2%. However, these marginal peak discharge reductions at one point in the basin do not provide a good description of the potential for flood mitigation using the alternative reservoir operation rules. In the event of immense flooding, river channels will have most likely exceeded their storage capacity and excessive overbank flows may already be occurring in floodplain: reductions in peak discharge in river channels may be marginal but the total reduction in the volume of flood water in floodplains may be significant. More rigorous techniques for quantifying the flood mitigation potential of the alternative operation rules are hereby applied by assessing and quantifying the impacts of the alternative reservoir operation rules to the (1) reduction in the occurrence storage overflows and dry ups in the reservoirs, (2) reduction in flood volume, (3) reduction in flood depth, and (4) extent and progression of areas inundated by the floods.

Examining the storage of the reservoirs from 1981-2004, the number of months wherein the total capacity of a reservoir was exceeded (overflows) was greatly reduced in all the alternative operation rules in both reservoirs (Table 4.4); this is primarily because of the lower target level as compare with *ThaiOp\_kRls*. As expected, the number of overflows decreases as target level,  $K_r \cdot C$  is lowered, making the *Rev0.25* alternatives more preferable than the *Rev0.5* alternative in terms of flood risk reduction.

On the other hand, the number of years wherein the effective storage by the end of October in the two dams is below the mean target storage set by the Thai Government (3.67 billion  $\text{m}^3$  for Bhumibol Reservoir, 2.53 billion  $\text{m}^3$  for Sirikit Reservoir, 6.2 billion  $\text{m}^3$  in total, JICA report, in Japanese) significantly increased in the alternative reservoir operation rules. The number of years below target storage, a measure of potential supply deficit, increase as the target level,  $K_r \cdot C$  is lowered; hence, *Rev0.5 Jul* outperforms the three other alternative reservoir operation rules in providing adequate water supply.



The number of months wherein the effective storage of the reservoirs reached zero (reservoir empty) is used as an indicator of the reliability of water supply during dry seasons; a lower frequency of reservoir emptying indicates less severe droughts or a higher likelihood that water was available for use during the latter days of the dry season (cropping season). Any effective water storage level less than 0.5% of the effective storage was considered to be in “reservoir empty” condition. As a result of the adjustment of dry season releases according to the available stored water at the beginning of the year through release coefficient,  $k_{rls}$ , all the reservoir operation rules simulated never resulted to empty reservoirs.

**Table 4.4. Reliability of the reservoir operation schemes.** Measured by the number of months the storage capacity was exceeded (overflows), number of years when storage is below the mean target set by the government, and the number of months when minimum storage level was reached.

| Sirikit Reservoir  |                       |  |                                   | Bhumibol Reservoir  |                       |  |                                   |
|--|-----------------------|--|-----------------------------------|---|-----------------------|--|-----------------------------------|
| 9.51 billion m <sup>3</sup> total storage capacity<br>(6.66 billion m <sup>3</sup> effective storage capacity) |                       |  |                                   | 13.46 billion m <sup>3</sup> total storage capacity<br>(9.66 billion m <sup>3</sup> effective storage capacity) |                       |  |                                   |
| Operation  | Overflow<br>(months*) | Below<br>target<br>storage<br>(years*) | Reservoir<br>Empty**<br>(months*) | Operation   | Overflow<br>(months*) | Below<br>target<br>storage<br>(years*) | Reservoir<br>Empty**<br>(months*) |
| <i>ThaiOp_kRls</i>   | 12                    | 2                                      | 0                                 | <i>ThaiOp_kRls</i>  | 6                     | 0                                      | 0                                 |
| <i>Rev0.5 Jul</i>  | 8                     | 5                                      | 0                                 | <i>Rev0.5 Jul</i>   | 6                     | 1                                      | 0                                 |
| <i>Rev0.25 Jul</i>   | 4                     | 11                                     | 0                                 | <i>Rev0.25 Jul</i>  | 1                     | 6                                      | 0                                 |
| <i>Rev0.25 Apr</i>   | 4                     | 11                                     | 0                                 | <i>Rev0.25 Apr</i>  | 2                     | 7                                      | 0                                 |
| <i>Rev0.25 Apr F3</i>  | 4                     | 11                                     | 0                                 | <i>Rev0.25 Apr F3</i>   | 1                     | 7                                      | 0                                 |

\*Simulation period in consideration spans for a total of 24 years or 288 months.

\*\* Less than 0.5% of storage capacity above the dead storage level

[Modified from Mateo et al., 2013, 2014b]

The low storage set in the alternative reservoir rules and the reduced occurrence of overflows result to the reduction in flood volume downstream of both reservoirs (see Figure 4.10). Here, the percent reduction in each alternative reservoir rules is obtained by getting the difference between the flood volume downstream of both reservoirs as compared with those of the natural flows,  $Nat - H08-CaMa$ .

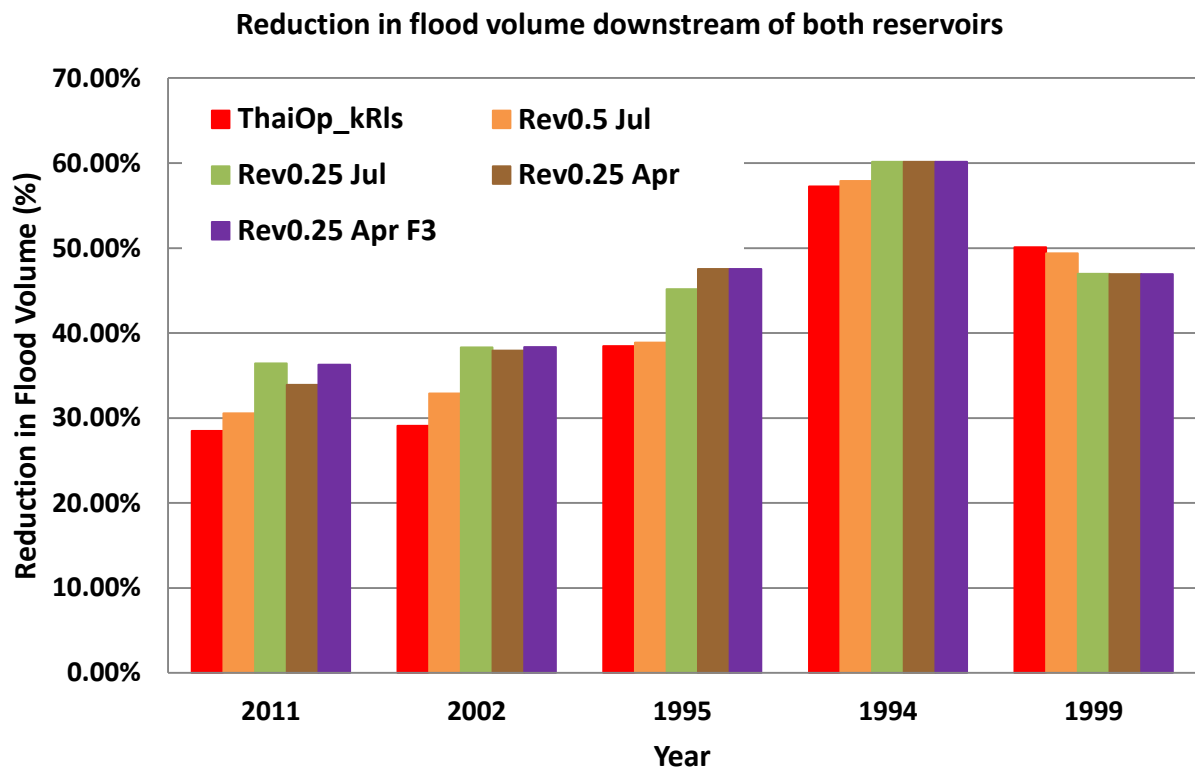


**Figure 4.10. Reduction in flood volume downstream of both reservoirs.** Percent reduction is computed as the percent difference in flood volume between each reservoir operation scheme and the  $Nat - H08-CaMa$ . [Modified from Mateo et al., 2014b]

Comparing the percent reduction between alternative operation rules and *ThaiOp\_kRIs*, it can be observed that flood volume can still be significantly reduced through very simple modifications in operating rules. In 2011, the flood volume is further reduced in all the four alternative reservoir operation rules; among the four alternatives, reduction is at least 3% in *Rev0.5 Jul* and at most 11% in

both *Rev0.25 Jul* and *Rev0.25 Apr F3*. The total reduction in both *Rev0.25 Jul* and *Rev0.25 Apr F3* is approximately 2.35 million m<sup>3</sup>. This verifies the initial estimate of an additional 1 million m<sup>3</sup> of flood volume stored in each of the two reservoirs if water had not been stored prior to the onset of heavy rainfall season [Komori et al., 2012].

As flood volume is reduced, consequently, the inundated area and flood depth will also be reduced through each alternative reservoir operation rules. The total inundated area at various flood depth threshold levels in flood years 2011, 2002, and 1995 were calculated for all grid cells downstream of the two reservoirs and shown in Figure 4.11. The curves were generated by calculating the maximum daily flood depth and corresponding flood area in each grid cell; subsequently, flood area in each grid cell that exceeded flood depth threshold levels at 0.4m intervals were summed. The three graphs indicate that *ThaiOp\_kRs* had significantly reduced flooding as compared with natural flow in the three flood years; in 2011, mean reduction in flood area at each flood depth threshold was about 40%.

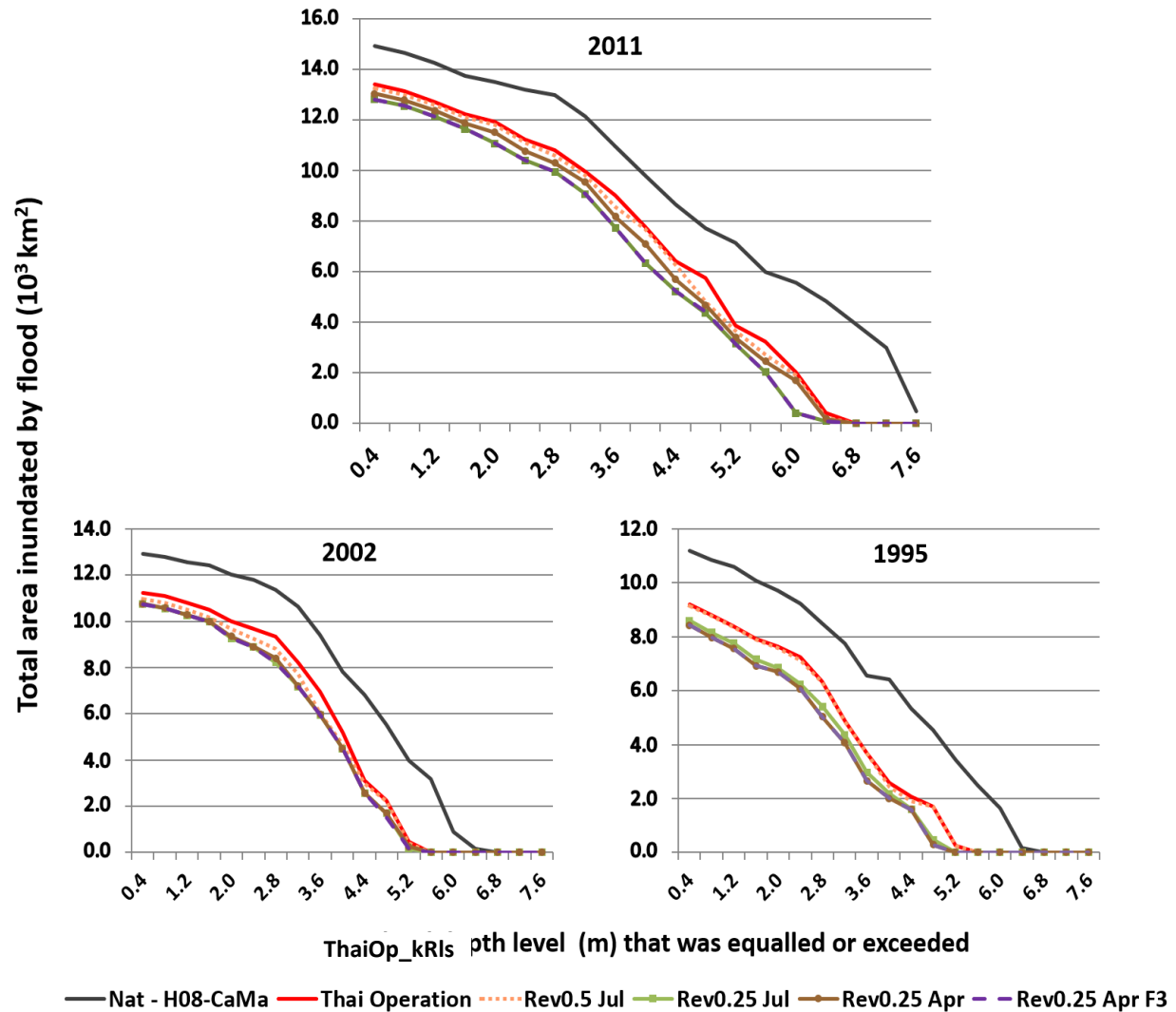


**Figure 4.11. Total area inundated by flood at increasing flood depth threshold levels.** The maximum daily flood depth and corresponding flood area were calculated for each grid cell located downstream of both reservoirs; after then, the sum of the flood area in all grid cells that exceeded each flood depth threshold level (interval of 0.4m) were totalled. Only the grid cells downstream of both reservoirs were included in order to focus on the impacts of reservoir operation on flood inundation. [Modified from Mateo et al., 2014b]

Nonetheless, both flooded areas and flood depth levels can be further reduced through simple modifications in the reservoir operation rules. The total inundated area is reduced at each flood depth threshold level in all the alternative reservoir operation rules; the reduction in total inundated area

increases with increasing flood depth threshold level. In 2011, maximum reduction in flood depth and total inundated area can be obtained through *Rev0.25 Jul* and *Rev0.25 Apr F3*; on average, these alternative operation schemes can reduce the total inundated area by 20% in each flood depth threshold level.

The progression of reduction in flood depth between each of the four alternative reservoir operations and *Thai Operation* are shown in Figure 4.12; significant reductions in flood depth are evident as indicated by the dark red pixels. Both *Rev0.25 Jul* and *Rev0.25 Apr F3* can potentially reduce flood depth by more than 80% when flood inundation in the basin is worst (late September to early November). The lower target level  $K_r$  primarily results to greater flood depth reduction. This is evident in the relatively lower flood depth reduction in the three *Rev0.25* operation rules as compared with that of *Rev0.5 Jul*. The target date  $T_r$  primarily influences the progression of flood inundation. *Rev0.25 Apr* resulted to greater flood depth reduction in the earlier months of the flood event as it started to store water by the beginning of May; however, eventually, the two reservoirs are filled to their capacity which resulted to relatively higher reservoir releases and consequently, lower flood depth reduction, as compared with those of *Rev0.25 Jul* and *Rev0.25 Apr F3* during the worst months of flooding.

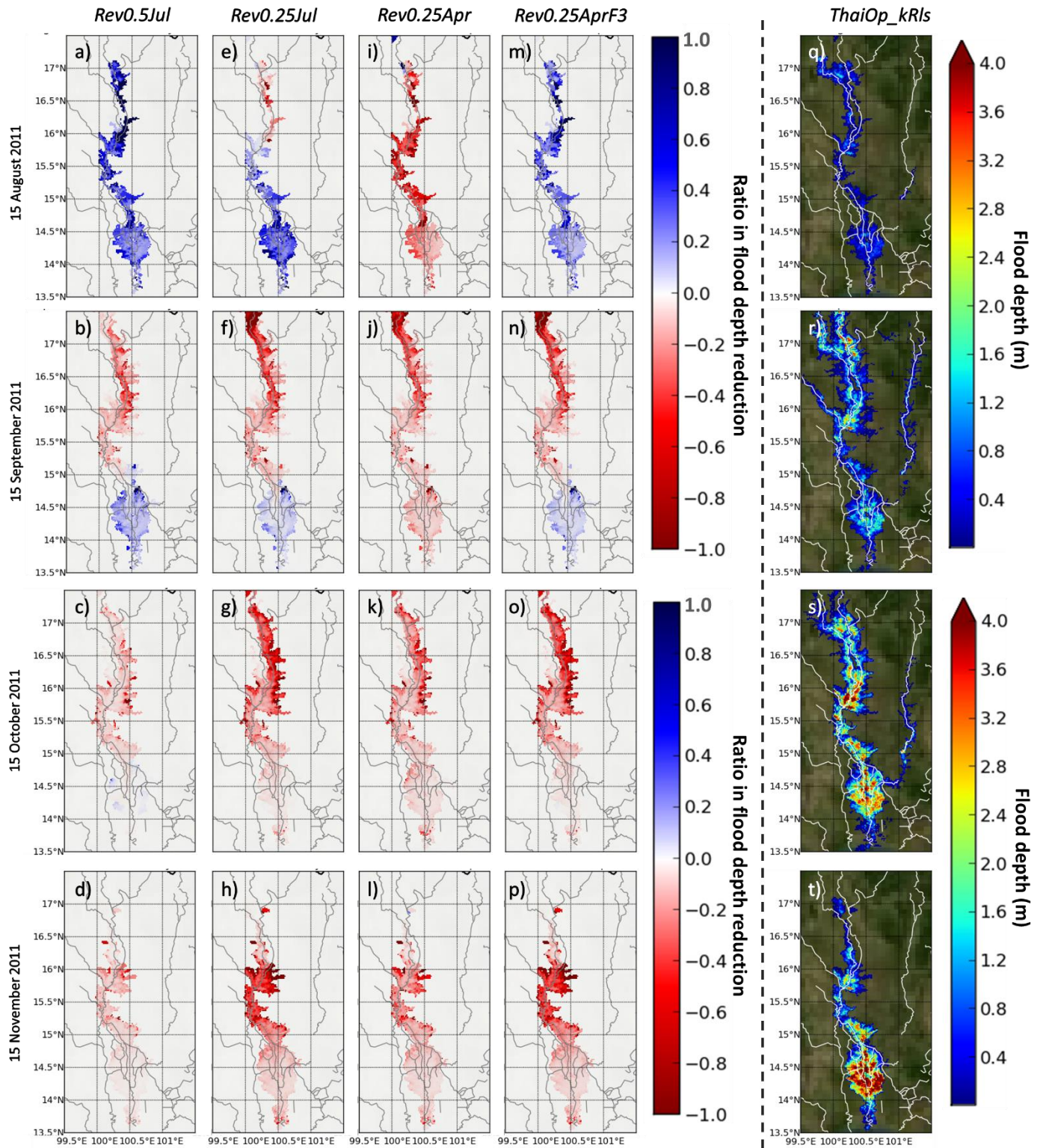


**Figure 4.12. Reduction in flood depth (FD) in 1-minute  $\times$  1-minute spatial resolution; FD reduction using *Rev0.5 Jul* scheme is shown in the left most column; FD reduction using *Rev0.25 Jul* scheme is shown in the second column; FD reduction using *Rev0.25 Apr* is shown in the third column; FD reduction using *Rev0.25 AprF3* is shown in the fourth column; Simulated FD using the *ThaiOp\_kRIs* scheme is shown in the**



right most column for reference. Flood reduction is shown at 1-month intervals from August 15 to November 15 to show the progression of reduction in flood depth. Figures are zoomed in to downstream of Bhumibol and Sirikit Reservoirs. [Modified from Mateo et al., 2014b]

Up to this point, the four alternative reservoir operation rules presented proved to be effective in mitigating flooding in the Chao Phraya River Basin. Both the lower target level and the target date affect the extent of flood reduction; the target level primarily affects the total flood volume whereas the date when this storage limit level is attained impacts the progression of flood depth and flood inundated area. Generally, the alternative reservoir operations that attained or maintained a low storage by the end of July (just prior to the occurrence of heavy rainfall in August and September) and then stored inflows thereafter performed better in reducing flood volume as compared with the alternative that attained a low storage by the end of April and then stored inflows thereafter. Further, an operation rule that set a low target level by the end of July had almost the same potential for flood reduction as that of an operation that set a low target level by the end of April and maintained the low storage level until the end of July. These imply that in improving the flood mitigation of the reservoirs, the date when reservoirs are allowed to be filled to their capacity ( $T_r + f_r$ ) is more critical than the date when target date is attained ( $T_r$ ); to improve the operation of the two reservoirs in the event of extreme floods, a later  $T_r + f_r$  should be set after the initial rainy season (May to June) or just before the onset of heavy rainfall season (August to September) to apportion reservoir storage for the heavy reservoir inflows.

#### 4.5 PROJECTION OF THE COMBINED IMPACTS OF CLIMATE CHANGE AND RESERVOIR OPERATION

*This section was omitted in the abridged version of the dissertation because it is being prepared for journal publication.*

*A preliminary version of the findings contained in this section have been presented in a conference. Please refer to Mateo et al., 2014a for the initial findings.*

*The full version of the dissertation will be available online by year 2020.*



#### 4.6 CONTRIBUTIONS, CAVEATS, AND FUTURE WORKS

This study became possible because of the detailed and long-term hydrologic records kindly provided by the RID, Thai Meteorological Department (TMD) and EGAT. The vast availability of data makes Chao Phraya River Basin one of the best river basins for conducting detailed examinations of the performances of advanced global models for analytical and operational purposes. This study can then provide insights on how such detailed tests can be performed. Thus, this paper can potentially benefit the following groups: 1) the operational agencies and researchers concerned about floods in Chao Phraya River Basin and other basins with similar characteristics, and 2) anthropogenic impact, climate change impact, and flood modellers. The contributions, applicability, points for improvement, and future works of the results presented in this chapter are further discussed in the next sections.

##### 4.6.1 On improving the operation of Bhumibol and Sirikit Reservoirs

Intended to be applicable and favourable for practical use, this study aptly used simulation modelling approach which are easier to understand and permits realistic representations of reservoir systems [Simonovic, 1992]. The alternative reservoir operation rules applied simple modifications on the historical operation rules; hence, it is deemed that they are easy to apply practically.

Although the reduction in peak discharge between *ThaiOp\_kRLs* and each of the four alternative reservoir operation is marginal, the reduction in depth, area, and volume of flood inundation proved to be significant. Practically, these reductions will result to significantly lower flood damages. In the future, a flood damage index which takes into account the depth, area, volume, and days of flood inundation as well as land cover or land type can be developed and/or applied to determine the optimum operation of the two reservoirs.

In the present climate, none of the presented alternative operating rules caused reservoir emptying or the depletion of water storage during the dry period primarily because of the adjustment of the release according to the amount of water stored at the beginning of the year. However, all the alternative

operation rules caused an increase in potential supply deficit in the present climate. In the combined climate change and reservoir operation studies, Sirikit reservoir was found to be vulnerable to the depletion of water. This was primarily caused by the smaller capacity of Sirikit reservoir and the use of a constant low target level for all years regardless of the currently available stored water or seasonal forecasts. It may also be caused by the relatively lower increase in precipitation and consequently, runoff, in the catchment basin of Sirikit reservoir. These indicate that a multiple objective approach in setting the reservoir operation have to be taken in future studies. A possible approach can be a more dynamic reservoir operation which adjusts the target level appropriately; the use of a target level coefficient that is inversely proportional to the initial reservoir storage at the beginning of each year or the use of advanced seasonal forecasting techniques can be investigated in the future. Such developments may not only improve the reliability in satisfying target demands but the flood mitigation potential of the reservoirs as well.

It should be noted that the reservoir operation used in both the present and future climate scenarios do not explicitly take into account the changes in irrigation and water supply demands. In the present climate simulations, the irrigation and water supply demands are implicitly taken into account by setting the reservoir operation algorithm according to observed trends in the historical operation. Hypothetically, the irrigation and water supply demands would likely change with socioeconomic and climate changes. The current simulation setup does not yet take such changes into account. A more dynamic reservoir operation algorithm that takes such projected changes into account must be developed in the future in order to provide more dependable future projections. Nonetheless, the results shown in this study provide reliable information on the direction of change of and boundary estimates to projected changes in water availability.

#### 4.6.2 On improving water resources management representation in global models

To the authors' knowledge, no basin scale physically-based hydrological models have been developed for assessing or optimizing the operation of Bhumibol and Sirikit Reservoirs. Thus, this study leveraged on the advancements in free and open source global models. Given that global models have been used in this study, global application of the simulation framework to assess the impacts of reservoirs to flood mitigation may be explored in future studies. However, replication of this study on a global scale requires massive data for establishing reservoir rules and/or validating the reliability of the model; with the current availability of comprehensive databases on reservoir operation, replication of this study on a global scale may be very challenging. Nevertheless, the methodology used in this study may help improve the representation of water resources management, particularly of local reservoir operation, in global models.

One of the distinguishing features of the reservoir operation algorithm introduced in this paper is the use of both storage targets and release rules. A recently published study concluded that combined flood control storage targets and irrigation release targets can best improve the representation of sub-regional water resources management into earth system models [Voisin et al., 2013]. A big difference between this study and that of Voisin et al. is in the methodology used for setting up the storage target and release rules; this study inferred the storage targets and release rules from the long-term mean observed reservoir operation, while Voisin et al. suggested that these rules can be best determined from mean annual natural flows and mean monthly withdrawals. The parameters used by Voisin et al. can be easily computed globally as compared with those used in this study. Hence, for easier global application of this study, the current reservoir operation algorithm may be revised in the future to calculate  $K_o$ ,  $T_o$ ,  $R_m$ , and  $R_d$  using mean annual natural flows and mean monthly withdrawals.

#### 4.6.3 On improving the simulation and assessment of flood events

This study is one of the first studies that have successfully simulated the impacts of reservoir operation on flood inundation using advanced global hydrological models. The combined model was shown to be effective in simulating one of the catastrophic flood events in recent history considering both reservoir operation and flood inundation. This development can potentially improve the integrated analysis of flood events taking into account the confounding impacts of water management.

In most studies done in the past, the impact of reservoir operation to flooding within a basin was commonly assessed by calculating the reduction in peak discharge in several gauging stations downstream of reservoirs. The flood inundation within the river basin is usually inferred from statistical correlation between historical peak discharges and inundation. As flood inundation within a river basin is influenced not only by reservoir operation but also by other hydrologic factors such as rainfall pattern within the basin, this assessment methodology would only be accurate if the other hydrologic factors do not significantly vary in history and in the future (i.e. linearity can be assumed). Through the combined H08-CaMa model, this study took a valuable step forward in explicitly assessing the impacts of alternative reservoir operation rules to the depth, spatial extent, and volume of flood inundation. These inundation metrics are valuable in assessing and clarifying the impacts of reservoir operation decisions at a level that is more understandable and relevant for planning, operational, management, and forecasting purposes. The studies in this chapter, therefore, demonstrated the applicability of advanced global models for analytical as well as practical purposes in regional to basin scales. However, the spatial resolution at which these studies have been conducted (5minute or approximately 9km) may still be too coarse for operational purposes.

Another caveat to the modelling framework is the rigorous calibration required to make the global model applicable on the Chao Phraya River Basin. A significant and promising improvement which can ease this concern has been published recently: a global width database for large rivers using an

algorithm that automatically calculates river width from satellite-based water marks and flow directions has been developed [Yamazaki et al., 2014]. As for the land parameters calibrated in H08, an algorithm for determining land parameters based on land cover and soil type may be developed in the future. Another issue that needs to be addressed is the slight overestimation in calculated flood volume. Incorporation of currently unaccounted anthropogenic factors such as the use of levees, diversion channels and discharge pumps may improve simulation results. The new implementation of CaMa-Flood which takes river bifurcation and diversion channels into account may also help solve this issue. In the next chapter, the roles of representing more complex flows and that of simulating at finer spatial resolutions in improving the flood simulations will be assessed and analysed.

## CHAPTER HIGHLIGHTS

- The relative impacts of spatial resolution and representation of complex flow processes to flood prediction were quantified
- The mechanisms which influence the accurate simulation of flood were explained
- CaMa-Flood model was shown to be suitable for hyper-resolution modelling

### Related publications:

- Mateo et al. (in preparation), Will hyper-resolution modelling always simulate flood inundation in large-scales better?

## CHAPTER 5

### Impacts of varying spatial resolution and representation of complex flow processes on large-scale flood predictions

*This section was omitted in the abridged version of the dissertation because it is being prepared for journal publication.*

*The full version of the dissertation will be available online by year 2020.*

## CHAPTER HIGHLIGHTS

- A new algorithm for detecting and representing dams and their reservoirs was developed
- Reservoirs and their operation were integrated in CaMa-Flood model
- The impacts of reservoir representation and spatial resolution on flood prediction were quantified

## CHAPTER 6

### Physical representation and integration of reservoir operation in CaMa-Flood

*This section was omitted in the abridged version of the dissertation because it is being prepared for journal publication.*

*The full version of the dissertation will be available online by year 2020.*

## DISSERTATION HIGHLIGHTS

- A new algorithm for representing the effects of annual and seasonal variations in the availability of water to reservoir operation was developed
- Better reservoir operation rules for reducing flood inundation were proposed and assessed for the present and future climate
- The impacts of varying complexity of physical representations in a hydrodynamic model and of varying finer spatial resolution to flood predictions were quantified
- A new algorithm for detecting and representing dams and their reservoirs was developed
- Reservoirs and their operation were integrated in CaMa-Flood hydrodynamic model

## CHAPTER 7

### Summary, contributions, future works, and conclusions

#### 7.1 SUMMARY

The accelerating human interventions to the hydrological cycle necessitates the representation of coupled human-natural systems in analysing and understanding water management options. The operation of artificial reservoirs is among the human interventions with the largest impact to the hydrological cycle. While the impacts of the operation of large reservoirs on augmenting limited water supply (e.g. through irrigation, water scarcity, water withdrawal related studies) have been assessed through global hydrological models, their impacts on large scale flooding and flood inundation are rarely assessed. The increasing flood risks necessitates the development of better tools which takes into account the impacts of artificial reservoirs to flood inundation.

This dissertation addressed the aforementioned issues through the development of modelling frameworks which combine or integrate a reservoir operation algorithm with a global hydrologic and hydrodynamic models. The developed models have been applied and tested in a flood prone regional basin, the Chao Phraya River Basin



in Thailand, which is largely impacted by large reservoirs, Bhumibol and Sirikit Reservoirs.

In Chapter 3, the simulation of natural flows by using H08 integrated water resources model with CaMa-Flood hydrodynamic model have been demonstrated. By using the runoff from the calibrated land surface module of H08 model as input to the calibrated CaMa-Flood model, natural flows that adequately resemble the naturalized observed flows in several gauge stations throughout the basin were simulated. In Chapter 4, a new reservoir operation algorithm that considers the seasonal and annual variation in the historical operation of Bhumibol and Sirikit Reservoirs have been developed and coupled with the H08 model. A modelling framework which uses the runoff and dam release outputs from H08 as forcing inputs to CaMa-Flood have been developed. A major advantage of the system is that it can simulate the impacts of large reservoirs to flood inundation in the entire basin. The combined model were used for (1) simulating the immense 2011 Thai Flood, (2) proposing and assessing alternative reservoir operation schemes, and (3) assessing the combined impacts of climate change and reservoir operation in the near and far future. The model was found to adequately simulate the spatio-temporal characteristics of flood inundation during the 2011 Thai flood. However, it tends to overestimate at the low-lying floodplains where the flood flow processes are more complex than in the upstream sections of the river basin. To improve the simulation of flood inundation, the contribution of finer spatial resolution and representation of complex flow processes in CaMa-Flood were examined in Chapter 5. It was found that the simulated extent of inundation improves with finer resolution primarily due to the finer topographical detail. However, it was also found that the capability of the model to simulate discharge and its peaking significantly declines with finer spatial resolution when single downstream connectivity in each grid cell is assumed. On the other hand, simulation results became better with finer spatial resolution when multi-directional downstream connectivity between grid cells is assumed. In Chapter 6, a new algorithm for identifying artificial dams and their reservoirs have been developed. Further, a simple algorithm for representing the bathymetry of the reservoirs have been developed. For consistency, the reservoir operation algorithm used in Chapter 4 was

integrated with CaMa-Flood in order to reduce inconsistencies in the modelling chain. It was found that the representation of the bathymetry of large reservoirs critically affect the accuracy of natural and dam-influenced (regulated) simulations.

## 7.2 CONTRIBUTIONS

The main contributions of this dissertation to the field of hydrology and hydrodynamics can be summarized in the following statements:

- 1) A hydrologic-hydrodynamic modelling framework with improved reservoir operation algorithm that can simulate the impacts of annual and seasonal variability of water on reservoir operation decisions had been developed. The modelling framework can simulate the impacts of large-scale operation of reservoirs on regional flood inundation.
- 2) The modelling framework was shown to be relevant for assessing alternative reservoir operation schemes to mitigate future flood risks, and adapt to climate change.
- 3) The relative impacts of varying spatial resolution and varying flow complexity on improving the predictability of regional scale floods using a global hydrodynamic have been assessed and explained.
- 4) New algorithms to detect dams and their reservoirs in DEMs, and correct the representation of the bathymetry inundated by the reservoirs have been developed. The corrected elevation maps have been used to physically represent reservoirs and integrate their operation with a hydrodynamic model. The technique enabled the simulation of more realistic water levels, storage, and inundated area in the areas within and surrounding the reservoirs.

To the best of the author's knowledge, this dissertation is the first to demonstrate the integration of artificial reservoirs with a global hydrodynamic model for application in regional domains. Further, it is the first to demonstrate an approach to physically represent large reservoirs and assess their impacts on improving the simulation of regional scale flood inundation. This dissertation is also the first to assess the impacts of spatial resolution and subgrid flow physics representation in

a regional to global scale hydrodynamic model; the assessment proved to improve our understanding of the important flow processes in modelling floodplain inundation at multiple spatial scales. While the modelling frameworks have only been applied in one regional river basin, this dissertation demonstrates the applicability of global models for practical uses in the local scale.

### 7.3 LIMITATIONS AND FUTURE WORKS

In spite of these advancements, several challenges and issues still remain. Probably the most apparent source of concern is the applicability of this dissertation, its methods, and its findings in other river basins or in a global scale. The most difficult issue to address in this respect is probably the calibration of the model and setting the parameters for reservoir operation. A more detailed discussion about this issue had been provided in chapter 4. While this issue remains to be addressed either by more advanced calibration techniques or by more physically-based parameterization through the use of globally-available data (i.e. through remotely-sensed physical characteristics or through inferring relationships from globally existing observations), it can be said that generally, the models used still require less parameters to be calibrated as compared with local or smaller scale, more complex models. It is expected that with the increasing availability of data and ongoing community efforts to share information, more physically-based estimation of parameters may be possible in the future and calibration may not have to be rigorously conducted. Meanwhile, the methodology and modelling framework should be assessed and replicated in a similar region with a low lying floodplain that is heavily impacted by large reservoirs (e.g. Three Gorges Dam in China, multiple dams in Danube River Basin in Europe, multiple dams in Parana River Basin in South America). Doing so will identify the strengths and weaknesses of the modelling framework and may identify possible means of simplification or generalization of the parameters used.

While canals, diversion channels, and smaller subgrid channels have been represented in the dissertation through the use of the multi-direction downstream connectivity scheme, the artificial operation of such channels have not been conducted. An approach similar to the generalization of

reservoir operation rules may be used to achieve such capability. In addition, the development of algorithms for automatically detecting other anthropogenic impacts which critically affect hydrodynamics such as dikes, barrages, and pumps may also be explored. However, it is deemed that such modelling efforts in the large scale will be hindered by the limited availability of information on the specific location of such structures, the rules used to operate them, and the data needed for validation.

While a very simple technique to represent the bathymetry of reservoirs have been introduced, the simplification and estimation provides another layer of uncertainty in the modelling chain. Such uncertainties will have to be quantified. The quantification of uncertainties will be beneficial and necessary in case the system is to be used with forecasting techniques or with any efforts for future prediction.

Despite these shortcomings, the new techniques hereby developed disclose opportunities for assessments and analyses that were deemed to be difficult in the past. An interesting study that can be conducted once calibration and replication issues are addressed is the recalculation of global flood risks in the future climate while evaluating the adaptive capability through the existing reservoirs. Reservoir “reoperation” techniques may be assessed or generalized as necessary. A more holistic approach to evaluating multiple benefits from reservoir operation, one that takes into account the benefits from provision of water supply (i.e. drought mitigation), provision of energy, flood control (i.e. flood mitigation), and ecological services, among others, may also be explored and proposed. Such studies are essential for identifying hotspots and where the construction of large reservoirs are necessary for mitigating multiple risks.

Another research project worth conducting would be the integration of other physical, biogeochemical, or ecological process with the system. For example, the integration of a simple sedimentation and sediment flow module will enable the analysis of the effects of large-scale damming of rivers to reducing sediment transfer and deposition in deltas. While reservoirs have been found to delay the global sea level rise, they also significantly reduce the delivery of sediments

to downstream sections of the river basin. This increases the vulnerability of deltas and low-lying floodplains to coastal erosion and flood risks [Syvitski et al., 2005]. The coupling of the system with atmospheric models similar with ISBA-TRIP [Decharme et al., 2008] will result to more realistic estimates of the changes in evapotranspiration due to the fluctuating area of the exposed surface waters in the reservoirs as well as in the floodplain downstream of the reservoirs.

## 7.4 CONCLUSIONS

To conclude, this dissertation has shown the importance of taking into account the human components to realistically model and understand complex natural-human processes such as floods and droughts. The new algorithms for representing reservoirs and modelling frameworks developed in this study proved to be essential tools for understanding and operating reservoirs in order to mitigate floods, ensure the availability of water supply, and to adapt better to the changing climate. This dissertation also highlights the importance of physical representation of processes in modelling natural-human systems. The physically-based representation of reservoirs and flood flow processes have been shown to lead to better predictions of flood flows and inundation in the river basin.

Despite being tested in only one river basin, the tools and techniques presented are essential for directing developments towards improved modelling of human-natural systems and their impacts on flood inundation in regional to global scales. The discussions provided are essential for improving our understanding of the underlying issues of scale and the necessary representation of physical processes. Overall, this dissertation contributes towards progress in physically-based modelling and their application for better prediction of large-scale floods.

## References

1. Adhikari, P., Hong, Y., Douglas, K. R., Kirschbaum, D. B., Gourley, J., Adler, R., & Brakenridge, G. R. (2010). A digitized global flood inventory (1998-2008): Compilation and preliminary results. *Natural Hazards*, 55(2), 405–422. doi:10.1007/s11069-010-9537-2
2. Arduino, G., Reggiani, P., & Todini, E. (2005). Recent advances in flood forecasting and flood risk assessment. *Hydrology and Earth System Sciences*, 9(4), 280–284. doi:10.5194/hess-9-280-2005
3. Baird, L., & Anderson, M. G. (1992). Ungauged catchment modelling I. Assessment of flood plain flow model enhancements. *Catena*, 19(1), 17–31. doi:10.1016/0341-8162(92)90014-3
4. Baird, L., Gee, D. M., & Anderson, M. G. (1992). Ungauged catchment modelling II. Utilization of hydraulic models for validation. *Catena*, 19(1), 33–42. doi:10.1016/0341-8162(92)90015-4
5. Bates, P. D. (2004). Remote sensing and flood inundation modelling. *Hydrological Processes*, 18(13), 2593–2597. doi:10.1002/hyp.5649
6. Bates, P. D. (2012). Integrating remote sensing data with flood inundation models: How far have we got? *Hydrological Processes*, 26(16), 2515–2521. doi:10.1002/hyp.9374
7. Bates, P. D., Anderson, M. G., Baird, L., Walling, D. E., & Simm, D. (1992). Modelling floodplain flows using a two-dimensional finite element model. *Earth Surface Processes and Landforms*, 17(6), 575–588. doi:10.1002/esp.3290170604
8. Bates, P. D., Horritt, M. S., & Fewtrell, T. J. (2010). A simple inertial formulation of the shallow water equations for efficient two-dimensional flood inundation modelling. *Journal of Hydrology*, 387(1-2), 33–45. doi:10.1016/j.jhydrol.2010.03.027
9. Bates, P. D., Horritt, M., & Hervouet, J. M. (1998). Investigating two-dimensional, finite element predictions of floodplain inundation using fractal generated topography. *Hydrological Processes*, 12(8), 1257–1277. doi:10.1002/(SICI)1099-1085(19980630)12:8<1257::AID-HYP672>3.0.CO;2-P
10. Beven, K. (2002). Towards a coherent philosophy for modelling the environment, *Proceedings of the Royal Society of London. Series A: Mathematical, Physical and Engineering Sciences*, 458(2026), 2465–2484, doi: 10.1098/rspa.2002.0986.
11. Beven, K. J., & Cloke, H. L. (2012). Comment on “Hyperresolution global land surface modeling: Meeting a grand challenge for monitoring Earth’s terrestrial water” by Eric F. Wood et al. *Water Resources Research*, 48(1), 2–4. doi:10.1029/2010WR010090

12. Bierkens, M. F. P., Bell, V. A., Burek, P., Chaney, N., Condon, L. E., David, C. H., ... Wood, E. F. (2015). Hyper-resolution global hydrological modelling: what is next? *Hydrological Processes*, 29(2), 310–320. doi:10.1002/hyp.10391
13. Bower, B. T., M. M. Hufschmidt, & W. H. Reedy (1962). Operating procedures: Their role in the design and implementation of water resource systems by simulation analysis, in *Design of Water Resource Systems*, edited by A. Maass et al., chap. 11, pp. 443–358, Harvard Univ. Press, Cambridge, Mass.
14. Brakenridge, G. R. (2015). "Global Active Archive of Large Flood Events", Dartmouth Flood Observatory, University of Colorado, <http://floodobservatory.colorado.edu/Archives/index.html> [last accessed: March 2015].
15. Bhumralkar, C. (1975). Numerical experiments on the computation of ground surface temperature in an atmospheric general circulation model, *J. Appl. Meteorol.*, 14, 1246-1258.
16. Chang, H., Franczyk, J., & Kim, C. (2009). What is responsible for increasing flood risks? The case of Gangwon Province, Korea. *Natural Hazards*, 48(3), 339–354. doi:10.1007/s11069-008-9266-y
17. Chongvilaivan, A. (2012). Thailand's 2011 flooding: Its impact on direct exports, and disruption of global supply chains, in *ARTNET Policy Brief No. 34*, UN Economic and Social Commission for Asia and the Pacific, Bangkok. [Available at [www.artnetontrade.org](http://www.artnetontrade.org).]
18. Christensen, N. S., Wood, A. W., Voisin, N., Lettenmaier, D. P., & Palmer, R. N. (2004). The Effects of Climate Change on the Hydrology and Water Resources of the Colorado River Basin. *Climate Change*, (Figure 1), 337–363. doi:10.1023/B:CLIM.00000013684.13621.1f
19. Coe, M. T. (2000). Modeling terrestrial hydrological systems at the continental scale: Testing the accuracy of an atmospheric GCM. *Journal of Climate*, 13(4), 686–704. doi:10.1175/1520-0442(2000)013<0686:MTHSAT>2.0.CO;2
20. Coe, M. T., Costa, M. H., & Howard, E. A. (2008). Simulating the surface waters of the Amazon River basin: impacts of new river geomorphic and flow parameterizations. *Hydrological Processes*, 22(14), 2542–2553. doi:10.1002/hyp
21. Cook, A., & Merwade, V. (2009). Effect of topographic data, geometric configuration and modeling approach on flood inundation mapping. *Journal of Hydrology*, 377(1-2), 131–142. doi:10.1016/j.jhydrol.2009.08.015
22. Dankers, R., Arnell, N. W., Clark, D. B., Falloon, P. D., Fekete, B. M., Gosling, S. N., ... Wisser, D. (2014). First look at changes in flood hazard in the Inter-Sectoral Impact Model Intercomparison Project ensemble. *Proceedings of the National Academy of Sciences of the United States of America*, 111(9), 3257–61. doi:10.1073/pnas.1302078110

23. De Paes, R. P., & Brandão, J. L. B. (2013). Flood Control in the Cuiabá River Basin, Brazil, with Multipurpose Reservoir Operation. *Water Resources Management*, 27(11), 3929–3944. doi:10.1007/s11269-013-0388-y
24. Deardoff, J. W. (1978). Efficient prediction of ground surface temperature and moisture, with inclusion of a layer of vegetation, *J. Geophys. Res.*, 83-C4, 1889-1903.
25. Decharme, B., Douville, H., Prigent, C., Papa, F., & Aires, F. (2008). A new river flooding scheme for global climate applications: Off-line evaluation over South America. *Journal of Geophysical Research: Atmospheres*, 113(11), 1–11. doi:10.1029/2007JD009376
26. DHI (2012), Thailand Floods 2011—The Need for Holistic Flood Risk Management, DHI-NTU Res. Cent., Singapore.
27. Di Baldassarre, G., & Uhlenbrook, S. (2012). Is the current flood of data enough? A treatise on research needs for the improvement of flood modelling. *Hydrological Processes*, 26(1), 153–158. doi:10.1002/hyp.8226
28. Di Baldassarre, G., A. Montanari, H. F. Lins, D. Koutsoyiannis, L. Brandimarte, & G. Blöschl (2010). Flood fatalities in Africa: From diagnosis to mitigation, *Geophys. Res. Lett.*, 37, L22402, doi:10.1029/2010GL045467.
29. Di Baldassarre, G., Kooy, M., Kemerink, J. S., & Brandimarte, L. (2013). Towards understanding the dynamic behaviour of floodplains as human-water systems. *Hydrology and Earth System Sciences*, 17, 3235–3244. doi:10.5194/hess-17-3235-2013
30. Döll, P., Fiedler, K., & Zhang, J. (2009). Global-scale analysis of river flow alterations due to water withdrawals and reservoirs. *Hydrology and Earth System Sciences*, 13, 2413–2432. doi:10.5194/hess-13-2413-2009
31. Döll, P., Kaspar, F., & Lehner, B. (2003). A global hydrological model for deriving water availability indicators: Model tuning and validation. *Journal of Hydrology*, 270(1-2), 105–134. doi:10.1016/S0022-1694(02)00283-4
32. Dutta, D., S. Herath, & K. Musiake (2003). A mathematical model for flood loss estimation, *J. Hydrol.*, 277, 24–29, doi:10.1016/S0022-1694(03)00084-2.
33. EM-DAT (2015), The OFDA/CRED International Disaster Database, Version 12.07, Univ. Catholique de Louvain, Brussels. [Available at [www.emdat.be](http://www.emdat.be), last accessed Jan 2015.]
34. Eum, H. I., & Simonovic, S. P. (2010). Integrated Reservoir Management System for Adaptation to Climate Change: The Nakdong River Basin in Korea. *Water Resources Management*, 24(13), 3397–3417. doi:10.1007/s11269-010-9612-1
35. Eum, H. I., Vasan, A., & Simonovic, S. P. (2012). Integrated Reservoir Management System for Flood Risk Assessment Under Climate Change. *Water Resources Management*, 26(13), 3785–3802. doi:10.1007/s11269-012-0103-4



36. FAO (2015), Aquastat database, Food and Agriculture Organization of the United Nations (FAO), Rome, Italy. [Available at: [www.fao.org/nr/water/aquastat/countries\\_regions/index.stm](http://www.fao.org/nr/water/aquastat/countries_regions/index.stm), last accessed Apr 2014.]
37. Farr, T. G., et al. (2007), The Shuttle Radar Topography Mission, *Rev. Geophys.*, 45, RG2004, doi:10.1029/2005RG000183.
38. GAME-T2 Data Center (2004), Thailand Routine Observation, Musiaka and Oki Lab (GAME-T headquarters), IIS, University of Tokyo, Japan [Available at <http://hydro.iis.u-tokyo.ac.jp/GAME-T/GAIN-T/routine/thailand/index.html>, last accessed Jan 2015.]
39. Gerten, D., S. Schaphoff, U. Haberlandt, W. Lucht, & S. Sitch (2004). Terrestrial vegetation and water balance - hydrological evaluation of a dynamic global vegetation model, *J. Hydrol.*, 286, 249–270.
40. Getirana, A., Boone, A., Yamazaki, D., Decharme, B., Papa, F., & Mognard, N. (2012). The Hydrological Modeling and Analysis Platform (HyMAP): evaluation in the Amazon basin. *Journal of Hydrometeorology*, 120630073030006. doi:10.1175/JHM-D-12-021.1
41. Haddeland, I., Skaugen, T., & Lettenmaier, D. P. (2006). Anthropogenic impacts on continental surface water fluxes. *Geophysical Research Letters*, 33(8), 2–5. doi:10.1029/2006GL026047
42. Hanasaki, N., Kanae, S., & Oki, T. (2006). A reservoir operation scheme for global river routing models. *Journal of Hydrology*, 327(1-2), 22–41. doi:10.1016/j.jhydrol.2005.11.011
43. Hanasaki, N., Kanae, S., Oki, T., Masuda, K., Motoya, K., Shirakawa, N., ... Tanaka, K. (2008a). An integrated model for the assessment of global water resources – Part 1 : Model description and input meteorological forcing. *Hydrol. Earth Syst. Sci.*, 12, 1007–1025. doi:10.5194/hess-12-1027-2008
44. Hanasaki, N., Kanae, S., Oki, T., Masuda, K., Motoya, K., Shirakawa, N., ... Tanaka, K. (2008b). An integrated model for the assessment of global water resources – Part 2: Applications and assessments. *Hydrology and Earth System Sciences*. doi:10.5194/hess-12-1027-2008
45. Hardy, R. J., Bates, P. D., & Anderson, M. G. (1999). The importance of spatial resolution in hydraulic models for floodplain environments. *Journal of Hydrology*, 216(1-2), 124–136. doi:10.1016/S0022-1694(99)00002-5
46. Hardy, R. J., Bates, P. D., & Anderson, M. G. (2000). Modelling suspended sediment deposition on a fluvial floodplain using a two-dimensional dynamic finite element model. *Journal of Hydrology*, 229(3-4), 202–218. doi:10.1016/S0022-1694(00)00159-1

47. Harrison, J. A., Maranger, R. J., Alexander, R. B., Giblin, A. E., Jacinthe, P. A., Mayorga, E., ... Wollheim, W. M. (2009). The regional and global significance of nitrogen removal in lakes and reservoirs. *Biogeochemistry*, 93(1-2), 143–157. doi:10.1007/s10533-008-9272-x
48. Hatcher, K. L., & Jones, J. A. (2013). Climate and Streamflow Trends in the Columbia River Basin: Evidence for Ecological and Engineering Resilience to Climate Change. *Atmosphere-Ocean*, 51(4), 436–455. doi:10.1080/07055900.2013.808167
49. Hirabayashi, Y., Mahendran, R., Koirala, S., Konoshima, L., Yamazaki, D., Watanabe, S., ... Kanae, S. (2013). Global flood risk under climate change. *Nature Climate Change*, 3(6), 1–6. doi:10.1038/nclimate1911
50. Hirabayashi, Y., S. Kanae, K. Motoya, K. Masuda, & P. Döll (2008). A 59-year (1948–2006) global near-surface meteorological data set for land surface models. Part I: Development of daily forcing and assessment of precipitation intensity, *Hydrol. Res. Lett.*, 2, 36–40, doi:10.3178/HRL.2.36.
51. Hirsch, R. M., & K. R. Ryberg (2012). Has the magnitude of floods across the USA changed with global CO2 levels?, *Hydrol. Sci. J.*, 57(1), 1–9, doi:10.1080/02626667.2011.621895.
52. Horritt, M. S., & Bates, P. D. (2002). Evaluation of 1D and 2D numerical models for predicting river flood inundation. *Journal of Hydrology*, 268(1-4), 87–99. doi:10.1016/S0022-1694(02)00121-X
53. Hunter, N. M., Bates, P. D., Horritt, M. S., & Wilson, M. D. (2007). Simple spatially-distributed models for predicting flood inundation: A review. *Geomorphology*, 90(3-4), 208–225. doi:10.1016/j.geomorph.2006.10.021
54. IPCC (2012), Managing the risks of extreme events and disasters to advance climate change adaptation, in *A Special Report of Working Groups I and II of the Intergovernmental Panel on Climate Change*, edited by C. B. Field et al., 582 pp., Cambridge Univ. Press, Cambridge, U. K.
55. IPCC Working Groups I & II. (2012). *Managing the Risks of Extreme Events and Disasters to Advance Climate Change Adaptation - SUMMARY FOR POLICYMAKERS*. doi:10.1017/CBO9781139177245
56. Junk, W. J., Bayley, P. B., & Sparks, R. E. (1989). The flood pulse concept in river-floodplain systems. In D. P. Dodge (Ed.), *Proceedings of the International Large River Symposium*, 106(1), (pp. 110–127). Canadian Special Publication on Fisheries and Aquatic Sciences.
57. Kirchner, J. W. (2006). Getting the right answers for the right reasons: Linking measurements, analyses, and models to advance the science of hydrology. *Water Resources Research*, 42(3), 1–5. doi:10.1029/2005WR004362

58. Komori, D. et al., (2013). Application of the probability evaluation for the seasonal reservoir operation on flood mitigation and water supply in the Chao Phraya River Watershed, Thailand, *J. Disaster Res.*, 8(3), 432–446.
59. Komori, D., S. Nakamura, M. Kiguchi, A. Nishijima, D. Yamazaki, S. Suzuki, A. Kawasaki, K. Oki, & T. Oki (2012). Characteristics of the 2011 Chao Phraya River flood in Central Thailand, *Hydrol. Res. Lett.*, 6, 41–46, doi:10.3178/HRL.6.41.
60. Kotsuki, S., & K. Tanaka (2013). Uncertainties of precipitation products and their impacts on runoff estimates through hydrological land surface simulation in Southeast Asia, *Hydrol. Res. Lett.*, 7(4), 79–84, doi:10.3178/hrl.7.79.
61. Kundzewicz, Z. W., Kanae, S., Seneviratne, S. I., Handmer, J., Nicholls, N., Peduzzi, P., ... Sherstyukov, B. (2014). Flood risk and climate change: global and regional perspectives. *Hydrological Sciences Journal*, 59(1), 1–28. doi:10.1080/02626667.2013.857411
62. Labadie, J. (2004), Optimal operation of multireservoir systems: State-of-the-art review, *J. Water Resour. Plann.*, 130(2), 93–111.
63. Lee, S. Y., Hamlet, A. F., Fitzgerald, C. J., & Burges, S. J. (2009). Optimized Flood Control in the Columbia River Basin for a Global Warming Scenario. *Journal of Water Resources Planning and Management*, 135(6), 440–450. doi:10.1061/(ASCE)0733-9496(2009)135:6(440)
64. Lehner, B., & Grill, G. (2013). Global river hydrography and network routing: Baseline data and new approaches to study the world's large river systems. *Hydrological Processes*, 27(15), 2171–2186. doi:10.1002/hyp.9740
65. Lehner, B., K. Verdin, & A. Jarvis (2008). New global hydrography derived from spaceborne elevation data, *Eos Trans. AGU*, 89(10), 93–94, doi:10.1029/2008EO100001.
66. Lehner, B., R-Liermann, C., Revenga, C., Vörösmarty, C., Fekete, B., Crouzet, P., Döll, P. et al.: High resolution mapping of the world's reservoirs and dams for sustainable river flow management. *Frontiers in Ecology and the Environment*. Source: GWSP Digital Water Atlas (2008). Map 81: GRanD Database (V1.0). Available online at <http://atlas.gwsp.org>.
67. Lima, I. B. T., Ramos, F. M., Bambace, L. A. W., & Rosa, R. R. (2008). Methane emissions from large dams as renewable energy resources: A developing nation perspective. *Mitigation and Adaptation Strategies for Global Change*, 13(2), 193–206. doi:10.1007/s11027-007-9086-5
68. Lund, J., & I. Ferreira (1996). Operating rule optimization for Missouri River Reservoir System, *J. Water Resour. Plann.*, 122(4), 287–295.
69. Lund, J., & J. Guzman (1999). Derived operating rules for reservoirs in series or in parallel, *J. Water Resour. Plann.*, 125(3), 143–153.
70. Manabe, S. (1969). Climate and the ocean circulation – 1: The atmospheric circulation and the hydrology of the Earth's surface, *Mon. Weather Rev.*, 97-11, 739-774.

71. Mateo, C. M., N. Hanasaki, D. Komori, K. Tanaka, M. Kiguchi, A. Champathong, T. Sukhapunnaphan, D. Yamazaki, & T. Oki (2014a). Assessing the impacts of reservoir operation to floodplain inundation by combining hydrological, reservoir management, and hydrodynamic models, *Water Resour. Res.*, 50, 7245–7266, doi:10.1002/2013WR014845.
72. Mateo, C. M. R., et al. (2014b). Modeling the impacts of climate change to reservoir operation and flood inundation in Chao Phraya River Basin, *Proceedings of the 7th International Scientific Conference on the Global Water and Energy Cycle (GEWEX 2014)*, 14-17 July 2014, The Hague, Netherlands.
73. Mateo, C., N. Hanasaki, D. Komori, K. Yoshimura, M. Kiguchi, A. Champathong, T. Sukhapunnaphan, D. Yamazaki, & T. Oki (2013). A simulation study on modifying reservoir operation rules: Tradeoffs between flood mitigation and water supply, in *Considering Hydrological Change in Reservoir Planning and Management*, edited by A. Schumann (IAHS Publ. 362) pp. 33–40, IAHS Press, Wallingford, U. K.
74. McMillan, H. K., & Brasington, J. (2007). Reduced complexity strategies for modelling urban floodplain inundation. *Geomorphology*, 90(3-4), 226–243. doi:10.1016/j.geomorph.2006.10.031
75. Merz, R., & Blöschl, G. (2008). Flood frequency hydrology: 1. Temporal, spatial, and causal expansion of information. *Water Resources Research*, 44(8), 1–17. doi:10.1029/2007WR006744
76. Milly, P. C. D., Wetherald, R. T., Dunne, K. A., & Delworth, T. L. (2002). Increasing risk of great floods in a changing climate. *Nature*, 415(6871), 514–517. doi:10.1038/415514a
77. Montanari, A., Young, G., Savenije, H. H. G., Hughes, D., Wagener, T., Ren, L. L., ... Belyaev, V. (2013). “Panta Rhei—Everything Flows”: Change in hydrology and society—The IAHS Scientific Decade 2013–2022. *Hydrological Sciences Journal*, 58(6), 1256–1275. doi:10.1080/02626667.2013.809088
78. Moriasi, D. N., J. G. Arnold, M. W. Van Liew, R. L. Bingner, R. D. Harmel, & T. L. Veith (2007). Model evaluation guidelines for systematic quantification of accuracy in watershed simulations, *Trans. Am. Soc. Agric. Biol. Eng.*, 50(3), 885–900.
79. Munich, R. E. (2013). Significant natural catastrophes 1980–2012: 10 costliest floods worldwide ordered by overall losses, Munchener Ruckversicherungs-Gesellschaft, *Geo Risks Res.*, NatCatSERVICE, Munich, Germany. [Available at <https://www.munichre.com/touch/site/touchnaturalhazards>, last accessed Mar 2014.]
80. Nalbantis, I., & D. Koutsoyiannis (1997). A parametric rule for planning and management of multiple reservoir systems, *Water Resour. Res.*, 33(9), 2165–2177.
81. Nalbantis, I., Efstratiadis, A., Rozos, E., Kopsiafti, M., & Koutsoyiannis, D. (2011). Holistic versus monomeric strategies for hydrological modelling of human-modified hydrosystems. *Hydrology and Earth System Sciences*, 15(3), 743–758. doi:10.5194/hess-15-743-2011

82. Neal, J., Schumann, G., & Bates, P. (2012). A subgrid channel model for simulating river hydraulics and floodplain inundation over large and data sparse areas. *Water Resources Research*, 48(11), 1–16. doi:10.1029/2012WR012514
83. Neal, J., Villanueva, I., Wright, N., Willis, T., Fewtrell, T., & Bates, P. (2012). How much physical complexity is needed to model flood inundation? *Hydrological Processes*, 26(15), 2264–2282. doi:10.1002/hyp.8339
84. Ngo-Duc, T., Oki, T., Kanae, S., & Ngo, T. (2007). A variable stream flow velocity method for global river routing model: model description and preliminary results. *Hydrology and Earth System Sciences*, 4(6), 4389–4414. doi:10.5194/hessd-4-4389-2007
85. Ngo-Duc, T., Polcher, J., & Laval, K. (2005). A 53-year forcing data set for land surface models. *Journal of Geophysical Research D: Atmospheres*, 110(6), 1–13. doi:10.1029/2004JD005434
86. Office of Natural Water Resources Committee (ONWRC) of Thailand Working Group (2003), Chao Phraya River Basin, Thailand, in: *World Water Development Report – 2003*, Bangkok, Thailand, part V, chap. 16, pp. 387–400, UNESCO Publishing and Bergahn Books, Paris, France. [Available at [www.wvvc.uwaterloo.ca](http://www.wvvc.uwaterloo.ca).]
87. Oki, T., & Sud, Y. C. (1998). Design of Total Runoff Integrating Pathways (TRIP)—A Global River Channel Network. *Earth Interactions*, 2(1), 1–1. doi:10.1175/1087-3562(1998)002<0001:DoTRIP>2.0.CO;2
88. Oldenborgh, G., A. Urk, & M. Allen (2012). The absence of a role of climate change in the 2011 Thailand floods, *Am. Meteorol. Soc.*, 93(7), 1041–1067, doi:10.1175/BAMS-D-12-00021.1.
89. Oliveri, E., & Santoro, M. (2000). Estimation of urban structural flood damages: the case study of Palermo. *Urban Water*, 2(3), 223–234. doi:10.1016/S1462-0758(00)00062-5
90. Opperman, J. J., Galloway, G. E., Fargione, J., Mount, J. F., Richter, B. D., & Secchi, S. (2009). Large-Scale Reconnection to Rivers. *Science*, 326(5959), 1487–1488. doi:10.1126/science.1178256
91. Paiva, R. C. D., Collischonn, W., & Buarque, D. C. (2013). Validation of a full hydrodynamic model for large-scale hydrologic modelling in the Amazon. *Hydrological Processes*, 27(3), 333–346. doi:10.1002/hyp.8425
92. Paiva, R. C. D., Collischonn, W., & Tucci, C. E. M. (2011). Large scale hydrologic and hydrodynamic modeling using limited data and a GIS based approach. *Journal of Hydrology*, 406(3-4), 170–181. doi:10.1016/j.jhydrol.2011.06.007
93. Pall, P., T. Aina, D. Stone, P. Stott, T. Nozawa, A. Hilberts, D. Lohmann, & M. Allen (2011). Anthropogenic greenhouse gas contribution to flood risk in England and Wales in autumn 2000, *Nature*, 470, 382–385, doi:10.1038/nature09762.

94. Papanicolaou, A. N. T., Krallis, G., & Edinger, J. (2008). Sediment Transport Modeling Review — Current and, (January), 1–14.
95. Pappenberger, F., Bartholmes, J., Thielen, J., Cloke, H. L., Buizza, R., & de Roo, A. (2008). New dimensions in early flood warning across the globe using grand-ensemble weather predictions. *Geophysical Research Letters*, 35(10), 1–7. doi:10.1029/2008GL033837
96. Payne, J., Wood, A., & Hamlet, A. (2004). Mitigating the effects of climate change on the water resources of the Columbia River basin. *Climatic Change*, 62, 233–256. doi:10.1023/B:CLIM.0000013694.18154.d6
97. Pinthong, P., A. Das Gupta, M. S. Babel, & S. Weesakul (2009). Improved reservoir operation using hybrid genetic algorithm and neurofuzzy computing, *Water Resour. Manage.*, 23(4), 697–720, doi:10.1007/s11269-008-9295-z.
98. Rakwatin, P., T. Sansena, N. Marjang, & A. Rungsipanich (2013), Using multi-temporal remote-sensing data to estimate 2011 flood area and volume over Chao Phraya River basin, Thailand, *Remote Sens. Lett.*, 4(3), 243–250, doi:10.1080/2150704X.2012.723833.
99. Robock, A., Vinnikov, K. Y., Schlosser, C. A., Sperskaya, N. A., & Xue, Y. K. (1995). Use of mid-latitude soil-moisture and meteorological observations to validate soil-moisture simulations with biosphere and bucket models, *J. Climate*, 8, 15-35.
100. Rost, S., Gerten, D., Bondeau, A., Lucht, W., Rohwer, J., & Schaphoff, S. (2008). Agricultural green and blue water consumption and its influence on the global water system. *Water Resources Research*, 44(9), 1–17. doi:10.1029/2007WR006331
101. Schumann, G., Bates, P. D., Horritt, M. S., Matgen, P., & Pappenberger, F. (2009). Progress in integration of remote sensing-derived flood extent and stage data and hydraulic models. *Reviews of Geophysics*, 47(3), 1–20. doi:10.1029/2008RG000274
102. Seibert, S. P., Skublics, D., & Ehret, U. (2014). The potential of coordinated reservoir operation for flood mitigation in large basins – A case study on the Bavarian Danube using coupled hydrological–hydrodynamic models. *Journal of Hydrology*, 517, 1128–1144. doi:10.1016/j.jhydrol.2014.06.048
103. Simonovic, S. P. (1992). Reservoir systems analysis: Closing gap between theory and practice, *J. Water Resour. Plann. Manage.*, 118, 262–280, doi:10.1061/(ASCE)0733–9496(1992)118:3(262).
104. Sivapalan, M., Thompson, S. E., Harman, C. J., Basu, N. B., & Kumar, P. (2011). Water cycle dynamics in a changing environment: Improving predictability through synthesis. *Water Resources Research*, 47(10), 1–7. doi:10.1029/2011WR011377
105. Smith, A., Sampson, C., & Bates, P. (2015). Regional flood frequency analysis at the global scale. *Water Resources Research*, 51(1), 539–553. doi:10.1002/2014WR015814



106. Sripong, H., W. Khao-uppatum, & S. Thanopanuwat (2000). Flood management in Chao Phraya River Basin, in *Proceedings of the International Conference on The Chao Phraya Delta: Historical Development, Dynamics and Challenges of Thailand's Rice Bowl*, Kasetsart Univ., Bangkok. [Available at <http://www.std.cpc.ku.ac.th/delta/deltacp/home.htm> in, last accessed Aug 2012.]
107. St. Louis, V. L., Kelly, C. a., Duchemin, É., Rudd, J. W. M., & Rosenberg, D. M. (2000). Reservoir Surfaces as Sources of Greenhouse Gases to the Atmosphere: A Global Estimate. *BioScience*, 50(9), 766. doi:10.1641/0006-3568(2000)050[0766:RSASOG]2.0.CO;2
108. Suiadee, W., & T. Tingsanchali (2007). A combined simulation-genetic algorithm optimization for optimal rule curves of a reservoir: A case study of the Nam Oon Irrigation Project, Thailand, *Hydrol. Processes*, 21(23), 3211–3225, doi:10.1002/hyp.6528.
109. Swiss Re (2012). Natural catastrophes and man-made disasters in 2011: Historic losses surface from record earthquakes and floods, *Sigma*, 2, Swiss Reinsurance Co. Ltd., Econ. Res. & Consult., Zurich, Switz. [Available at [http://media.swissre.com/documents/sigma2\\_2012\\_en.pdf](http://media.swissre.com/documents/sigma2_2012_en.pdf), last accessed Mar 2014.]
110. Syvitski, J. P. M., Vörösmarty, C. J., Kettner, A. J., & Green, P. (2005). Impact of Humans on the Flux of Terrestrial Sediment to the Global Coastal Ocean. *Science*, 308, 376–380. doi:10.1126/science.1109454
111. Tebakari, T., J. Yoshitani, & P. Suvanpimol (2012), Impact of large-scale reservoir operation on flow regime in the Chao Phraya River Basin, Thailand, *Hydrol. Processes*, 26, 2411–2420, doi:10.1002/hyp.9345.
112. Tospornsampan, J., I. Kita, M. Ishii, & Y. Kitamura (2005a), Optimization of a multiple reservoir system operation using a combination of genetic algorithm and discrete differential dynamic programming: A case study in Mae Klong system, Thailand, *Paddy Water Environ.*, 3, 29–38, doi:10.1007/s10333-005-0070-y.
113. Tospornsampan, J., I. Kita, M. Ishii, & Y. Kitamura (2005b), Optimization of a multiple reservoir system operation using a simulated annealing: A case study in Mae Klong system, Thailand, *Paddy Water Environ.*, 3, 137–147, doi:10.1007/s10333-005-0010-x.
114. US Army Corps of Engineers (1996), Developing seasonal and long-term reservoir system operation plans using HEC-PRM, US Army Corps of Eng. Rep. RD-40, *Hydrol. Eng. Cent.*, Davis, Calif.
115. Van Beek, L. P. H., Wada, Y., & Bierkens, M. F. P. (2011). Global monthly water stress: 1. Water balance and water availability. *Water Resources Research*, 47(7), n/a–n/a. doi:10.1029/2010WR009791

116. Van Der Knijff, J. M., Younis, J., & De Roo, A. P. J. (2010). LISFLOOD: a GIS-based distributed model for river basin scale water balance and flood simulation. *International Journal of Geographical Information Science*, 24(2), 189–212. doi:10.1080/13658810802549154
117. Vergnes, J. P., & Decharme, B. (2012). A simple groundwater scheme in the TRIP river routing model: Global off-line evaluation against GRACE terrestrial water storage estimates and observed river discharges. *Hydrology and Earth System Sciences*, 16(10), 3889–3908. doi:10.5194/hess-16-3889-2012
118. Voisin, N., Li, H., Ward, D., Huang, M., Wigmosta, M., & Leung, L. R. (2013). On an improved sub-regional water resources management representation for integration into earth system models. *Hydrology and Earth System Sciences*, 17(9), 3605–3622. doi:10.5194/hess-17-3605-2013
119. Vörösmarty, C. J., & Sahagian, D. (2000). Anthropogenic Disturbance of the Terrestrial Water Cycle. *BioScience*, 50(9), 753. doi:10.1641/0006-3568(2000)050[0753:ADOT\*TW]2.0.CO;2
120. Vörösmarty, C. J., Green, P., Salisbury, J., & Lammers, R. B. (2000). Global Water Resources: Vulnerability from Climate Change and Population Growth. *Science*, 289(5477), 284–288. doi:10.1126/science.289.5477.284
121. Vörösmarty, C. J., Meybeck, M., Fekete, B., Sharma, K., Green, P., & Syvitski, J. P. M. (2003). Anthropogenic sediment retention: Major global impact from registered river impoundments. *Global and Planetary Change*, 39(1-2), 169–190. doi:10.1016/S0921-8181(03)00023-7
122. Vörösmarty, C. J., Sharma, K., Fekete, B. M., Copeland, A. H., Holden, J., Marble, J., & Lough, J. (1997). The Storage and Aging of Continental Runoff in Large Reservoir Systems of the World. *Ambio*, 26(4), 210–219.
123. Wada, Y., van Beek, L. P. H., Viviroli, D., Dürr, H. H., Weingartner, R., & Bierkens, M. F. P. (2011). Global monthly water stress: 2. Water demand and severity of water stress. *Water Resources Research*, 47(7), n/a–n/a. doi:10.1029/2010WR009792
124. Wagener, T., Sivapalan, M., Troch, P. A., McGlynn, B. L., Harman, C. J., Gupta, H. V., ... Wilson, J. S. (2010). The future of hydrology: An evolving science for a changing world. *Water Resources Research*, 46(5), 1–10. doi:10.1029/2009WR008906
125. Water Resources System Research Unit (2013). *The Impact of Climate Change on Irrigation Systems and Adaptation Measures (Dam Operation Analysis)*. Final Report on February 2013, Faculty of Engineering, Chulalongkorn University, Bangkok, Thailand. [Available at <http://project->



- wre.eng.chula.ac.th/watercu\_eng/sites/default/files/publication/Final%20Report\_JIID%2004\_2013.03.09.pdf, last accessed Jun 2014.]
126. Wichakul, S., Y. Tachikawa, M. Shiiba, & K. Yorozu (2013a). Developing a regional distributed hydrological model for water resources assessment and its application to the Chao Phraya River Basin, *J. Jpn. Soc. Civ. Eng.*, 69(4), I\_43–I\_48.
  127. Wichakul, S., Y. Tachikawa, M. Shiiba, & K. Yorozu (2013b). Development of a flow routing model including inundation effect for the extreme flood in the Chao Phraya River Basin, Thailand 2011, *J. of Disaster Res.*, 8(3), 415–423.
  128. Wilson, M. D., Bates, P., Alsdorf, D., Forsberg, B., Horritt, M., Melack, J., ... Famiglietti, J. (2007). Modeling large-scale inundation of Amazonian seasonally flooded wetlands. *Geophysical Research Letters*, 34(15), 4–9. doi:10.1029/2007GL030156
  129. Wisser, D., Fekete, B. M., Vörösmarty, C. J., & Schumann, A. H. (2010). Reconstructing 20th century global hydrography: a contribution to the Global Terrestrial Network-Hydrology (GTN-H). *Hydrology and Earth System Sciences*, 14, 1–24. doi:10.5194/hess-14-1-2010
  130. Wood, E. F., Roundy, J. K., Troy, T. J., Van Beek, L. P. H., Bierkens, M. F. P., Blyth, E., ... Whitehead, P. (2011). Hyperresolution global land surface modeling: Meeting a grand challenge for monitoring Earth's terrestrial water. *Water Resources Research*, 47(5), 1–10. doi:10.1029/2010WR010090
  131. Wood, E. F., Roundy, J. K., Troy, T. J., Van Beek, R., Bierkens, M., Blyth, E., ... Whitehead, P. (2012). Reply to comment by Keith J. Beven and Hannah L. Cloke on “hyperresolution global land surface modeling: Meeting a grand challenge for monitoring Earth's terrestrial water.” *Water Resources Research*, 48(1), 10–12. doi:10.1029/2011WR011202
  132. World Bank (2012). *Rapid Assessment for Resilient Recovery and Reconstruction Planning*. Joint Publ. of World Bank and Global Facil. for Disaster Reduct. and Recovery, Bangkok.
  133. Wurbs, R. (1993). Reservoir-system simulation and optimization models, *J. Water Resour. Plann.*, 119(4), 455–472.
  134. Yamazaki, D., Baugh, C. A., Bates, P. D., Kanae, S., Alsdorf, D. E., & Oki, T. (2012). Adjustment of a spaceborne DEM for use in floodplain hydrodynamic modeling. *Journal of Hydrology*, 436–437, 81–91. doi:10.1016/j.jhydrol.2012.02.045
  135. Yamazaki, D., De Almeida, G. A. M., & Bates, P. D. (2013). Improving computational efficiency in global river models by implementing the local inertial flow equation and a vector-based river network map. *Water Resources Research*, 49(11), 7221–7235. doi:10.1002/wrcr.20552

136. Yamazaki, D., Kanae, S., Kim, H., & Oki, T. (2011). A physically based description of floodplain inundation dynamics in a global river routing model. *Water Resources Research*, 47(4), 1–21. doi:10.1029/2010WR009726
137. Yamazaki, D., Lee, H., Alsdorf, D. E., Dutra, E., Kim, H., Kanae, S., & Oki, T. (2012). Analysis of the water level dynamics simulated by a global river model: A case study in the Amazon River. *Water Resources Research*, 48(9), 1–15. doi:10.1029/2012WR011869
138. Yamazaki, D., O’Loughlin, F., Trigg, M. A., Miller, Z. F., Pavelsky, T. M., & Bates, P. D. (2014). Development of Global Width Database for Large Rivers. *Water Resources Research*, 50(4), 3467–3480. doi:10.1002/2013WR014664
139. Yamazaki, D., Oki, T., & Kanae, S. (2009). Deriving a global river network map and its sub-grid topographic characteristics from a fine-resolution flow direction map, *Hydrol. Earth Syst. Sci.*, 13, 2241–2251, doi:10.5194/hess-13-2241-2009.
140. Yamazaki, D., Sato, T., Kanae, S., Hirabayashi, Y., & Bates, P. D. (2014). Regional flood dynamics in a bifurcating mega delta simulated in a global river model. *Geophysical Research Letters*, 41, 3127–3135. doi:10.1002/2014GL059744.

# Appendix

## A. CALIBRATION OF MODEL PARAMETERS

The calibration of parameters was carried out at Nakhon Sawan Station, also known as C2 Station, a critical station that is located just after the confluence of the four main tributaries of the Chao Phraya River Basin (Figure 3.3). Seven parameters have been calibrated in this study: 1) bulk transfer coefficient ( $C_D$ ), 2) soil depth ( $SD$ ), 3) time constant for daily maximum subsurface runoff ( $\tau$ ), and 4) shape parameter which sets the relationship between subsurface flow and soil moisture ( $\gamma$ ) were calibrated in the H08 model; 5) river channel width, 6) bank height, and 7) Manning's roughness coefficient were calibrated in the CaMa-Flood model.

The default and calibrated values of  $C_D$ ,  $SD$ ,  $\gamma$ ,  $\tau$ , and Manning's coefficient are shown in Table A1. Equations A1 and A2 show the calibrated river width and river bank height equations, respectively, as functions of the mean 30-day runoff from upstream of the cell ( $R_{up}$ ):

$$W = \max[16.6 * R_{up}^{0.35}, 3.0] \quad (A1)$$

$$B = \max[0.70 * R_{up}^{0.23}, 0.20] \quad (A2)$$

**Table A1. Model parameters calibrated in the study** [Modified after Mateo et al., 2014]

| Parameter                 | Default Value | Calibrated Value H08-Plain | Calibrated Value H08-CaMa | Typical Values in Tropical Forests                          |
|---------------------------|---------------|----------------------------|---------------------------|---|
| Bulk transfer coefficient | 0.003         | 0.007                      | 0.007                     | 0.006 in paddy fields; 0.007 in well-irrigated paddy fields |
| Soil depth (m)            | 1.00          | 3.50                       | 2.50                      | <i>not applicable</i>                                       |
| Time constant (d), $\tau$ | 100           | 155                        | 140                       | 100*  |
| Shape parameter, $\gamma$ | 2.00          | 2.30                       | 2.40                      | 2.00*   |
| Manning's coefficient     | 0.03          | <i>not applicable</i>      | 0.024                     | <i>not applicable</i>                                       |

\*Hanasaki et al., 2008a

Calibration of natural flow simulation was carried out manually in daily, monthly, and annual time scales. Primarily, daily flow was calibrated to reduce errors in simulating the peak discharge and timing from 1993-1995. Further tuning was carried out to increase the NSE-coefficient in the monthly flows and reduce the PBIAS in the annual flows from 1981-2004.